MOLECULAR ANALYSIS OF SENESCENCE-ASSOCIATED PROTEIN PHOSPHATASES DUSP10 AND MTMR11

A THESIS SUBMITTED TO
THE DEPARTMENT OF MOLECULAR BIOLOGY AND GENETICS AND THE INSTITUTE OF ENGINEERING AND SCIENCE OF BILKENT UNIVERSITY
IN PARTIAL FULFILLMENT OF THE REQUIREMENTS
FOR THE DEGREE OF
MASTER OF SCIENCE

BY
SUNA PELİN GÜLAY
JULY 2009

I certify that I have read this thesis and that in my opinion it is fully adequate, in scope and in quality, as a thesis for the degree of Master of Science.

_____

Assoc. Prof. Dr. Rengül Atalay

I certify that I have read this thesis and that in my opinion it is fully adequate, in scope and in quality, as a thesis for the degree of Master of Science.

_____

Prof. Dr. Mehmet Öztürk

I certify that I have read this thesis and that in my opinion it is fully adequate, in scope and in quality, as a thesis for the degree of Master of Science.

_____

Assist. Prof. Dr. Ali Osmay Güre

I certify that I have read this thesis and that in my opinion it is fully adequate, in scope and in quality, as a thesis for the degree of Master of Science.

_____

Assist. Prof. Dr. Ayşe Elif Erson

Approved for the Institute of Engineering and Science

_____

Director of Institute of Engineering and Science
Prof. Dr. Mehmet Baray

ABSTRACT

MOLECULAR ANALYSIS OF SENESCENCE-ASSOCIATED PROTEIN PHOSPHATASES DUSP10 AND MTMR11

Suna Pelin Gülay
MSc. in Molecular Biology and Genetics
Supervisor: Assoc. Prof. Rengül Atalay
July 2009, 129 Pages

Liver cancer is the fifth most common cancer in the world. Until recently, tumor cells were thought to proliferate indefinitely. In a previous study, our group showed spontaneous induction of replicative senescence in p53- and p16INK4a-deficient HCC (hepatocellular carcinoma) cell clones. The gene expression profiling was later done for these different clones, in an attempt to find novel therapeutic targets in HCC. Since protein kinases are known to be very important in disease formation and carcinogenesis, their partners in signaling, protein phosphatases should also be important in these processes. Hence analysis and targeting of protein phosphatases genes with differential expression between immortal and senescent clones might prove beneficial for HCC therapeutics. Among the phosphatase genes with differential expression patterns, we focused on two most upregulated genes in senescent clones with respect to immortal clones, DUSP10 and MTMR11. After gathering detailed information on these genes and their products by bioinformatics analysis, we confirmed the upregulation of the two genes in our senescent clones compared to our immortal clones by semi-quantitative RT-PCR. We then checked DUSP10 and MTMR11 expression in HCC and breast cancer cell lines to see if a differential expression of these genes are observed in different subtypes of these cell lines. Other experiments on MTMR11 focused on discovery of novel transcripts of this gene in HCC and breast cancer cell lines and checking the amounts of different transcripts in different subtypes of these cell lines, to form a bridge between MTMR11 transcript variants and carcinogenesis, however we did not observe differential expression. Two microarray studies comparing non-tumor and HCC tissues have listed MTMR11 as upregulated in HCC. Hence, upregulation of this gene in senescent clones may not be significant in hepatocarcinogenesis or replicative senescence, and further experiments should be performed. Considering DUSP10, we checked the subcellular localization of this protein in HCC cell lines by immunostaining, to see if the two subtypes (well-differentiated and poorly-differentiated) of HCC cell lines differed in DUSP10 localization. We observed some cell lines having only nuclear or only cytoplasmic DUSP10, whereas most had both nuclear and cytoplasmic DUSP10. This lead the way for us to explore the factors that may be important in changing this protein's localization, as this may be a type of regulation on this protein, and may change during carcinogenesis or upon induction of senescence. For this purpose, we checked to see if DUSP10 changed its localization in aging MRC-5 cell passages compared to young, proliferating ones and in premature senescence-induced cells compared to normal ones. Interestingly, it was found that upon replicative senescence induction, but not premature senescence, DUSP10 localized more to the cell nucleus which indicated a connection between DUSP10

localization and replicative senescence. We also checked to see if DUSP10 changed its localization upon disruption of the MAPK pathways it participates in, by kinase inhibitor experiments. Interestingly, it was found that DUSP10 localized significantly more to the cell nucleus upon inhibition of JNK pathway but not p38 pathway, in well-differentiated subtype of HCC cell lines. DUSP10 localization did not change significantly in poorly-differentiated subtype of HCC cell lines. Although JNKs, which seem to regulate DUSP10 through its localization according to this study, act as oncogenes in HCC, the significance of the change in DUSP10 localization should be characterized further before stating that DUSP10 can be a putative tumor suppressor. However, our other results indicate a relationship between DUSP10 localization and replicative senescence, which is promising because DUSP10 has emerged from our group's microarray data as a replicative senescence-associated gene, and this connection should be analyzed further.

ÖZET

HÜCRE YAŞLANMASIYLA İLİNTİLİ DUSP10 VE MTMR11 FOSFATAZ GENLERİNİN MOLEKÜLER ANALİZİ

Suna Pelin Gülay
Moleküler Biyoloji ve Genetik Yüksek Lisansı
Tez Yöneticisi: Doç. Dr. Rengül Atalay
Temmuz 2009, 129 Sayfa

Karaciğer kanseri (hepatosellüler karsinom) dünya çapında en sık görülen beşinci kanser türüdür. Yakın bir zamana kadar, tümör hücrelerinin sonsuz bölünme kapasitesine sahip olduğu düşünülmekteydi. Grubumuzun önceki bir çalışmasında p53 ve p16INK4a proteinlerine sahip olmayan karaciğer kanseri hücre klonlarında kendiliğinden gelişen bir hücre yaşlanması olayı gösterildi. Elde edilen senesant ve ölümsüz klonlarda değişen gen ifadelerinin incelenmesi karaciğer kanseri için tedavi amaçlı yeni hedef gen ve proteinlerinin bulunmasini sağlayabilirdi. Biz de bu amaçla, yakın zamanda hücre içi sinyal iletiminde ve bunun zarar görmesi sonucunda oluşan hastalıklarda önemleri anlaşılmaya başlanmış olan fosfataz genlerine odaklandık ve çalışmamız için senesant klonlarda ifadesi ölümsüz klonlara göre en yüksek anlamlı artışı gösteren DUSP10 ve MTMR11 fosfataz genlerini seçtik. DUSP10, mitojenler tarafindan aktive edilen protein kinazlardan (MAPK) JNK ve p38'i deaktive eder. MTMR11 ise myotubularin fosfataz ailesindendir. Bu genlerin ve gen ürünlerinin detaylı biyoinformatik analizinden sonra, revers transkriptaz polimeraz zincir reaksiyonu (RT-PZR) ile senesant klonlarda ölümsüz klonlara göre ifadelerinin arttığını doğruladık. Değişik kökenli ve değişik farklılaşma oranlarına sahip karaciğer ve meme kanseri hücre hatlarında, RT-PZR ile DUSP10 ve MTMR11 genlerinin ifadesine baktik. Amacımız bu genleri kanser oluşumu ve hücre yaşlanmasıyla ilişiklendirmekti. MTMR11 konusundaki diğer deneyler, elimizdeki hücre hatlarında bu genin yeni ve değişik transkript formlarinin bulunmasina ve bu farklı transkriptlerin miktarının karaciğer ve meme kanseri hücre hattı alt-türlerinde değişiminin saptanmasına odaklandı. Bu konuda farklı alt-türleri farklı transkriptler ile ilişiklendiremedik. Başka iki mikrodizilim çalışmasında da MTMR11'in karaciğer kanserinde ifadesi artmış bir gen olarak gösterildiğini de göz önünde bulundurursak, grubumuzun mikrodizilim çalışmasında MTMR11'in ifadesinin senesant klonlarda artmış olması, bu gen ve ürününün kanserleşme veya senesansta fonksiyonel bir rolü olduğu anlamına gelmiyor olabilir. Bunu ileriki çalışmalar gösterecektir. DUSP10 için ise, yine değişik karaciğer kanseri hücre hattı alt-türlerinde (epitel veya mezenkim kökenli) bir fark yakalayabilmek için, bu proteinin hücre içindeki lokalizasyonunu immüno-boyama ile tespit ettik. Bu proteinin bazı hücre hatlarında sadece çekirdekte veya sadece sitoplazmada, çoğundaysa her iki yerde de olduğunu gözlemledik. Bir proteinin hücre içi lokalizasyonunun değişimi bir çeşit kontrol mekanizması olabileceği, bu da bu proteini kanserleşme veya hücre yaşlanmasıyla ilişkilendirebileceği için, hücre içi DUSP10 lokalizasyonunu değiştirebilecek faktörleri incelemeye yöneldik. Öncelikle telomere bağlı olan ve olmayan hücre yaşlanması tiplerinde bu proteinin lokalizasyonunun değişimine baktık. Bunun için genç MRC-5 fibroblast hücre hattı pasajları ile yaşlanmakta olan pasajları

karşılaştırdık. İlginç bir şekilde, DUSP10'un yaşlanmakta olan hücrelerde çekirdeğe lokalize olmaya başladığını gözlemledik. Değişik kimyasallarla erken (prematüre) hücre yaşlanmasına sebep olunduğunda ise DUSP10'un lokalizasyonunun değişmediğini gördük. Mikrodizileme çalışmasının yapıldığı klonlarda gözlemlenen hücre yaşlanmasının telomere bağlı olduğu düşünüldüğünde aldığımız sonuç DUSP10'un bu tip hücre yaşlanmasında kontrolünün değiştiğini göstermesi açısından umut vericiydi. Bunlara ilaveten, DUSP10 lokalizasyonunun p38 ve JNK sinyal yolaklarının kimyasal ilaçlarla engellenmesi üzerine değişip değişmediğine de baktık. İlginç bir şekilde, DUSP10'un JNK'nin inhibisyonu sonucunda anlamlı bir şekilde çekirdeğe lokalize olduğunu, bu sonucun p38'in inhibisyonu sonucunda ise oluşmadığını gördük. Ayrıca bu gözlemimizi epitel kökenli hepatosellüler karsinom hücre hatlarında yapabildik. Mezenkim kökenli hücre hatlarında ise DUSP10 lokalizasyonunda bir değişiklik göremedik. Bu çalışmada DUSP10 lokalizasyonunu kontrol ettiği görülen JNK'ların hepatosellüler karsinomda onkoprotein olarak işlev gördükleri bilinmektedir. Yine de DUSP10'un tümör inhibisyonuyla veya telomere bağlı hücre yaşlanması ile olan ilişkisinin kesinleştirilmesi için bu proteinin hücre içi lokalizasyonundaki değişiminin öneminin başka deneyler aracılığıyla daha iyi anlaşılması gerekmektedir.

TO MY FAMILY

ACKNOWLEDGEMENTS

First of all, I would like to express my gratitude for my thesis advisor Assoc. Prof. Dr. Rengül Atalay for her guidance throughout this study. Being her student was a true privilege since she was always accessible for questions and discussions, and very supportive during hard times.

I would like to thank my co-advisor and the founder of KANİLTEK project, Prof. Dr. Mehmet Öztürk, for his guidance throughout this study and for providing me with inspiration.

I would like to thank the entire MBG faculty. I had the chance to interact with almost all of them through the courses I took or the ones I was involved in as a teaching assistant, and I learned a lot from each. I would also like to thank Dr. Hani Al-Otaibi for providing me with experimental support in the earlier parts of my research.

I would like to express my deepest thanks to Şerif Şentürk who has provided me with experimental support right from the beginning of my study until the very end, always being there when I needed to ask something or borrow a reagent.

I would like to thank all the past and present members of the MBG lab for creating a friendly, comfortable and helpful atmosphere to do research in. Many thanks go to the members of Molecular Oncology Group, especially to Ayça Arslan-Ergül, Mine Mumcuoğlu, Sevgi Bağışlar, Tülin Erşahin, Eylül Harputlugil, Gökhan Yıldız, Bilge Kılıçoğlu, Ebru Bilget-Güven and the past member Nilgün Taşdemir, as all of these people has done at least one thing to make my life easier in one or more aspects. Same is true for Duygu Akbaş-Avcı, Ender Avcı and Ceyhan Ceran, as I have enjoyed their friendships very much.

I am indebted to Füsun Elvan, Sevim Baran, Abdullah Ünnü and Pelin Telkoparan for their help in various ways, and especially for providing an ideal environment for research by making everything run smoothly.

Last but of course not the least, my deepest gratitude goes to my family for their patience, unconditional love and support throughout my life, and I dedicate this thesis to them.

This work was supported by the KANİLTEK project from State Planning Office (coordinator M. Ozturk). Additionally, during my MSc research, I was personally supported by TÜBİTAK with scholarship 2228.

The confocal microscopy images were taken at Central Laboratory Molecular Biology and Biotechnology R&D Center at Middle East Technical University, Ankara, with the help of Dr. Can Özen.

TABLE OF CONTENTS

LIST OF TABLES

LIST OF FIGURES

CHAPTER 1. INTRODUCTION

1.1 Protein phosphorylation and its regulation by kinases and phosphatases

Reversible post-translational modification is a very important process in regulating protein activity and thus crucial in cell signaling pathways. Many types of post-translational modifications exist, including but not limited to phosphorylation, ubiquitination, acetylation, methylation, glycosylation and myristoylation. Historically, phosphorylation is the best studied of these modifications mostly due to the relative ease of detecting protein phosphorylation *in vitro* and *in vivo* (see Hunter T, 2007). Phosphoproteomic analysis has shown the extent of protein phosphorylation in mammalian cells and the temporal dynamics of this post-translational modification through mass spectrometry. A recent study has detected 6600 phosphorylation sites in 2244 proteins of HeLa cell line and has further found that 14% of these sites are modulated at least 2-fold by epidermal growth factor (EGF) within 20 minutes (Olsen JV et al, 2006). These phosphoproteins include enzymes (specifically kinases), ubiquitin ligases, guanidine nucleotide exchange factors (GEFs), GTPase activating proteins (GAPs), transcription factors and other transcriptional regulators.

Phosphorylation is a well-characterized biochemical process in which a phosphate group is added through a phosphoester bond (O-phosphate) to the hydroxyl side chain of serine, threonine or tyrosine residues (Fig.1.1). The relative ratio of phosphorylation of these aminoacids in mammalian cells is about 1000:100:1 respectively. Of lower frequency, N-phosphorylation of histidine residues is also observed (see Kowluru A, 2008). The low frequency of phosphorylation of a specific residue does not show its insignificance in signaling as tyrosine phosphorylation is a very important process regulating activities of various growth factor receptors (see Arena S et al, 2005).

Phosphates are negatively charged groups and their addition to a protein can cause a conformational change in that protein, regulating its binding affinities to other proteins and its substrates thus controlling its function in a signaling cascade. In addition to this allosteric regulation, the phosphate groups may exert steric effects on

proteins such as shielding their positive charges as seen in the case of histones (see Grant PA, 2001). In addition, when coupled to ubiquitination, protein phosphorylation may also be a step in the degradation of a protein. Hence, protein phosphorylation can be considered as a molecular switch, turning the protein activity on or off. Additionally, it is a rapid and reversible process, all of which must have contributed to its selection during evolution as a key mechanism for the control of cell homeostasis (see Hunter T, 2007; Arena S et al, 2005).

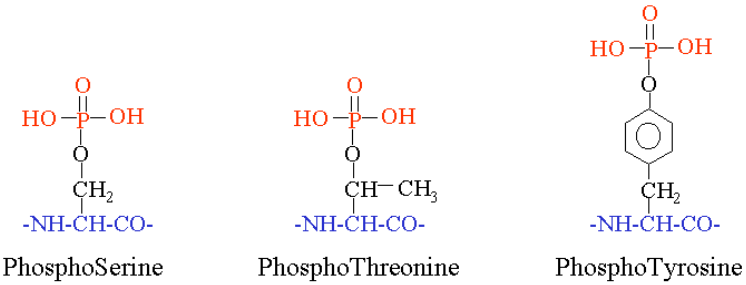

Fig.1.1: Frequently phosphorylated residues in humans: This image was retrieved from http://www.ionsource.com/Card/phos/phos.h1.gif on July 15th, 2009.

The key players in protein phosphorylation are kinases and phosphatases. Kinases are in charge of transferring phosphate groups from ATP molecules to their substrates, while phosphatases remove the phosphate groups from their substrates, reversing the action of kinases (see Arena S et al, 2005).

1.1.1 Kinase gene family

Kinases represent 1.5-2.5% of all eukaryotic genes, thus confirming the prominent role of these enzymes in controlling key cellular functions. There are 478 classical kinases which can be characterized by the presence of a conserved catalytic domain. A kinome tree can be seen in www.sciencemag.org/cgi/data/298/5600/1912/DC2/1. Kinases can be grouped into seven according to the sequence similarity between protein kinase domains: AGC (containing PKA, PKG, PKC families), CAMK (calcium/calmodulin dependent protein kinase), CK-1 (casein kinase 1), CMGC (containing CDK, MAPK, GSK3, CLK families), STE (homologs of yeast Sterile 7, Sterile 11, Sterile 20 kinases), TK (tyrosine kinase) and TKL (tyrosine kinase-like). There are also 40 atypical kinases including lipid kinases. Serine-threonine kinases comprise 67% of all kinases whereas tyrosine kinases comprise 17%. Tyrosine kinase-like kinases and atypical kinases comprise 8% of all kinases each. Despite their

relatively low number, tyrosine kinases are involved in key signaling pathways, including the transduction of extracellular stimuli to the cell nucleus. Tyrosine kinases can further be divided into two subgroups: Receptor tyrosine kinases (RTKs) which include membrane-spanning receptors, such as EGFR, FGFR and c-MET, characterized by an extracellular ligand-binding domain and an intracellular kinase domain, and non-receptor tyrosine kinases (NRTKs) which include cytoplasmic proteins, such as SRC, ABL and Janus kinases, generally involved in the intracellular signaling cascades. There are also a number of dual-specificity kinases (phosphorylating both serine-threonine and tyrosine residues) including mitogen-activated protein kinase kinases (MAPKKs, also known as MKKs) and cdc2-like kinases (CLKs), listed under different kinase groups (see Arena S et al, 2005).

1.1.2 Phosphatase gene family

Phosphatases generally counteract kinases in phosphorylation process by dephosphorylating proteins. They are newly acquiring a central importance in the control of proliferation, differentiation, cell adhesion and motility. There are 153 protein phosphatases in the human genome, and they can be classified into three: Protein serine-threonine phosphatases (PSTPs), protein tyrosine phosphatases (PTPs) and dual specificity phosphatases (DSPs) which include both serine-threonine and tyrosine dephosphorylating phosphatases such as MAPK phosphatases (MKPs), and protein and lipid dephosphorylating phosphatases such as myotubularin related phosphatases (MTMRs). 54% of all phosphatases are PTPs, 27% are DSPs and 19% are PSTPs. In contrast with the kinome, in the phosphatome serine-threonine phosphatases are lower in number which is because of the relatively low number of PSTP catalytic subunits. However, PSTP function is mostly determined by regulatory subunits, exceeding 50 subunits for some PSTPs such as protein phosphatase 1 (PPP1). Hence, the reactions PSTPs take part in are still numerous, including glycogen synthesis, muscle contractility, protein synthesis, stress response and regulation of circadian rhythm. PSTPs can be divided into three subgroups: PPPs (PPP1-7), PPMs (magnesium-dependent phosphatases, PPM1A-M and PPM2C) and FCP1 (dephosphorylation of RNA polymerase II carboxy-terminal-domain). Like TKs, PTPs can be divided into two subgroups: Receptor tyrosine phosphatases (RPTPs, further grouped according to protein structure and domains: R1-8, containing

phosphatases PTPRA-Z and PTPN5/STEP) and non-receptor tyrosine phosphatases (NRPTPs, further grouped according to protein structure and domains: NT1-9, containing phosphatases PTPN1-23 except PTPN5). RPTPs are generally implicated in processes that involve cell-cell and cell-matrix contact since they resemble cell-adhesion molecules in their extracellular segment. NRPTPs are generally found to be associated with a variety of TKs and hence are important in regulation of signal transduction. Finally, DSPs can be divided into many families of various functions according to their conserved domains, the major ones being: DUSPs (DUSP1-DUSP26 and DUPD1) (which bear yet another subfamily within: MAPK phosphatases/MKPs), Slingshots (SSH1-3), PRLs (PRL1-3), PTENs, MTMRs (MTM1 and MTMR1-13, this family includes pseudophosphatases with inactive catalytic sites that are important in regulation through binding) and CDC25 (CDC25A-C). The phosphatase tree is shown in Fig.1.2. PTENs and MTMRs have both lipid and protein phosphatase activity, however their preferred substrates are lipids (see Arena S et al, 2005; Tonks NK, 2006; Alonso A et al, 2004).

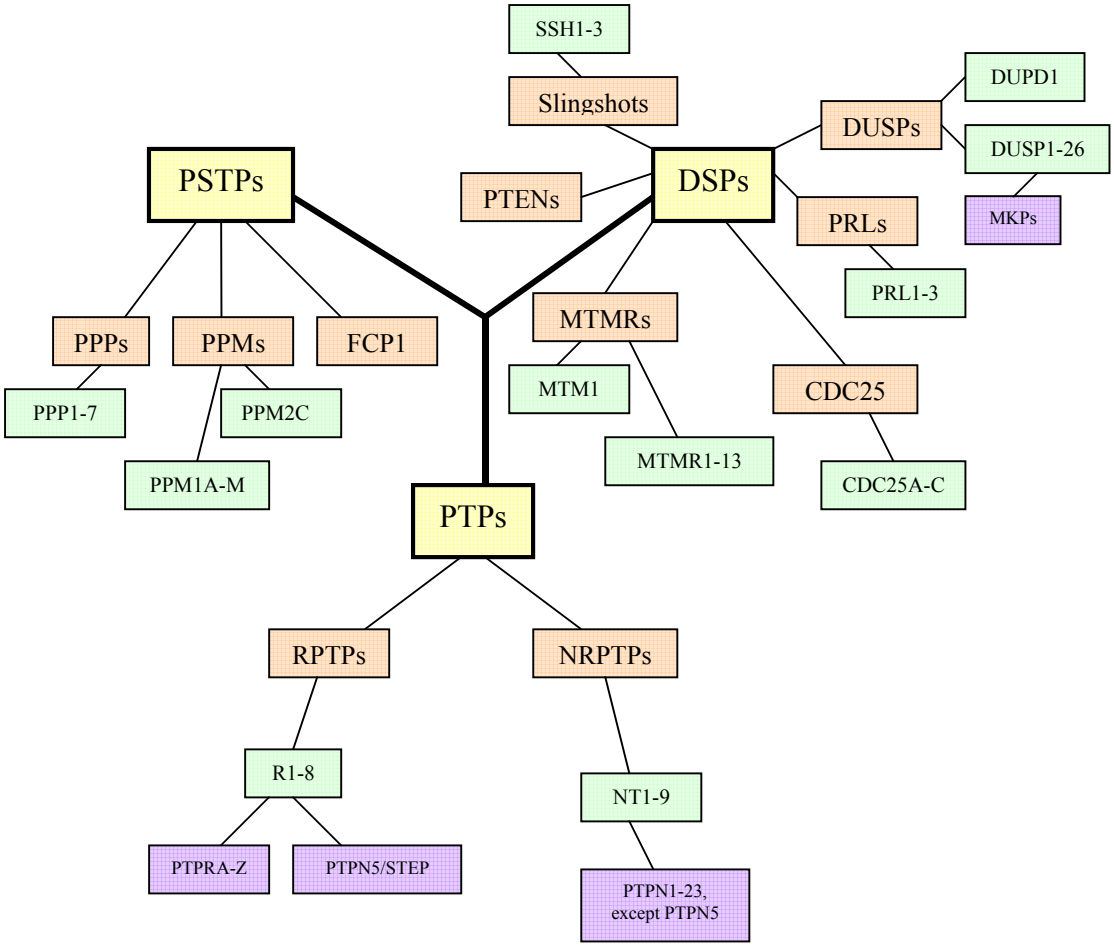

Fig.1.2: Protein phosphatase tree.

1.1.3 Deregulation of protein kinases and phosphatases in cancer and other diseases

Through phosphorylation, the cell regulates complex functions such as proliferation, differentiation, adhesion, metabolism and apoptosis (Fig.1.3). It is therefore not surprising that aberrant phosphorylation correlates strongly with the development of cancer and other complex diseases. Aberrant phosphorylation occurs through inactivation or hyperactivation of kinases and phosphatases.

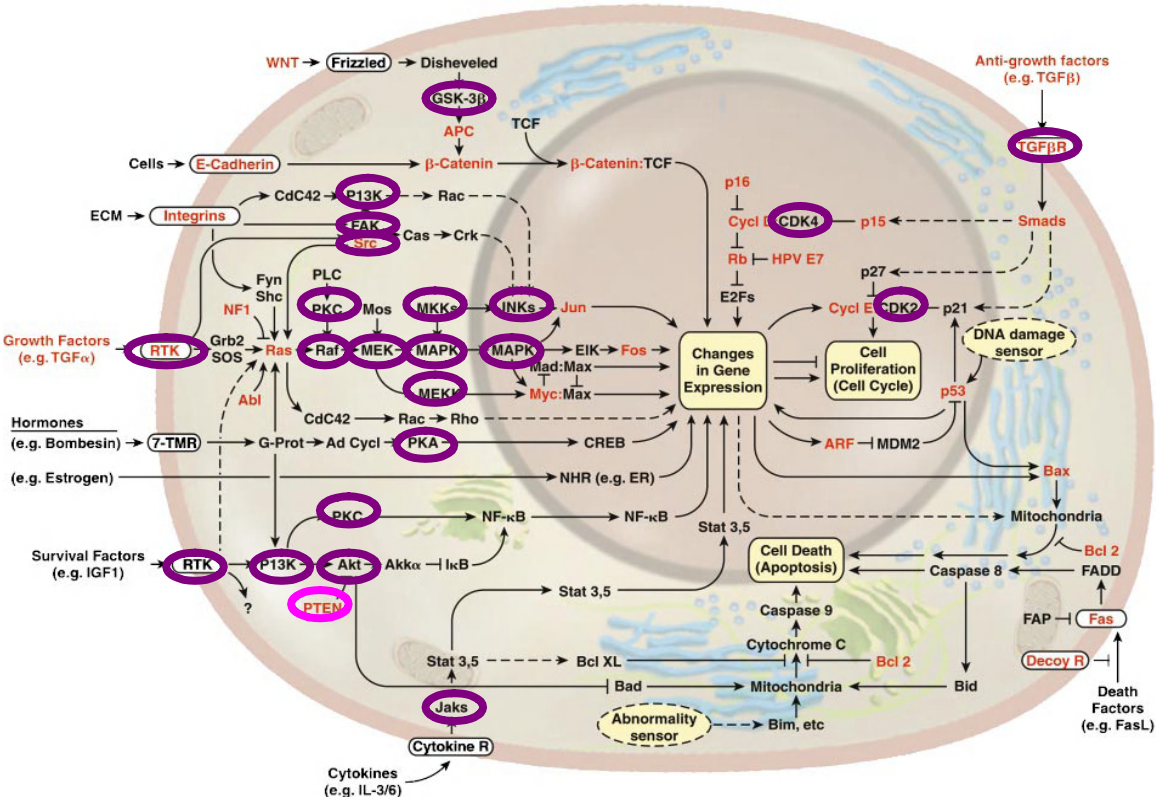

Fig.1.3: Cell signaling circuitry: The proteins known to be functionally altered in cancer are highlighted in red. Kinases are circled in purple and phosphatases in pink (there is only one phosphatase in this scheme, PTEN, which is a dual specificity phosphatase acting mainly on PIP_3). The abundance of protein kinases in signaling pathways resemble their importance for the cell (modified from Hanahan D, Weinberg RA, 2000).

Kinases are more studied than phosphatases in diseases and mostly are products of protooncogenes in case of cancer (Table 1.1). Kinase products of tumor suppressor genes also exist. For example, deletion of LKB1 (STK11) has been found to cause Peutz-Jeghers syndrome characterized by polyp formation in gastrointestinal tract. Downregulation of LATS1 (large tumor suppressor kinase 1) has been associated with an aggressive phenotype in breast cancers and molecular alterations of this gene have

been found in soft tissue sarcoma. Role of LATS1 in formation of soft tissue sarcomas has also been supported with knockout mice studies. MKK4 has been found to be mutated or deleted in a variety of human cancer cell lines, including pancreatic, testis, breast and colon cancer cell lines (Teng DH et al, 1997). Other well known examples of tumor suppressor kinases include CHEK2 and ATM which are important in DNA damage response, loss of function mutations of which cause Li-Fraumeni syndrome (characterized as a cancer predisposition syndrome) and ataxia telangiectasia (characterized by an increased sensitivity to ionizing radiation, this disease is neurodegenerative, it affects many parts of the body causing severe disability and susceptibility to cancer), respectively. Death-associated protein kinase 1 (DAPK1) is also a tumor suppressor candidate as its expression is lost in some human B-cell lymphoma, bladder, breast and renal carcinoma cell lines (Kissil JL et al, 1997). Interestingly, all these tumor suppressor and candidate kinases are either serine-threonine or dual-specificity kinases. Many growth factor receptors (RTKs) are known to be encoded by protooncogenes or candidates (including EGFR, PDGFR, FGFR). Additionally, there are well known examples of protooncogenes among NRTK genes, including SRC and ABL. Other than cancer, kinases also take part in formation of a variety of diseases ranging from metabolic diseases such as diabetes to severe chronic immunodeficiencies and neurodevelopmental disorders (Table 1.1).

Gene Name	Cancer	Other Disease	Effect in Cancer
LIMK1		Williams syndrome	
INSR		Leprechaunism, diabetes	
PDGFRA	Atypical CML, gastrointestinal stromal tumors (GIST), pulmonary artery intimal sarcoma, glioblastoma, osteosarcoma, dermatofibrosarcoma protuberans	Hypereosinophilic syndrome (HES), systemic mastocytosis (SM)	Oncogenic
PDGFRB	CMML, GIST, atypical CML, AML		Oncogenic
ABL	CML, ALL, AML, GIST		Oncogenic
ALK	Non-Hodgkins lymphoma, anaplastic large cell lymphoma (ALCL), inflammatory myofibroblastic tumor		Oncogenic
ABL2 (ARG)	AML		Oncogenic
RPS6KA3		Coffin-Lowry syndrome	
ATM		Ataxia-telangiectasia	Tumor suppressive
CHEK2		Li-Fraumeni syndrome	Tumor suppressive
AMPK		Wolff-Parkinson-White syndrome	
EIF2AK3		Wolcott-Rallison syndrome	
LKB1		Peutz-Jeghers syndrome	Tumor suppressive

MET	Papillary renal cancer, HCC, HPRCC, HNSCC, gastric cancer, malignant melanoma, SCLC, musculoskeletal tumors,		Oncogenic
FGFR1	Atypical CML	Craniosynostosis, Eosinophilia-myalgia syndrome (EMS)	Oncogenic
FGFR3	Multiple myeloma, T lymphoma		Oncogenic
FLT3	AML		Oncogenic
CSF1R (c-FMS)	AML	Myelodysplastic syndrome	Oncogenic
NTRK1	Papillary thyroid carcinoma		Oncogenic
NTRK3	AML, congenital fibrosarcoma, mesoblastic nephroma, secretory breast carcinoma		Oncogenic
JAK3		X-linked SCID	
ZAP70		Autosomal recessive SCID	
RET	Familial medullary thyroid cancer, radiation-associated papillary thyroid carcinoma, multiple endocrine neoplasia types 2A and 2B, neuroblastoma	Hirschsprung disease	Oncogenic
ROS1	Glioblastoma, astrocytoma		Oncogenic
BTK		X-Linked agammaglobulinaemia	
DMPK		Myotonic muscular dystrophy	
VEGFR-1 and -2	NSCLC and breast, prostate, renal, colorectal cancers (through overexpression of their ligands)		Oncogenic
KIT	AML, GIST, seminoma, SCLC, sarcomas	Systemic mastocytosis (SM), myelodysplastic syndrome	Oncogenic
PIK3CA	NSCLC, colorectal, brain and breast cancer		Oncogenic
CDKs	CLL, Non-Hodgkins' lymphoma, breast and lung cancer		Oncogenic
SYK		Myelodysplastic syndrome	
RAF1	Kidney cancer, melanoma		Oncogenic
P38		Rheumatoid arthritis	
BRAF	Melanoma, colorectal cancer		Oncogenic
EGFR (ERBB1)	Glioblastoma, NSCLC, colorectal cancer, squamous cell carcinoma of head/neck (SCCHN), pancreatic cancer, ovarian cancer		Oncogenic
ERBB2 (HER-2)	Breast, lung, ovarian cancer		Oncogenic
ERBB3	Soft tissue clear-cell sarcoma		Oncogenic
AKT2	Ovarian and pancreatic cancer		Oncogenic
JAK2	Colorectal, lung, brain and breast cancer, AML, ALL, atypical CML	Polycythemia vera, myeloproliferative diseases	Oncogenic
PP2A*	SV40 transformation		Tumor suppressive
PRL-3*	Colorectal cancer, HCC		Oncogenic
PTPN11*	AML, CML, ALL	Polycythemia vera, Noonan syndrome, LEOPARD syndrome	Oncogenic
PTPRG*	Colorectal cancer		Tumor suppressive
PTPN14*	Colorectal cancer		Tumor suppressive
PTPN13*	Colorectal cancer		Tumor suppressive
PTPRT*	Colorectal, gastric, brain cancer		Tumor suppressive
PTEN*	Glioma, prostate, breast, endometrial and colorectal cancer	Cowden syndrome, Bannayan-Zonana syndrome, Lhermitte-Duclos disease	Tumor suppressive
PPM1D*	Breast and ovarian cancer		Oncogenic
MTM1*		X-linked myotubular myopathy	

PTPRE*	Breast cancer		Oncogenic
PTPN1*		Insulin resistance, obesity	
MTMR2*		CMT syndrome type 4B	
MTMR13*		CMT syndrome type 4B	
PTPN9*		Autism	
PTPRC*		SCID, multiple sclerosis	
PTPN6*		Sezary syndrome	
PTPRN1/2*		Markers for autoimmune diabetes	
PTPN22*		SNP polymorphism in Type I diabetes	

Table 1.1: Kinases and phosphatases that are implicated in various diseases: Various kinases and phosphatases, and the diseases they have a role in are shown. Also their effect in cancer (oncogenicity vs. tumor suppression) has been noted. (*) shows phosphatases (see Cohen P, 2001; Krause DS, Van Etten RA, 2005; Arena S et al, 2005; Janssens V et al, 2005; Gallego M, Virshup DM, 2005; Ventura J-J, Nebreda AR, 2006).

Since phosphatases reverse the action of kinases, they can be considered as equally significant in disease formation, although their importance has been started to be discovered only recently. In the case of cancers, phosphatases are generally expected to be products of tumor suppressor genes. However just like there are tumor suppressor kinases, there are phosphatases encoded by protooncogenes and candidates (Table 1.1). For example, wild-type p53-induced phosphatase 1 (Wip1 or PPM1D) has been shown to be amplified and overexpressed in multiple cancer types, including breast and ovarian carcinomas. This phosphatase is known to suppress important tumor suppressors such as p53, ATM, p16INK4A and ARF, hence its overexpression may mediate carcinogenesis through inactivation of these proteins (see Lu X et al, 2008). Phosphatases of regenerating liver (PRLs), especially PRL-1 and PRL-3 have been associated with tumor progression, metastasis and angiogenesis. PRL-3 has been found to be amplified in colorectal cancer (see Arena S et al, 2005; Bessette DC et al, 2008). PTPN11 (Shp2) has been found to be mutated in polycythemia vera (a myeloproliferative disorder characterized by overproduction of red blood cells), Noonan syndrome (a genetic disease affecting the whole body characterized by congenital heart malformation and neurological problems) and LEOPARD syndrome ("*l*entigines, *e*lectrocardiogram abnormalities, *o*cular hypertelorism, *p*ulmonic stenosis, *a*bnormalities of genitalia, *r*etardation of growth, and *d*eafness," a multisystem disease). Additionally, somatic mutations of PTPN11 have been found in approximately 35% of patients with sporadic JMML (juvenile myelomonocytic leukemia) (see Chan G et al, 2008). Furthermore PTPN11 overexpression has been implicated in primary adult AML, CML and ALL (Xu R et al, 2005). PTPRE has been

implicated in aiding Neu (HER-2 or ERBB2) -induced mammary tumorigenesis (see Berman-Golan D et al, 2008). In addition to oncogenic phosphatases, there are also tumor suppressor and candidate phosphatases. One of the best known tumor suppressor phosphatase is PTEN, a dual specificity phosphatase that can act both on proteins and lipids, and its main target is PIP_3. Deletion of PTEN has been observed in a variety of cancers including glioma, prostate, breast, endometrial and colorectal cancer. Another well known tumor suppressor phosphatase is PP2A, as it is known that small t antigen of SV40 tumor virus targets this phosphatase system to promote tumor formation. This is thought to occur by activation of PIP_3 signaling pathway and stabilization of c-myc oncoprotein as both are targets of PP2A under normal physiological conditions (see Gallego M, Virshup DM, 2005). Just like kinases, phosphatases take part in a number of other diseases ranging from insulin resistance and obesity to myopathies and sensory neuropathies such as Charcot-Marie-Tooth (CMT) disease (Table 1.1).

Although there are many kinases and phosphatases whose role in cancer is well known as already mentioned, not everything is black and white for the functions of rest of these enzyme families in cancer development and progression. For example, there are controversial data on the role of MKPs in carcinogenesis. This is only normal because although ERK mainly shows oncogenic effect, the effects of JNK and p38 MAPKs changes according to the cancer type and stage. They act to suppress some cancers mainly through induction of apoptosis, whereas in some other cancers in which inflammation contributes to carcinogenesis, they act in favor of cancer development. Another complication especially important for JNK is that the duration and magnitude of signal mediated through it causes differential results such as proliferation versus apoptosis. Hence negative regulators of these two MAPK subtypes act either as oncoproteins or tumor suppressors depending on the cancer type, stage, the duration and magnitude of signaling (see Keyse SM, 2008; Krishna M, Narang H, 2008).

In an additional study, researchers have employed RNA interference to downregulate each known kinase and phosphatase in HeLa cell line, and have found that 73 kinases and 72 phosphatases are necessary for survival and growth and 12 other phosphatases function in sensitizing cells to apoptosis (MacKeigan JP et al, 2005), further

suggesting that kinases and phosphatases are vital for cells and that knowledge on these enzymes may lead to new treatment options for a large variety of diseases.

1.2 Hepatocellular carcinoma

Liver cancer is the fifth most common cancer in men and the eighth in women worldwide. It is also one of the leading causes of cancer-related deaths worldwide, ranking third in men and sixth in women (American Cancer Society, 2007). This high lethality rate is attributable in part to a resistance to existing anticancer agents, a lack of biomarkers that can detect surgically resectable incipient disease, and underlying liver disease that limits the use of chemotherapeutic drugs. Primary liver cancers include hepatocellular carcinoma, intrahepatic bile duct carcinoma (cholangiocarcinoma), hepatoblastoma, bile duct cystadenocarcinoma, haemangiosarcoma and epitheloid haemangioendothelioma, of which hepatocellular carcinoma is the most common (see Farazi PA, DePinho RA, 2006).

Hepatocarcinogenesis proceeds through a multi-step histological course. The discussed risk factors act to promote rounds of hepatocyte necrosis and regeneration that pave the way for development of a chronic liver disease. Liver injury and exposure to various cytokines, in a chronic liver disease condition, provoke stellate cell activation, which is associated with cellular proliferation and the robust synthesis of extracellular matrix components such as collagen, therefore contributing to liver fibrosis. Meanwhile the destruction-proliferation cycles also promote hepatocyte proliferative arrest due to telomere shortening (telomerase reactivation has also been associated with hepatocarcinogenesis, although the exact timing is not known). These changes lead to cirrhosis which is characterized by regenerative nodules surrounded by fibrous scar tissue (collagen). These nodules transform into hyperplastic nodules of regenerating hepatocytes which represent a potential first step towards HCC. Hyperproliferation of hepatocytes in these nodules causes accumulation of mutations and chromosome aberrations that leads to genomic instability, and results in pre-malignant dysplastic nodules characterized by accumulation of lipids or glycogen inside the cell and nuclear crowding. Also abnormal liver architecture is seen at this stage. The dysplastic nodules can evolve into HCC due to high genomic instability and loss of p53. HCC has the capacity to invade the surrounding fibrous stroma and

vessels, and occasionally has metastatic potential. HCC can be further classified into well differentiated, moderately differentiated and poorly differentiated tumors, the last being the most malignant form of primary HCC. (see Goodman ZD, 2007; Farazi PA, DePinho RA, 2006).

1.2.1 Aetiologies of hepatocellular carcinoma

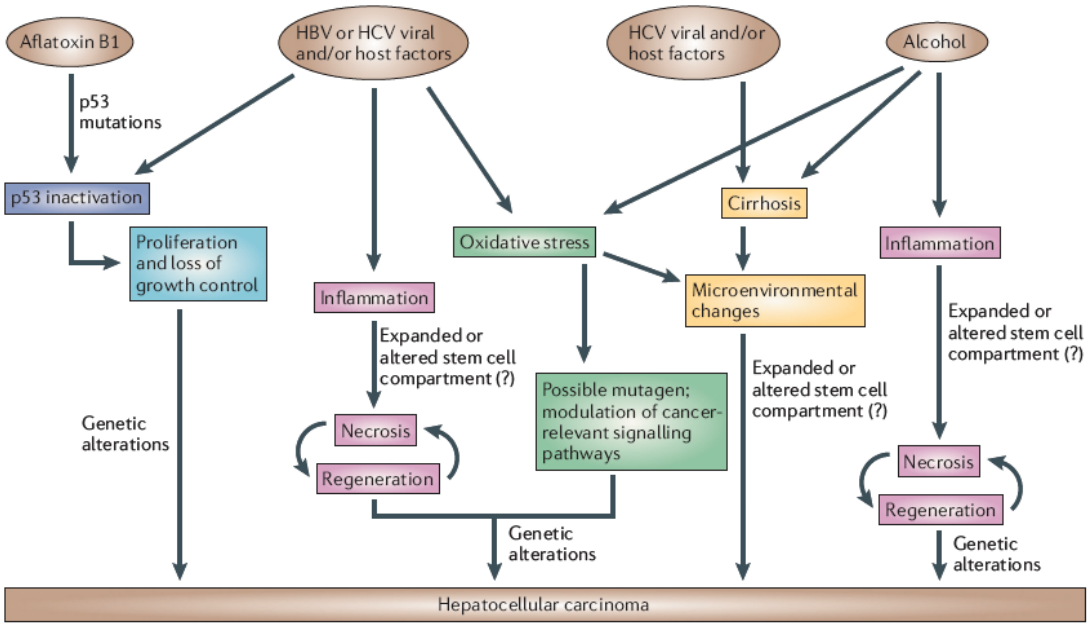

Fig.1.4: Risk factors and mechanisms of hepatocarcinogenesis (see Farazi PA, DePinho RA, 2006).

Hepatitis B virus (HBV) is the main causal factor of HCC globally, due to the fact that it is one of the most common diseases in the world, with an estimated 350 million chronically infected carriers worldwide. HBV is a single-stranded DNA virus of the hepadnavirus family that is integrated into the host genome. The integration of virus DNA may activate cellular proto-oncogenes or cause microdeletions that can target cancer-relevant genes, although no consistent integration sites have been observed (see Lok AS, 2000). HBx protein has transcriptional activation activity that has been shown to alter the expression of growth-control genes, such as *src* tyrosine kinases, Ras, Raf, ERK and JNK (Tarn C et al, 2001). HBx protein has also been shown to bind and inactivate p53 by sequestration *in vitro* and to block p53 mediated apoptosis in vivo. ER stress and oxidative stress might also result due to viral-ER physical interactions (see Farazi PA, DePinho RA, 2006).

Hepatitis C virus (HCV) is known to be the greatest risk factor for development of HCC, increasing the rate of HCC formation in patients with HCV approximately 17-fold (Degos F et al, 2000). It is an RNA virus of the flaviviridae family. It has no reverse transcriptase activity and hence does not integrate itself into the host genome. Still, HCV shows a higher propensity to yield chronic infection which might relate to immune evasion by this virus, and that HCV shows a higher propensity to promote liver cirrhosis (see Farazi PA, DePinho RA, 2006). HCV core proteins have transcription regulatory functions on many different host genes, including the proto-oncogene *c-myc* (Ray RB et al, 1995). HCV core proteins are also known to inhibit multiple activators of apoptosis, including Fas and tumor necrosis factor-α (TNF-α) (Marusawa H et al, 1999; Jin X et al, 2006). These effects of HCV core proteins may be exerted through the constitutive activation of ERK signaling cascade (Hayashi J et al, 2000). In addition to the core proteins, HCV nonstructural protein NS5A have been shown to interact with and inactivate p53 by sequestration to the perinuclear membrane (Majumder M et al, 2001). ER-stress and oxidative-stress-mediated mechanisms might also be possible for HCV-induced HCC (see Farazi PA, DePinho RA, 2006). Additionally HCV might be impairing immune system by interfering with T-cell activation (see Pachiadakis I et al, 2005).

Chronic alcohol intake has been implicated in causing production of pro-inflammatory cytokines through monocyte activation, in increasing intestinal permeability to bacteria/lipopolysaccharides, leading to Küpffer cell activation. Küpffer cells are specialized macrophages located in the liver and they release many chemokines and cytokines upon activation (including TNF-α, interleukin-1β, interleukin-6 and prostaglandin E) with adverse effects on hepatocyte survival. Chronic ethanol exposure causes hepatocytes to show increased sensitivity to the cytotoxic effects of TNF-α which may be responsible for chronic hepatocyte destruction-regeneration cycles leading to stellate cell activation, fibrosis, cirrhosis and ultimately HCC (see Farazi PA, DePinho RA, 2006; McKillop IH et al, 2006). Alcohol also damages the liver through oxidative stress mechanisms that result upon hepatic ethanol metabolism (see McKillop IH et al, 2006).

Aflatoxins are mycotoxins from *Aspergillus flavus* and *Aspergillus parasiticus*. Hepatic cytochrome p450 metabolizes aflatoxin (AFB_1) and converts it to its highly

reactive exo-8,9-epoxide form. This epoxide reacts with guanine nucleotides in the hepatocyte DNA to form a number of adducts, which lead to heritable mutations that result in hepatocarcinogenesis (see McKillop IH et al, 2006). The main mechanism of AFB_1 in hepatocarcinogenesis has been found to be GC→TA transversion at the third position of codon 249 of p53 gene (resulting in an Arg→Ser alteration in the protein) (Puisieux A et al, 1991).

Other aetiological factors in HCC can be listed as follows:

- Non-alcoholic fatty liver disorders (NAFLD) and non-alcoholic steatohepatitis (see Farrell GC, Larter CZ, 2006).
- Type 2 diabetes and its associated hyperinsulinemia and hyper-IGF-1 production (El-Serag HB et al, 2004).
- Certain metabolic disorders such as hereditary haemochromatosis, porphyria cutanea tarda, Wilson's disease and primary biliary cirrhosis (see McKillop IH et al, 2006; Farazi PA, DePinho RA, 2006).
- Possibly use of oral contraceptives through their estrogen and progesterone components (see Maheshwari S et al, 2007; El-Serag HB, Rudolph KL, 2007).

1.3 Protein kinases and phosphatases implicated in hepatocarcinogenesis

Disruption of cell signaling is frequently seen in hepatocarcinogenesis. Mutations and other regulatory problems in p53 tumor suppressor, Wnt/β-Catenin pathway, growth factor receptors (including ErbB receptor family and c-MET) and their associated pathways, pRb tumor suppressor, Ras proteins and associated pathways, Janus kinases / signal transducers and activators of transcription (JAK/STAT) pathway are observed.

Deregulation of protein phosphorylation in important signaling pathways is very important in initiation and progression of HCC. For example, in a recent study, PRL-3 has been found to be significantly upregulated in HCC tumor tissues compared to the paired noncancerous liver tissues. The mRNA level of PRL-3 in tissues was also correlated with serum α-fetoprotein level, vascular invasion and metastasis in this study. Furthermore, a significant correlation between PRL-3 mRNA expression and

MMP-2, MMP-9 and E-cadherin has been found (Zhao WB et al, 2008). Another example is the tyrosine kinase $p60^{c\text{-}src}$ (SRC), which is overactivated in hepatoma cells and this is thought to account for the desensitization of liver tumor cells to TRAIL and CD95. SRC works with EGFR in desensitizing cells to apoptosis (De Toni EN et al, 2007). Another recent example may be DUSP1 (MKP-1). The expression of this MAPK phosphatase, a negative regulator of ERK, is dysregulated in liver tumors with poor prognosis. This is suggested to be through increased ubiquitination of DUSP1 by S-phase kinase-associated protein 2 (SKP2)/CDC28 protein kinase 1b (CKS1) ubiquitin ligase complex which leads to increased proteasomal degradation of DUSP1 (Calvisi DF et al, 2008). A final example comes from a very recent study on Rho-associated, coiled-coil containing protein kinase 2 (ROCK2) which has been found to be overexpressed in about 54% of the 41 HCC samples and this overexpression has correlated with a more aggressive phenotype. Further experiments have also associated ROCK2 with increased invasiveness in HCC, which is in accordance with the fact that ROCKs normally regulate actin cytoskeleton and cell motility (Wong CC et al, 2009).

In addition to these specific and novel examples, there are a number of important signaling pathways known to be deregulated in HCC, in which kinases and phosphatases play major roles (Fig.1.5).

1.3.1 Growth factor receptor tyrosine kinases

ErbB family of receptor tyrosine kinases consists of ERBB1 (EGFR), ERBB2 (HER2/neu), ERBB3 and ERBB4. EGFR has been found to be overexpressed in 4-70% of HCC cases, HER2 in 0-30%, ERBB3 in 84% and ERBB4 in 61% (see Breuhahn K et al, 2006; Höpfner M et al, 2008; Farazi PA, DePinho RA, 2006).

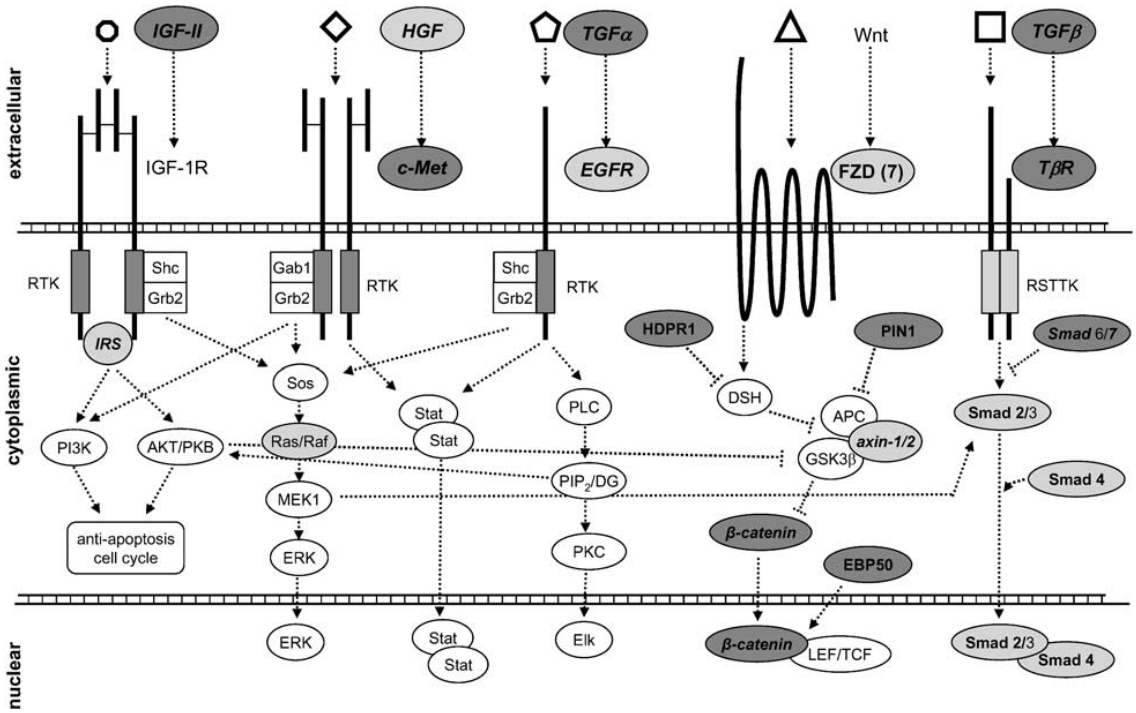

Fig.1.5: Major growth factor receptor signaling pathways important in HCC: Predominantly dysregulated components of signaling pathways are highlighted in dark gray. Seldom regulated components (eg. Smad 2/3), molecules not expressed by tumor cells (eg. HGF), and distinct protein family members dysregulated in HCC (eg. FZD-7) are highlighted in light gray (see Breuhahn K et al, 2006).

Considering IGF signaling, expression of IGF-2R has been found to be reduced in 63% of human HCC. Loss of heterozygosity at the *igf-2r* locus has also been observed in HCC and its premalignant lesions coupled to inactivating mutations of the second allele in 25% of the cases. Furthermore, several missense mutations are reported in HCC which target the extracellular domain of IGF-2R (see Breuhahn K et al, 2006; Höpfner M et al, 2008).

Mesenchymal-epithelial transition factor (MET) is a proto-oncogene encoding for a membrane receptor tyrosine kinase, of which hepatocyte growth factor (HGF) is the only known ligand. Overexpression of the MET receptor has been observed in 20-48% of tumor samples. This induction in HCC cells may be attributed to genomic alterations (7q gains have been observed in 16.8% of HCCs), tumor hypoxia or HGF-dependent transcriptional activation of MET (Breuhahn K et al, 2006; Höpfner M et al, 2008; Farazi PA, DePinho RA, 2006).

There are different data on the expression of TGFβ receptors, which are serine-threonine kinases, in HCC. There are studies that have not detected a change in

expression levels of the receptors. In another study, upregulation of TGF-βRI levels has been detected in 60% of the cases. In yet another one, downregulation of TGF-βRI levels has been detected in 80% of the cases. In some studies, including this latter study, downregulation of TGF-βRII levels has been detected in 37-70% of the cases. Overall, most studies document a reduction of the receptors in up to 70% of HCCs. (Breuhahn K et al, 2006).

1.3.2 Kinases and phosphatases of PI3K/PTEN/AKT/mTOR pathway

A major activation of this pathway can be either due to higher activity of receptor tyrosine kinases or to the reduced expression of PTEN, a negative regulator of the pathway. 10q loss is a genomic alteration that occurs in 17-27% of HCC cases, and this region also contains the *PTEN* gene. Furthermore, somatic missense mutations, frame shifts, splice site mutations and loss of promoter activity of PTEN have also been observed in HCC tissues and cell lines (Kawamura N et al, 1999; Ma DZ et al, 2005; Fujiwara Y et al, 2000). Downstream of this pathway, mTOR, a serine-threonine kinase implicated in the regulation of translation, is overexpressed in %50 of HCC cases (n=314), as found in a recent broad study. Additionally, chromosomal gains in RICTOR were observed in 25% of patients (Villanueva A et al, 2008).

1.3.3 Mitogen-activated protein kinase (MAPK) pathways

The mitogen-activated protein kinase (MAPK) family consist of five subgroups, including the extracellular signal-regulated kinase homologs 1 and 2 (ERK1/2), big MAPK-1 (BMK-1/ERK5), c-Jun N-terminal kinase homologs 1, 2 and 3 (JNK1/2/3), stress-activated protein kinase 2 (SAPK-2) homologs α, β, and δ (p38α/β/δ), and ERK6 (p38γ). These kinases are activated through dual phosphorylation of T and Y residues located in their activation loop by their corresponding MAPK kinases (MKKs). MAPKs are implicated in diverse cellular processes such as cell growth and proliferation, differentiation, adhesion, apoptosis and stress response (see Pimienta G, Pascual J, 2007). Major MAPK pathways and their components are shown in Fig.1.6.

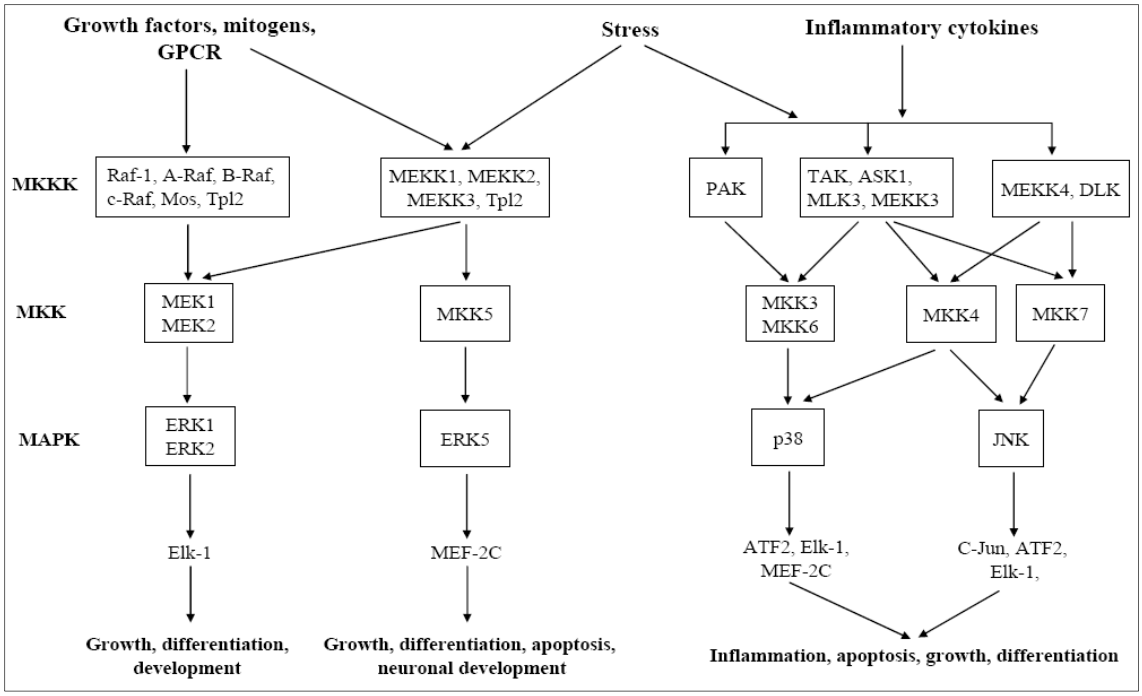

Fig.1.6: Mitogen-activated protein kinase pathways (see Zhang Y, Dong C, 2005).

Extracellular signal-regulated kinases (ERKs) or classical MAP kinases are widely expressed and are involved in functions including the regulation of cell proliferation and differentiation. Many different stimuli, including growth factors, cytokines, virus infection, ligands for heterotrimeric G protein-coupled receptors, transforming agents, and carcinogens, activate the ERK pathway. Main isoforms are ERK1 and ERK2 (Krishna M and Narang H, 2008).

c-Jun N-terminal kinases (JNKs), originally identified as kinases that phosphosphorylate c-Jun on Ser63 and Ser73 within its transcriptional activation domain, are responsive to stress stimuli, such as cytokines, ultraviolet irradiation, heat shock, and osmotic shock. They are involved in cell differentiation, proliferation and apoptosis. Main isoforms are JNK1 and JNK2 which are ubiquitiously expressed, and JNK3 which is only found in brain, heart and testes (Krishna M and Narang H, 2008).

Similar to JNK pathway, p38 MAP kinases are activated by a variety of cellular stresses including osmotic shock, heat shock, inflammatory cytokines, lipopolysaccharides (LPS), ultraviolet light and growth factors. They are involved in cell differentiation, apoptosis and Ras-induced senescence. Main isoforms are p38α, p38β, p38γ (also known as ERK6) and p38δ (Krishna M and Narang H, 2008).

Other MAPKs are: ERK5, found recently, is activated both by growth factors and stress stimuli, and participates in regulation of cell proliferation, and, atypical MAPKs ERK3/4 and ERK7/8 which are cytoplasmic proteins and possess a C-terminal extension. Atypical MAPKs are also recently found and not much is known on them (Krishna M and Narang H, 2008).

Proteins of HBV, HCV and hepatitis E virus target and modulate multiple steps along MAPK pathway. In one study, it has been shown that HCV E2 protein, one of the two envelope glycoproteins of hepatitis C virus, activates the MAPK pathway in human hepatoma Huh-7 cells and promotes cell proliferation (Zhao LJ et al, 2005). Furthermore, increased levels of ERK have been observed in HCC and are known to correlate with tumor progression (Tsuboi Y et al, 2004). In another study, expression of Spred protein (Sprouty-related protein with Ena/vasodilator-stimulated phosphoprotein homology-1 domain), an inhibitor of the Ras/Raf-1/ERK pathway has been found to be deregulated in human HCC. Also in this study, ectopic overexpression of Spred has been observed to cause inhibition of ERK activation both in vivo and in vitro, resulting in reduced cancer cell proliferation and low secretion of MMP2 and MMP-9 (Yoshida T et al, 2006).

1.4 Cellular senescence and liver cirrhosis

Liver cirrhosis is the greatest clinical risk factor in hepatocarcinogenesis regardless of the aetiology underneath (HBV, HCV, aflatoxin or alcohol). In fact when compared to other cancers, HCC is characterized by an underlying cirrhosis condition, and 45-90% of all HCCs worldwide occur in the setting of liver cirrhosis. Cirrhosis has life-threatening complications other than HCC, ascites (fluid retention in the abdominal cavity) being the most common one, leading to an increased risk of infection and a poor long-term outcome (see Goodman ZD, 2007).

As already mentioned, liver cirrhosis is characterized by abnormal nodules of regenerating hepatocytes surrounded by fibrous scar tissue. Telomere shortening and senescence have been shown as the general markers of human liver cirrhosis, also correlating with progression of fibrosis in cirrhosis (Wiemann SU et al, 2002).

Cellular senescence was initially defined as the loss of proliferative capacity of cells in culture typically after cultures have been passaged 50 or more times (Sherwood SW et al, 1988; Hayflick L, 1965). Cellular senescence, the state of stable cell cycle arrest, can be provoked by a variety of stimuli, such as telomere shortening, DNA damage, activation of certain oncogenes and oxidative stress (Fig.1.7). Senescence is associated with a number of gross cellular changes including cell-cycle arrest (see Collado M et al, 2005; Herbig U and Sedivy JM, 2006), increase in cell size and size heterogeneity, and increase in the frequency of cells with chromosomal aberrations, including polyploidy (Sherwood SW et al, 1988). Senescent cells display SABG (senescence-associated β-galactosidase) activity at pH 6.0 and this activity can be used as a marker to identify senescent cells. Other characteristic features of senescent cells include presence of $p16^{INK4a}$, senescence-associated DNA-damage foci and senescence-associated heterochromatin foci (see Ozturk M et al, 2008). Cellular senescence acts as a barrier to cancer, preventing damaged cells from undergoing aberrant proliferation (see Chen JH et al, 2007, Campisi J, 2005), although it probably also has deleterious effects on organisms such as tissue aging (see Ozturk M et al, 2008). Two well-established tumor suppressor proteins, pRb and p53, have been shown to play key roles in cellular senescence (Fig.1.8) (see Ben-Porath I and Weinberg RA, 2004).

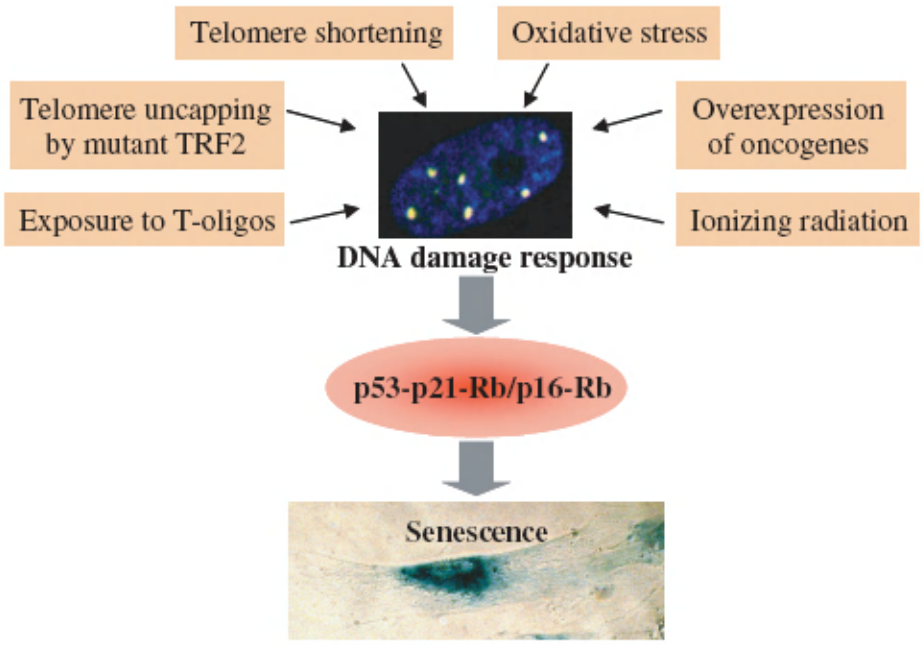

Fig.1.7: Stimuli that cause cells to undergo senescence (see Chen JH, Hales CN, Ozanne SE, 2007).

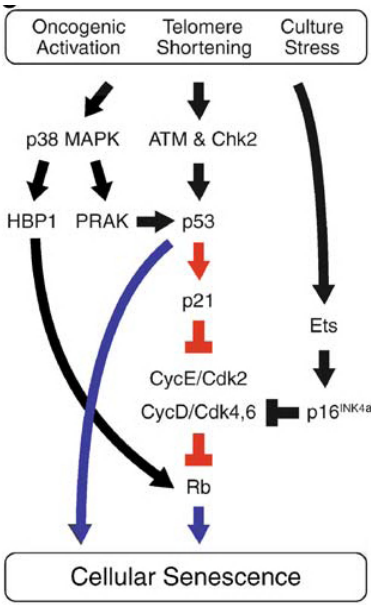

Fig.1.8: Molecular mechanisms of senescence (see Funayama R, Ishikawa F, 2007).

1.4.1 Replicative senescence and telomere shortening

Telomeres progressively shorten with age in somatic cells in culture and in vivo because DNA replication results in the loss of sequences at the 5' ends of double-stranded DNA. Whereas somatic cells do not express the enzyme telomerase which adds repeated telomere sequences to chromosome ends, telomerase activity is detected in immortalized and cancer cells in vitro and in primary tumor tissues. This represents an important difference between normal cells and cancer cells, suggesting that telomere shortening causes cellular senescence (see Oshimura M and Barrett JC, 1997). This form of senescence is called as replicative or telomere-dependent senescence. There is accumulating evidence that when only a few telomeres are shortened, they form end-associations, resulting in a DNA damage response which leads to replicative senescence (see Shay JW and Wright WE, 2004). This DNA damage signal leads to the activation of cell cycle checkpoint pathways involving p53, p16INK4a, and/or retinoblastoma (pRb) proteins (see Campisi J, 2005; Dimri GP, 2005). Inactivation of p53 and $p16^{INK4a}$ genes (see Shay JW and Bacchetti S, 1997) and reactivation of hTERT gene expression (see Sherr CJ and McCormick F, 2002) cause cells to gain replicative immortality (see Ozturk M et al, 2008).

1.4.2 Premature (stress-induced) senescence

Replicative senescence is not the only form of senescence, as telomere-independent senescence mechanisms are also known, namely oncogene-induced senescence and oxidative stress-induced senescence (see Ozturk M et al, 2008). Telomere-independent senescence is also known as premature senescence since it occurs in a short time after oncogenic activation or stress caused by reactive oxygen species (ROS), if the elements of the senescence or DNA damage pathways are intact. This is in contrast to telomere-dependent senescence which occurs roughly after 50 population doublings in normal cells (see Funayama R, Ishikawa F, 2007). Additionally, hTERT expression does not prevent premature senescence (Gorbunova V et al, 2002).

Activated oncogenes such as Ras, Raf, Mos, Mek, Myc and Cyclin E are known to cause senescence. Loss of PTEN tumor suppressor gene also leads to senescence. Like replicative senescence, oncogene-induced senescence is mainly a DNA damage response, having ATM/ATR, CHK1/2, p53 and pRb as key players (see Ozturk M et al, 2008). Other mechanisms also contribute to the formation of this senescence type. p38 MAPK is known to play an important role in Ras-induced senescence. One of its targets, high mobility group (HMG)-box transcription factor 1 (HBP1) cooperates with pRb to mediate senescence whereas another target, p38-regulated/activated protein kinase (PRAK) phosphorylates p53 (see Funayama R, Ishikawa F, 2007).

Oxidative stress-induced senescence is caused by the reactive oxygen species (ROS), for which mitochondria are the main source. ROS have also been identified as critical mediators of replicative and oncogene-induced senescence, as these forms of senescence are accelerated in cells under oxidative stress (see Ozturk M et al, 2008). Although the exact mechanism of ROS-induced senescence is not known, studies have shown that p38 MAPK pathway might be important in mediating it, since inactivation of p38 delays the onset of various forms of cellular senescence, including the three that have been mentioned (see Funayama R, Ishikawa F, 2007). Additionally, ROS have been found to induce senescence in hematopoietic stem cells by activating p38 MAPK (see Ozturk M et al, 2008). However, the p38 targets important in mediating ROS-induced senescence are currently not known.

1.5 Reprogramming of immortal cell lines for replicative senescence

Previously, Ozturk N and colleagues discovered spontaneous replicative senescence reprogramming in cultured cancer cell lines while working with empty vector-transfected clones. This study hinted at a possible novel therapeutical approach against HCC by reversal of immortality in cancerous cells (Ozturk N et al, 2006).

1.5.1 Induction of spontaneous replicative senescence in stable clones derived from parental HCC cell lines

In the work of Ozturk N et al, analysis of clones from established HCC cell lines revealed that some empty vector transfected Huh7-derived clones showed phenotypes similar to cellular senescence. Two sets of clones were established according to their potential to undergo replicative senescence: C1/C3 clones (pcDNA 3.1 transfected) and G11/G12 clones (pEGFP-N2 transfected). C3 clones (C3L) went through only 80 population doublings (PD), had very high senescence-associated-β-galactosidase (SABG) staining and very low BrdU staining, associated with very low rates of proliferation. On the other hand, C1 clones went through more than 150 population doublings and had very low SABG staining. Interestingly, parental Huh7 cells are composed of a heterogeneous population of cells on the basis of SABG staining, normally displaying about 20% staining. Early passage C3 clones (C3E; PD 57) also showed heterogeneous SABG staining and a normal phenotype. Similar results were obtained with G11/G12-Early/G12-Late clones. Hence this work showed that replicative immortality could be reversed and that cancer cells could generate senescent progeny spontaneously (Ozturk N et al, 2006).

1.5.2 Mechanism of spontaneous replicative senescence in stable clones derived from parental HCC cell lines

In an attempt to uncover the mechanism of spontaneous replicative senescence generated in these Huh7-derived stable clones, Ozturk N et al checked hTERT activity and telomere lengths in these cells. They found that the immortal C1 clones displayed hTERT activity and maintained their telomere length, whereas the senescent C3

clones displayed no detectable hTERT activity and had shortened telomeres. The researchers further analyzed the expression of known regulators of hTERT expression in the clones and found that a perfect reverse correlation was present between expression of hTERT and *SIP1* (Zinc finger E-box binding homeobox 2; ZEB2) genes. This gene encodes a transcriptional repressor that interacts with Smad proteins of TGF-β signaling pathway and with CtBP co-repressor. Bypass of senescence arrest was observed after shRNA-mediated inactivation of SIP1 expression in C3 clones, further indicating SIP1 protein as a key regulator in this senescence mechanism (Ozturk N et al, 2006).

1.6 Gene expression changes between senescent and immortal Huh7 clones

1.6.1 Gene expression profiling of senescent and immortal Huh7 clones

Affymetrix gene expression profiling of Huh7-derived clones was performed to analyze the differences between immortal, senescent and revertant (C3-Early, G12-Early) clones by our group (Ozturk M et al, unpublished results). Three copies of each cell clone were grown in a 175cm^2 flask and RNA was extracted separately from each using Promega SV RNA Isolation Kit. Hence, no RNA pooling was done and the data were processed in triplicates. The samples were treated extensively with DNAse and the qualities of the obtained RNA samples were assessed using Agilent 2100 Bioanalyzer and Agilent RNA 6000 Nano LapChip kit. RNA integrity was about 100%, indicating no significant RNA degradation. cDNAs and eventually cRNAs were synthesized from the RNA samples by employing One Cycle cDNA Synthesis Kit from Affymetrix. 5μg of cRNA from each clone was hybridized to Affymetrix HGU133Plus2 Chips for 16 hours, adding up to 18 chips in total. The signals were detected according to the manufacturer's protocol.

1.6.2 Analysis of genes differentially expressed between senescent and immortal clones

The signals received from the chips were automatically saved as `.CEL` files by Affymetrix Scanner. These files were accessed and processed by the statistical

computing and graphics software, “R,” which converts signal intensities obtained from chips into numeric expression values of genes. Background correction and normalization of expression data by “RMA” algorithm were performed using the open source bioinformatics software, “Bioconductor” on “R” software environment. The data was then subjected to t-test analysis (two-tailed, unpaired, unequal variance) where the p-value limit was set to 0.05. Hierarchical clustering of genes was performed by GenePattern software. Finally, significant gene lists were obtained which contained the names of the genes differentially expressed between revertant, senescent and immortal clones.

Affymetrix HGU133Plus2 chip used in this microarray analysis contained 54675 probes representing 47000 gene transcripts and variants corresponding to approximately 39000 human genes. The final Senescent vs. Immortal significant gene list contained 3073 genes represented by 3872 probes, the Revertant vs. Immortal significant gene list contained 2149 genes represented by 2552 probes and the Senescent vs. Revertant significant gene list contained 2023 genes represented by 2388 probes. In total, there were 8812 probes representing 7245 genes with significantly differential expression (Ozturk M et al, unpublished data).

1.6.3 Identification of DUSP10 and MTMR11 as senescence-associated genes

Given the importance of protein phosphatases in diseases and cancer (including HCC), generating a significant phosphatase gene list by comparison of significant gene lists with all known phosphatase genes were of great interest for further studies. Since the primary aim in analyzing differentially expressed genes between the Huh7-derived clones was to find therapeutically relevant novel genes important in “reversal” of immortality, the “Revertant” vs. Immortal gene list was of greatest importance. Other significant gene lists included genes also important in induction of senescence. Hence novel phosphatase genes in the Revertant vs. Immortal gene list were important the most, for our work. We initially aimed at finding phosphatase genes upregulated in immortal clones hinting at their possible oncogenicity in HCC. However, due to the fact that most upregulated genes were well-known and extensively studied, we turned to phosphatase genes downregulated in immortal clones compared to revertant and senescent ones demonstrating their possible tumor

suppressive activity in HCC. The significant phosphatase gene lists are shown in Table 1.2.

DUSP10 emerged as the most upregulated phosphatase gene in revertant clones compared to immortal ones with a fold change of 2.5 (1.3 fold in log2). Although this gene encodes a protein phosphatase that has been characterized in 1999 and has been studied thoroughly in immunology, it has not yet been studied in HCC. It is known to inactivate p38 and JNK MAPKs by dephosphorylation. Given the importance of MAPKs in hepatocarcinogenesis and the importance of p38 in mediating oxidative stress response and oncogene-induced senescence, DUSP10 (MKP-5) was of interest for our work. MTMR11 emerged as the most upregulated novel phosphatase gene in senescent clones compared to immortal ones with a fold change of 3.0 (1.6 fold in log2). This pseudophosphatase belongs to the myotubularin family of phosphatases and pseudophosphatases. Catalytically inactive phosphatases in this family are generally known to bind and regulate the active phosphatases. Upon these results, we chose DUSP10 and MTMR11 as our primary and secondary targets, respectively.

SENESCENT vs IMMORTAL		**REVERTANT vs IMMORTAL**		**SENESCENT vs REVERTANT**	
Phosphatase	**Fold Change**	**Phosphatase**	**Fold Change**	**Phosphatase**	**Fold Change**
CDC25C	-1.3	PTEN	-0.9	CDC25A	-1.233
PTEN	-1.1	PPM1A	-0.7	SSH1	-0.9
RNGTT	-0.8	PPP1CB	-0.7	CDC25B	-0.8
PPP3CB	-0.7	PTPN2	-0.7	CDC25C	-0.65
PTPN2	-0.7	TPTE	-0.6	PPP4C	-0.6
DUSP14	-0.4	CDC25C	-0.5	PTP4A2	-0.6
PPP2CA	-0.4	MTMR12	-0.4	PTPN1	-0.4
PTPMT1	0.2	DUSP1	0.3	PHPT1	-0.3
DUSP1	0.5	CTDSP2	0.4	SBF1	-0.3
SSH3	0.5	DUSP4	0.4	PPTC7	-0.2
PTPRE	0.6	PPP2CA	0.4	CDC14B	0.2
DUSP4	0.7	PTPLB	0.4	DUSP4	0.2
DUSP16	0.95	PTPRF	0.4	DUSP1	0.3
PTPN2	1.1	DUSP7	0.6	PTPRK	0.5
CDC14B	1.2	DUSP16	0.8	TPTE	0.6
DUSP10	**1.4**	CDC25A	0.9	PTPRM	0.7
MTMR11	**1.6**	**MTMR11**	**1.1**	PPM1B	0.8

		CDC14B	1.15		
		DUSP10	**1.3**		

Table 1.2: Differentially expressed phosphatases in significant lists: Fold changes are expressed in log2 base in this table. The protein phosphatases that were the foci of this study are shown in bold. The fold changes are in log2 base. This table was generated by Sevgi Bağışlar.

1.6.4 Cellular activities of DUSP10

Although it has been discovered in 1999 (Tanoue T et al, 1999; Theodosiou A et al, 1999), not much is known on DUSP10 and studies concentrate on its roles in prostate cancer and in immunology.

Vitamin D is implicated in prevention of prostate cancer. A cDNA microarray study has been done in an effort to understand the basis of antitumor effects of Vitamin D in prostate cancer. In this study it has been found that 1,25-dihydroxyvitamin-D3 (1,25D) form of Vitamin D causes an early, significant upregulation of DUSP10 (Peehl DM et al, 2004). Further experiments have shown that upon 1,25D treatment in early prostate cancer (primary prostatic adenocarcinoma), DUSP10 is upregulated due to the presence of putative vitamin D response elements in its promoter. Upon upregulation, it dephosphorylates and inactivates p38 MAPK which normally causes production of proinflammatory cytokines such as interleukin-6 (IL-6). Since prostatic inflammation and IL-6 overexpression are key factors in formation of prostate cancer, DUSP10 acts as a tumor suppressor in early prostate cancer when overexpressed (Nonn L et al, 2006). Additional experiments have shown that curcumin, resveratrol and [6]-gingerol also upregulate DUSP10 in normal prostate cells (Nonn L et al, 2007).

DUSP10 has been studied mainly in immunology and it has been found to regulate production of inflammatory cytokines and antigen presentation, showing its importance in both innate and adaptive immunity. In macrophages, TLR ligands induce DUSP10 expression which inhibits JNK activity and thereby constrains the production of cytokines and may reduce costimulation of T cells. In T cells, DUSP10 is constitutively expressed and inhibits early JNK activation after TCR ligation. Increased JNK activity in the absence of DUSP10 results in reduced proliferation and increased AP-1-dependent production of T cell cytokines since AP-1 transcription

factor complexes are targets of JNK (see Lang R et al, 2006).

DUSP10 knockout mice are reported to only have immunological and haemotological phenotypes. These include increased number of activated T cells and enhanced APC priming in response to lipopolysaccharides (LPS) activation, decreased T cell proliferation in response to antigen, increased interferon-gamma, tumor necrosis factor, IL-2, IL-4 and IL-6 secretion, and decreased susceptibility to experimental autoimmune encephalomyelitis (EAE). These mice have also shown a fatal response to secondary viral challenge (Zhang Y et al, 2004).

1.6.5 Cellular activities of MTMR11

The only article on MTMR11 in NCBI Pubmed reports a common duplicated DNA sequence at 1q21.2 (includes MTMR11 gene according to Ensembl database) in acute lymphoblastic leukemia and Burkitt lymphoma (La Starza R et al, 2007), indicating a possible role of MTMR11 in these types of cancers.

CHAPTER 2. OBJECTIVES AND RATIONALE

Hepatocellular carcinoma is among the most lethal and prevalent cancers in the human population. Despite its significance, there are only limited therapeutic options against it (Farazi PA, DePinho RA, 2006). Therefore, it is of ultimate importance to discover new approaches that could open up the way to novel therapeutic applications. The finding of Öztürk N et al that immortal cancer cells can be reprogrammed into replicative-senescent progeny that have lost tumorigenic potential is crucial in this aspect (Öztürk N et al, 2006).

Following the work of Öztürk N et al, gene expression profiling was performed on immortal and senescent clones since the differences between the expression profiles of these two types of clones could point out genes that are important in the reversion of the immortal phenotype of cancer cells. Further analysis of these genes may be important for new therapeutical approaches aiming to stop proliferation of cancer cells, or at least slow down tumor progression. After gene expression profiling, a set of genes were identified as differentially expressed between immortal and senescent clones. Of this set of significant genes, we were interested in protein phosphatase genes. Regulation of protein phosphorylation cascades is known to be disrupted in cancer and other diseases. Partnered to protein kinases, protein phosphatases are crucial players in protein phosphorylation which acts like a molecular switch mechanism turning target protein activities on and off. This renders protein phosphatases important in disease formation and carcinogenesis. In this study, we decided to focus on two novel protein phosphatases DUSP10 and MTMR11, which are significantly upregulated in senescent clones compared to immortal ones. Although information on these genes was limited and their tumor suppressive potentials were not known well, chromosomal aberrations targeting the chromosome arm they reside in (1q) in HCC bestowed an importance on them (mentioned in the Results chapter). We aimed the analysis of these two genes and their products to reveal their connection to hepatocarcinogenesis and replicative senescence, mainly by RT-PCR analysis to identify new potential transcript variants (MTMR11) in HCC cell lines, and by subcellular localization experiments to find out regulatory mechanisms related to replicative senescence (DUSP10). We expected to find significant difference

between the amounts of different transcripts of MTMR11 gene in subtypes of HCC cell lines (isolated from well-differentiated tumors vs. poorly-differentiated tumors) and breast cancer cell lines (originating from basal, luminal and mesenchymal tissues), leading to a possible explanation that different transcript variants of this gene is important in hepatocarcinogenesis or formation of breast cancer. For DUSP10, we expected to find a difference in subcellular localization between young and aging normal cells, indicating an importance of DUSP10 in replicative senescence, and between the mentioned subtypes of HCC cell lines, indicating a possible importance of DUSP10 in hepatocarcinogenesis. The results are shown and discussed in the following chapters.

CHAPTER 3. MATERIALS AND METHODS

3.1 MATERIALS

3.1.1 Reagents

All laboratory chemicals were analytical grade from Sigma (St. Louis, MO, USA), Farmitalia Carlo Erba (Milano, Italy) and Merck (Schucdarf, Germany) with the following exceptions: Ethanol used for sterilization purposes was from Delta Kim Sanayi ve Ticaret A.S (Turkey). Commercial Bradford reagent, haematoxylin and nuclear fast red counterstains were also from Sigma. Kinase inhibitors JNK inhibitor V (AS601245) and Ro-31-8220 were obtained from Calbiochem. X-Gal was from Fermentas.

3.1.2 Enzymes and nucleic acids

Restriction endonucleases and T4 DNA ligase used for gene cloning were purchased from MBI Fermentas GmbH (Germany). Recombinant Taq DNA Polymerase and Pfu DNA Polymerase used for polymerase chain reaction (PCR) were also purchased from the same company. DNA molecular weight standard and ultrapure deoxyribonucleotides were again from MBI Fermentas GmbH. pEGFP-N2 (Clontech, Palo Alto, CA, USA), pcDNA3.1/myc-His B (Invitrogen, Carlsbad, CA, USA) and pGEMT-Easy (Promega, Madison, WI, USA) were commercially obtained.

3.1.3 Oligonucleotides

The oligonucleotides used in PCR were synthesized by İONTEK (Istanbul, Turkey). The sequencing reactions for verifications of DNA sequences were also conducted by this company.

3.1.4 Electrophoresis, photography and spectrophotometer

Electrophoresis grade agarose was obtained from Sigma Biosciences Chemical

Company Ltd. (St. Louis, MO, USA). Horizontal electrophoresis apparatuses were from Stratagene (Heidelberg, Germany) and E-C Apparatus Corporation (Florida, USA). The power supply Power-PAC300 and Power-PAC200 was from Bio Rad Laboratories (CA, USA). The Molecular Analyst software used in agarose gel profile visualizing was from BioRad Laboratories (CA, USA). Spectrophotometer used for protein concentration measurements was from Beckman. For DNA and RNA concentration measurements, NanoDrop from Thermo Scientific was employed.

3.1.5 Tissue culture reagents and cell lines

Dulbecco's modified Eagle's medium (DMEM), Rosswell Park Memorial Institute (RPMI) medium 1640, fetal calf serum, L-glutamine, penicillin/streptomycin solution, trypsin and Geneticin (G418 sulfate) were obtained from GIBCO (Invitrogen, Carlsbad, CA, USA). Tissue culture flasks, petri dishes, cell plates were purchased from Corning Life Sciences Incorporated (USA).

3.1.6 Antibodies and chemiluminescence

The antibodies used in immunoblotting and immunohistochemistry were obtained from different sources, and their working dilutions are given in Table 3.1. ECL Western Blotting detection kit was purchased from Amersham Pharmacia Biotech Ltd. (Buckinghamshire, UK).

Antibody	Working dilution		Source
	Western Blot	Immunostaining	
DUSP10 (goat polyclonal)	1:200	1:50 (IF), 1:100 (immunoperoxidase)	Abcam
Tubulin (mouse monoclonal)	1:1000	-	Calbiochem
Calnexin (mouse monoclonal)	-	No dilution	Home-made (AF18)
B-actin (rabbit polyclonal)	-	1:60 – 1:100	Santa Cruz Biotechnology
p-JNK (rabbit polyclonal)	1:100	-	Cell Signaling Technologies
JNK (rabbit polyclonal)	1:300	-	Cell Signaling Technologies
p-p38 (rabbit polyclonal)	1:100	-	Cell Signaling Technologies
p38 (rabbit polyclonal)	1:300	-	Cell Signaling Technologies
p-c-Jun (mouse monoclonal)	1:80	-	Santa Cruz
c-Jun (rabbit polyclonal)	1:150	-	Santa Cruz Biotechnology
Anti-goat-HRP	1:6000	1:1000 – 1:1500	Sigma
Anti-mouse-HRP	1:5000	-	Sigma
Anti-rabbit-HRP	1:5000	-	Sigma

Anti-goat Alexa Fluor 568	-	1:200 – 1:300	Invitrogen
Anti-mouse Alexa Fluor 488	-	1:400	Invitrogen
Anti-rabbit Alexa Fluor 488	-	1:200	Invitrogen

Table 3.1: Antibody dilution table.

3.2 SOLUTIONS AND MEDIA

3.2.1 General Solutions

50X Tris-acetic acid-EDTA (TAE): 2 M Tris-acetate, 50 mM EDTA pH 8.5. Diluted to 1X for working solution.

Ethidium bromide: 10 mg/ml in water (stock solution), 30 ng/ml (working solution).

6x Loading dye solutions: 10mM Tris.HCl (pH 7.6), 0.03% bromophenol blue or 0.03% xylene cyanol, 60% glycerol, 60mM EDTA (0.5M pH 8.0).

3.2.2 Microbiological media, reagents and antibiotics

Luria-Bertani medium (LB) *Per liter:* 10 g Bacto-tryptone, 5 g Bacto-yeast extract, 10 g NaCl. For LB agar plates, add 15 g/L Bacto-agar.

Ampicillin: 100 mg/ml solution in double-distilled water, sterilized by filtration and stored at -20°C (stock solution). Workingsolution was 100 µg/ml.

Kanamycin: 300 mg/ml solution in double-distilled water sterilized by filtration and stored at -20°C (stock solution). Working solution was 30 µg/ml.

0.1 M IPTG: 1.41 g IPTG in 50 ml double-distilled water, sterilized by filtration and stored at -20C.

SOB medium: *Per liter:* 20 g tryptone (2%), 5 g yeastextract (0.5%), 0.584 g NaCl (10 mM), 0.186 g KCl (2.5 mM), 2.465 g $MgSO_4$ and 2.03 g $MgCl_2$ (10 mM) are put, autoclaved to sterilize, stored at room temperature.

Transformation Buffer (TB): 10 mM PIPES, 15 mM $CaCl_2$, 250 mM KCl are added, pH adjusted to 6.7 with KOH, 55 mM $MnCl_2$ is added only after pH adjustment. Filter sterilized and stored at 4ºC.

Glycerol stock solution: 50% glycerol was mixed with 50% bacterial culture and stored at -80ºC.

3.2.3 Tissue culture solutions

DMEM / RPMI working medium: 10% FBS, 1% penicillin/streptomycin, 1% Non-Essential Amino Acid were added and stored at 4ºC.

10X Phosphate-buffered saline (PBS) *Per liter:* 80 g NaCl, 2 g KCl, 14.4 g Na2HPO4, 2.4 g KH2PO4, pH 7.4, diluted to 1X and autoclaved before use.

3.2.4 SDS (Sodium Deodecyl Sulfate)-PAGE (Polyacrylamide Gel Electrophoresis) solutions

30% Acrylamide mix (1:29) *Per 100 ml*: 29 g acrylamide, 1 g bisacrylamide in double-distilled water, filtered, degassed, and stored at 4°C (stock solution).

5X SDS gel-loading buffer: 3.8 ml double-distilled water, 1 ml of 0.5 M Tris-HCl, 0.8 ml glycerol, 1.6 ml of 10% SDS, 0.4 ml of 0.05% bromophenol-blue. Before use, β-mercaptoethanol was added to 5% to reach 1% when mixed with samples.

10X SDS-electrophoresis running buffer *Per liter*: 30.3 g Tris base, 144.0 g Glycine, 10.0 g SDS. Diluted to 1X for working solution. Stored up to 1 month at 4°C.

10% Ammonium persulfate (APS): 0.1 g/ml solution in double distilled water (prepared freshly).
1.5 M Tris-HCl, pH 8.8 54.45 g: Tris base (18.15 g/100 ml) ~150 ml distilled water Adjust to pH 8.8 with 1 N HCl. Completed to 300 ml with distilled water and stored at 4°C.

1 M Tris-HCl, pH 6.8 12.14 g: Tris base ~ 60 ml distilled water. Adjust to pH 6.8 with 1 N HCl. Completed to 100 ml with distilled water and store at 4° C.

3.2.5 Immunoblotting solutions

1X Towbin wet transfer buffer with 10% Methanol *Per liter*: 3.03 g Tris-base, 14.4 g Glycine, 100 ml methanol, completed to 1 liter with double distilled water. pH is not adjusted.

10X Tris-buffer saline (TBS) *Per liter:* 100 mM Tris-base, 1.5 M NaCl, pH 7, in double distilled water.

TBS-Tween (TBS-T): 0.2 % Tween-20 solution in TBS (prepared freshly).

Blocking solution 5% (w/v): Non-fat milk, 0.2 % Tween-20 in TBS (prepared freshly).

3.2.6 Immunofluorescence and immunoperoxidase solutions

DAPI (4', 6-diamidino-2-phenylindole): 0.1-1 μg/ml (working solution in distilled water).

Immunofluorescence blocking solution: 5% BSA (bovine serum albumin) in 1X PBS.

Immunoperoxidase blocking solution: 10% FBS (fetal bovine serum) in 1X PBS.

3.2.7 SABG assay solutions

SABG buffer: Final concentrations of 40mM citric acid/sodium phosphate buffer (pH 6.0), 5mM potassium ferrocyanide, 5mM potassium ferricyanide, 150mM NaCl, 2mM MgCl2, 1mg/ml X-Gal.

3.3 METHODS

3.3.1 General Methods

3.3.1.1 Preparation of competent cells

3.3.1.1.1. Supercompetent *E. Coli* preparation

This method is based on a report by Inoue *et al*. 1990 (Inoue H et al, Gene, 1990). An overnight 10-20 ml E. *coli* DH5α culture was used to inoculate autoclaved SOB medium to an OD_{600} of 0.2. Bacteria were grown at 20ºC to an OD_{600} of 0.5-0.6 with vigorous shaking at 200 rpm and cooled down on ice for 10 minutes. Cells were transferred to 50 ml falcon tubes and centrifuged at 2500xg for 10 minutes (Hettich Rottina 420R, fixed-angle rotor, pre-cooled to 4ºC). The pellet was resuspended in ice-cold transformation buffer (1/3 of initial culture volume) by gently swirling and kept on ice for 10 minutes. The suspension was then centrifuged at 2500xg for 10 minutes. The pellet was gently resuspended in ice-cold transformation buffer (1/12.5 of initial culture volume) containing 7% DMSO and incubated on ice for 10 minutes. Bacteria were put into 1.5-ml eppendorf tubes as 150µl aliquots. Tubes were immersed in liquid nitrogen to freeze rapidly and stored at –80ºC. Supercompetent bacteria were transformed by heat-shock method as described in 3.3.1.2.1.

3.3.1.1.2 Electrocompetent *E. Coli* preparation

An overnight 10-20 ml *E. coli* DH5α culture was used to inoculate autoclaved SOB medium to an OD_{600} of 0.2. Bacteria were grown at 20ºC to an OD_{600} of 0.5-0.6 with vigorous shaking at 200 rpm and cooled down on ice for 10 minutes. Cells were transferred to 50 ml falcon tubes and centrifuged at 2500xg for 10 minutes (Hettich Rottina 420R, fixed-angle rotor, pre-cooled to 4ºC). The pellet was resuspended in ice-cold autoclaved ddH_2O (1/1.25 of initial culture volume) by gently swirling and kept on ice for 10 minutes. The suspension was then centrifuged at 2500xg for 10 minutes. The pellet was gently resuspended in ice-cold 10% glycerol (1/12.5 of initial culture volume) and kept on ice for 10 minutes. At this stage, contents of different folcon tubes were joined. Cells were pelleted at 2500xg for 10 minutes and

resuspended in ice-cold 10% glycerol (1/500 of initial culture volume). The OD_{600} of bacteria at this stage was approximately 200-250. Bacteria were put into 1.5-ml eppendorf tubes as 50µl aliquots. Tubes were immersed in liquid nitrogen to freeze rapidly and stored at -80ºC. Electrocompetent bacteria were transformed by electroporation method as described in 3.3.1.2.2.

3.3.1.2 Transformation of *E .coli*

Transformation of plasmid DNA into *E. coli* was achieved by using heat-shock method and electroporation.

3.3.1.2.1 Transformation by heat-shock method

Competent cells from -80ºC stock were thawed on ice. Bacteria were transfered into transformation tubes. 100-200 ng of ligation product or empty plasmid was added onto supercompetent cells. Then cells were incubated on ice for 30 minutes. After heat-shock for 45 seconds at 42ºC, the tubes were put on ice and 800 µl LB was added. Following incubation for 1 hour at 37ºC with vigorous shaking, cells with ligation products were pelleted for 1 min at highest speed in a bench microfuge (Heraeus Instruments Biofuge Pico), about 850µl of supernatant was discarded and pellet was resuspended in the remaining supernatant. Cells were plated out on LB-agar with selective agent(s). 50µl of cells with empty plasmid were plated out without concentrating the pellet.

3.3.1.2.2 Electroporation of bacteria

Electrocompetent cells from –80ºC stock were thawed on ice. 100-200ng of ligation product or empty plasmid was put along wall of 0.2cm electroporator cuvette. Bacteria were pipetted onto the DNA drop. The cuvette was flicked to settle the mixture to the bottom of the cuvette. Any moisture outside the cuvette was dried off and the cuvette was immediately placed into the holder of the electroporator. The parameters used were: 25µFD (capacitance), 200Ω (sample resistance) and 1.8 kV (volts). The holder was slided into position and electric current was given to cells. Immediately upon hearing a high constant tone (which generally occurs when the time

constant is 3-4msec), 1 ml of LB was added onto cells and they were transfered into 1.5-ml eppendorf tubes. The tubes were incubated at 37ºC for 1 hour with vigorous shaking. The remainder of the protocol was identical to the heat-shock method depicted in 3.3.1.2.1.

3.3.1.3 Long term storage of bacterial strains

To keep bacterial cells including plasmid in it or as empty for future experiments and to have a stock of strain in a laboratory is necessary. The most frequently used method is "Glycerol-Stock" method. A single colony picked from either an agar plate or a loop-full of bacterial stock was inoculated into 5 ml LB (with a selective agent if necessary) in 15 ml screw capped tubes. Tubes were incubated overnight at 37ºC and at 200 rpm. For glycerol stock, 500µl of saturated culture was added into 500µl of 50% glycerol v/v (1ml autoclaved 100% glycerol, 1ml ddH_2O). This mix was frozen and stored at -80ºC.

3.3.1.4 Purification of DNA

3.3.1.4.1 Purification of plasmid DNA using MN (Macherey-Nagel) miniprep kit

This method was preferred for isolation of plasmids in order to use in sequencing or cloning procedures. 5 ml of saturated culture was used for isolation of plasmid DNA by using "MN miniprep plasmid DNA purification kit" following manufacture's instructions.

3.3.1.4.2 Large-scale plasmid DNA purification

This method was used for isolation of plasmids in order to use in sequencing or mammalian cell transfection procedures by using "Qiagen large-scale plasmid DNA purification kit" and "Promega PureYield plasmid midiprep purification kit" following manufactures' instructions.

3.3.1.5 Quantification and qualification of nucleic acids

Quantification of DNA and RNA was done by NanoDrop ND-1000 Full-spectrum UV/Vis Spectrophotometer (Thermo Fisher Scientific, Wilmington, DE, USA). Calculation of the division of OD_{260} and OD_{280} gave information about possible contaminants and was used to assess quality of nucleic acids.

3.3.1.6 Restriction enzyme digestion of DNA

Restriction enzyme digestions were routinely performed in 20 µl reaction volumes and typically 0.5-5 µg DNA was used. Reactions were carried out with the appropriate reaction buffer and conditions according to the manufacturer's recommendations.

Digestion of DNA with two different restriction enzymes was performed in the same reaction buffer to provide the optimal condition for both restriction enzymes. If no single reaction buffer could be found to satisfy the buffer requirements of both enzymes, the reactions were carried out sequentially.

3.3.1.7 Gel electrophoresis of nucleic acids

DNA fragments were fractionated by horizontal electrophoresis by using standard buffers and solutions. DNA fragments less than 1 kb were generally separated on 2% agarose gel, those greater than 1 kb were separated on 1% agarose gels. Agarose gels were completely dissolved in 1x TAE electrophoresis buffer to required percentage in microwave and ethidium bromide was added to final concentration of 30 µg/ml. The DNA samples were mixed with 6x loading dye (bromophenol blue and/or xylene cyanol) and loaded onto gels. The gel was run in 1x TAE at different voltage and time depending on the size of the fragments at room temperature.

3.3.2 Computer analyses

Primers were designed by using the web software provided by Steve Rozen and Whitehead Institute for Biomedical Research at http://frodo.wi.mit.edu/cgi-bin/primer3/primer3_www.cgi. DUSP10 gene, mRNA and protein information were

obtained from National Center for Biotechnology Information website (NCBI; http://www.ncbi.nlm.nih.gov). SWISSPROT and TrEMBL databases listed under ExPASy Proteomics Server were used for bioinformatics analyses of protein domains and motifs (http://www.expasy.ch/sprot). Oncomine Research Platform (http://www.oncomine.org) was used to obtain microarray data on DUSP10. Also Oncogenomic Database of Hepatocellular Carcinoma was employed for obtaining information related to DUSP10 in hepatocellular carcinoma (http://oncodb.hcc.ibms.sinica.edu.tw/index.htm). Alignments of nucleic acid or protein sequence were performed by using NCBI BLAST at http://www.ncbi.nlm.nih.gov/BLAST. Multiple sequence alignments for were done by ClustalW2 online program at http://www.ebi.ac.uk/Tools/clustalw2/index.html.

3.3.3 Vector construction

pEGFP-DUSP10 vector was generated by cloning the coding sequence of human DUSP10 transcript variant 1 mRNA (cut with BamHI and HindIII) into BglII/HindIII digested pEGFP-N2 vector. pcDNA3.1-DUSP10 vector was generated by cloning the coding sequence of human DUSP10 transcript variant 1 mRNA (cut with KpnI and BamHI) into KpnI/BamHI digested pcDNA3.1/myc-His B vector. As an intermediate step to enrich DUSP10 transcript variant 1 coding region, TA cloning was done with pGEMT-Easy vector system according to the kit's specifications (Promega, Madison, WI, USA) and a bacterial cloning construct was obtained (pGEMT-DUSP10). All plasmids were verified by sequencing.

3.3.4 Tissue culture techniques

3.3.4.1 Cell lines

15 HCC derived cell lines (Huh7, Hep40, HepG2, Hep3B, Hep3B-TR [TGF-β-resistant], PLC, Snu182, Snu387, Snu398, Snu423, Snu449, Snu475, Mahlavu, Focus and SK-Hep1) were used in this study and cultured as described previously (Cagatay T, Ozturk M, Oncogene, 2002). 8 breast cancer derived cell lines (BT-20, HCC1937, MCF-7, BT-474, CAMA1, T47D, MDA-MB-453 and MDA-MB-231) were also used and were cultivated in DMEM with 10% FBS. For experiments where a specific

number of cells were to be seeded, cell counting was performed by a haemocytometer after trypsinization and resuspension of cells in culture medium.

3.3.4.2 Thawing cell lines

One vial of the frozen cell line from the liquid nitrogen tank was taken and immediately put into ice. The vial was left 1 minute on the bench to allow excess nitrogen to evaporate and then placed into 37ºC water bath until the external part of the cell solution was thawed (takes approximately 1-2 minutes). The cells were resuspended gently using a pipette and transferred immediately into a 15 ml sterile tube containing 10 ml cold fresh medium. The cells were centrifuged at 1200 rpm for 3 minutes (Beckman GS-15R centrifuge, fixed angle rotor; all cell culture centrifugations were done with the centrifuge unless written otherwise). Supernatant was discarded and the pellet was resuspended in 37ºC culture medium to be plated into 25cm^2 or 75cm^2 flasks. After overnight incubation in a humidified incubator at 37°C supplied with 5% CO_2, culture mediums were replenished.

3.3.4.3 Growth conditions of cells

Dulbecco's modified Eagle's medium (DMEM) or RPMI 1640 supplemented 10% FCS and penicillin and streptomycin (50 mg/ml), and 1% NEAA was used to culture the HCC cell lines. The cells were incubated in at 37°C in an incubator with an atmosphere of 5% CO2 in air. The cells were passaged before reaching confluence. The growth medium was aspirated and the cells were washed once with calcium and phosphate-free PBS. Trypsin was added to the flask to remove the monolayer cells from the surface. The fresh medium was added and the suspension was pipetted gently to disperse the cells. The cells were transferred to either fresh petri dishes or fresh flasks using different dilutions (from 1:2 to 1:10) depending on requirements. All media and solutions used for culture were kept at 4°C (except stock solutions) and warmed to 37°C before use.

3.3.4.4 Cryopreservation of cell lines

Exponentially growing cells were harvested by trypsinization and neutralized with

growth medium. The cells were counted and precipitated at 1500 rpm for 5 min at 4ºC. The pellet was suspended in a freezing solution (10% DMSO, 20% FCS and 70% DMEM for adherent cells; at a concentration of $4x10^6$ cells/ml. 1 ml of this solution was placed into 1 ml screw capped-cryotubes. The tubes were left at -80°C overnight. The next day, the tubes were transferred into the liquid nitrogen storage tank.

3.3.5 Extraction of total RNA from tissue culture cells and tissue samples

Total RNAs were isolated from cultured cells using the NucleoSpin RNA II Kit (MN Macherey-Nagel, Duren, Germany) according to the manufacturer's protocol.

3.3.6 First strand cDNA synthesis

First strand cDNA synthesis from total RNA was performed using RevertAid First Strand cDNA synthesis kit (MBI Fermantas, Germany). The RevertAid kit relies on genetically engineered version of Moloney Murine Leukemia Virus reverse transcriptase (RevertAid M-MuLV RT) with low RNase H activity. This allows the synthesis of full-length cDNA from long templates. The first strand reactions were primed with oligo(dT)18 primer to specifically amplified mRNA population with 3'-poly(A) tails. As the reaction conditions and components of this kit and those of conventional PCR are compatible, first strand synthesized with this system can be used as a template for PCR. 1 to 5 µg total RNA was used to synthesize the first stand cDNA following the manufacturer's instruction. After 1:1 dilution of total reaction products in DEPC-treated water, 2 µl of diluted first strand cDNA was used for PCR.

3.3.7 Primer design for expression analysis by semi-quantitative PCR

The primer pairs that have been used in expression profile analyses were designed carefully. Forward and reverse primer were positioned on different exons of the gene of interest, so that the primer pair would either produce a longer amplicon than expected (from genomic DNA, if there was genomic DNA contamination in total RNA) or only produce the expected amplicon in a PCR reaction. The other important parameteres in primer design were length of expected amplicon (100-200bp), a GC content of about 50%, no hairpin formation, and very low energies of interactions

between 3' ends of primers and primer pairs. Primers used for expression analysis have been designed strictly considering these criteria, and listed in Table 3.2.

Primer name	Sequence	Tm (ºC)	Number of cycles
DUSP10 transcript variant 1	F: TGCGAGTCCATAGCTGAAGA R: CAGGAGGGTGGCTGTTACTG	62	30
DUSP10 transcript variant 2	F: TTGGAAGATGCTCTGGTGGT R: TGACGTAGCCGATGTTCAGC	61	30
DUSP10 transcript variant 3	F: ATTTATGAAGTGGACTTAGT R: TGACGTAGCCGATGTTCAGC	58	30
DUSP10 isoform a cloning Bam/Hind	F: TATGCAGGATCCATGCCTCCGTCTCCTTTAG R: CCAGTAAAGCTTTCACACAACCGTCTCCACG	61	35
DUSP10 isoform a cloning Kpn/Bam	F: CAGCAAGGTACCATGCCTCCGTCTCCTTTAGAC R: CTATAAGGATCC(GCT)CACAACCGTCTCCACGCCCAT	61	35
DUSP10 isoform b cloning Bam/EcoRV	F: AAGCTTGGATCCAATGCAGCGGCTGAACATC R: GAATTCGATATC(GCT)CACACAACCGTCTCCAC	61	35
GAPDH	F: GGCTGAGAACGGGAAGCTTGTCAT R: CAGCCTTCTCCATGGTGGTGAAGA	60	19
T7 for sequencing	Available from İONTEK	60	-
SP6 for sequencing	Available from İONTEK	60	-
BGH for sequencing	Available from IONTEK	60	-
pEGFP-N2 sequencing	F: CGTGTACGGTGGGAGGTCTA R: GCTGAACTTGTGGCCGTTTA	62	-
MTMR11	F: GGGCATTCAGATGTTGTCCT R: CTGACATAGTCCAGCCATCG	60	30
MTMR11 cloning Kpn/Bam	F: ATTATAGGTACCATGCCTCCCAGGGTCACCTT R: GCGTGCGGATCC(TTA)CATCTGGTTATCCAGA	60	35
MTMR11 intron spanning	F: AGCTTGCCCTTTACCTCCAG R: GCCATCTTGTTGGGACTGAT	60	30

Table 3.2: Primer list for PCR and sequencing reactions: Considering the primers for cloning, stop codons are put inside parantheses in cases when reverse primers both with and without stop codon were synthesized.

3.3.8 Fidelity and DNA contamination control in first strand cDNAs

The fidelity and genomic DNA contamination of first strand cDNAs were checked before performing expression analyses. 2µl of diluted first strand cDNA was used for PCR amplification of the *glyceraldehyde-3-phosphate dehydrogenase (GAPDH)* transcript. *GAPDH* primer pair for this analysis was designed to produce a 151 bp fragment from cDNA and 250 bp fragment from genomic DNA.

3.3.9 Expression analysis of a gene by semi-quantitative PCR and GAPDH normalization

Equal volume (2µl) of all first strand cDNA samples was used for PCR amplification of *GAPDH* transcript using the pre-determined optimal cycle number for GAPDH. Then an equal volume of each sample was loaded onto agarose gel and intensity of each band was analyzed by BIO-1D software. After intensities were determined, intensity of sample with the highest densitometric reading and 2 µl loading volume were used as reference points for normalization of input loading volume of other samples for expression analysis of both *GAPDH* and gene of interest by PCR amplification. Amplification products were analyzed in computer.

3.3.10 Crude total protein extraction

Adherent monolayer cells were grown to 70% confluency in complete growth medium. After removal of growth medium, cells were washed twice with PBS to remove any serum residue. Cells were trypsinized and pelleted at 1200 rpm for 5 min (Beckman GS-15R centrifuge, swinging bucket rotor). Cell pellets were resuspended in NP40 lysis buffer (150 mM NaCl, 50 mM Tris-HCl pH 8.0, 0.5% sodium deoxycholate, 1 % NP-40, and 1X Complete Protein Inhibitor mix (Roche)) for total protein extraction. Complete lysis was achieved by pipetting of crude cell lysates several times and by incubating the lysates on ice for 30 min, and then centrifuging at 11000xg for 30 minutes at 4ºC. Total cell protein was collected as supernatant.

For studies with phosphoproteins, the lysis buffer employed contained the following: 10mM Tris.HCl (pH 7.6), 5mM EDTA, 50mM NaCl, 1% Triton X-100, 1X complete protein inhibitor mix and the phosphatase inhibitors 30mM Na-pyrophosphate, 50mM NaF and 100µM $NaVO_3$. Everything else was the same as the lysis procedure with NP40 buffer.

3.3.11 Western blotting

The conventional Bradford protein assay was employed to quantify the protein amounts in the lysates obtained. In this assay, known concentrations of bovine serum

albumin (BSA) are used to form a colored reaction with the brown Bradford reagent, for generation of a standard curve of OD_{595} vs. protein concentration. Blue color formation was measured at 595nm.

After protein quantification, protein lysates were aliquoted into fresh tubes and, stored at -80°C. 10% resolving gel and 5% stacking gel was used in SDS-PAGE analysis of protein lysates. EC-120 (E-C Apparatus Corp., Holbrook, NY, USA) and ProteanII-xi (BioRad) vertical gel system was set up according to manufacturer's instructions. The standard SDS-electrophoresis buffer system was used. Equal amounts of cell lysates were solubilized in 1X SDS gel-loading buffer, denatured at 100°C for 5 min and incubated on ice for 1 min. After a quick spin, samples were loaded onto SDS-polyacrylamide gel. After electrophoresis at 80 V for 20 minutes followed by 120 V for 1-2 hours, proteins were transferred onto PVDF western blotting membrane (Roche) by Transblot - Wet transfer electroblotting apparatus (BioRad) according to the manufacturer's instructions.

NuPAGE NOVEX pre-cast gel system from Invitrogen was also employed from time-to-time for running a denaturing protein gel and transferring proteins onto a PVDF membrane, according to the manufacturer's protocol. The gels employed were either 4-12% or 10% Bis-Tris gels, and the running buffer employed was MOPS buffer. The transfer buffer employed contained 10% methanol, in accordance with the manufacturer's protocol.

The resulting membrane was treated for an hour in blocking solution at room temperature and probed with primary antibody either for an hour at room temperature or overnight at 4°C. After washing 4 times for (5 min, 15 min, 5 min, 5 min) in TBS-T solution at room temperature, the membrane was incubated with appropriate HRP conjugated secondary antibody for 1 hr. The membrane was washed 4 times for (5 min, 15 min, 5 min, 5 min) in TBS-T solution at room temperature. After final wash, the blot was exposed to ECL western blot detection kit (Amersham) according to manufacturer's instructions. The chemiluminescence emitted was captured on X-ray film within 3 sec-1 min (for proteins of high amount in cells, such as α-tubulin) to 2-10 min (for proteins of low amount in cells, such as phosphorylated proteins) exposure times.

3.3.12 SABG assay

SABG activity was detected by using a described protocol (Dimri GP. et al., 1995). After Nuclear Fast Red counterstaining, SABG positive and negative cells were identified and counted.

3.3.13 Immunostaining

3.3.13.1 Immunofluorescence of cell culture monolayers

Cells were seeded onto coverslips in 6-well or 12-well plates. For experiments with inhibitors JNK inhibitor V, Ro-31-8220 (inhibits MKP-1), SB202190, SB203580 and SKF86002 (inhibit p38), cells were left to attach for 24 hours at 37ºC with 5% CO_2 and inhibitor was given. Control cells were not treated. Cells were left at 37ºC with 5% CO_2 for 48-72 hours before immunostaining. For experiments without inhibitors, cells were left overnight at 37ºC with 5% CO_2 after seeding before immunostaining.

On the day of immunostaining, cells were washed with PBS twice and fixed with 3% paraformaldehyde in dark at room temperature for 15 minutes. After fixation, cells were washed with PBS once and permeabilized with 0.3% Triton X-100 in PBS for 10 minutes at room temperature. After permeabilization, cells were washed with 150mM Glycine in PBS for three times with one-minute intervals. Blocking was done by incubating cells in 2% BSA in PBS for 1 hour at room temperature. Cells were washed with PBS-T (0.1% Triton X-100 in PBS) once, before the primary antibody (targeting the protein of interest; diluted in blocking solution) was put onto each coverslip. Only blocking solution was put onto negative control wells of immunostaining. After incubation of 2 hours at room temperature or overnight incubation at 4ºC, cells were washed with PBS-T three times with one-minute intervals. Secondary antibody (conjugated to a fluorochrome, targeting the primary antibody) in blocking solution was put onto each coverslip, including negative control wells. Cells were incubated in dark at room temperature for 1 hour and washed with PBS-T three times with one-minute intervals. Nuclear dye DAPI (diluted 1:10000-20000 in ddH_2O) was put into each well and cells were counterstained for 30 seconds. DAPI was aspirated and cells were washed with ddH_2O four times. Coverslips were

taken out of the wells and left to air-dry for a few minutes. Meanwhile slides were prepared and a drop of anti-fading reagent was put on each slide. Coverslips were placed on slides and the edges were sealed with nail polish. Slides were observed under Zeiss Axio Imager.A1 or Zeiss LSM 510 (laser scanning confocal microscope), and stored at 4ºC in dark.

3.3.13.2 Immunoperoxidase of cell culture monolayers

Seeding and inhibitor treatment of cells were same as of immunofluorescence protocol. On the day of immunostaining, cells were washed with PBS twice and fixed with ice-cold methanol for 5 minutes or 3% formaldehyde solution for 15 minutes at room temperature. Ice-cold methanol also permeabilizes cells, hence no additional permeabilization was done when using this fixative. After fixation with formaldehyde however, 10-minute permeabilization with 0.3% Triton X-100 in PBS was done at room temperature. After fixation (and permeabilization if required), cells were washed with PBS twice and blocked with 10% FCS in PBS for 1 hour at room temperature. After washing with PBS-T (0.1% Triton X-100 in PBS) once, cells were incubated with primary antibody in blocking solution for 1 hour at room temperature or overnight at 4ºC. Only blocking solution was put onto negative control wells of immunostaining. Cells were washed with PBS-T three times with one-minute intervals and secondary antibody (conjugated to horse-radish peroxidase) were put onto coverslips, including negative control wells. After an incubation of 1 hour at room temperature, cells were washed with PBS-T three times. DAB staining solution was prepared during the last washing step and put on each coverslip upon aspiration of PBS-T. Brown staining was checked for under light microscope and color reaction was stopped by putting ddH_2O to wells. Wells were further washed with ddH_2O for three times. Haematoxylin was used for counterstaining of the nuclei. Cells were stained with haematoxylin for 10-20 seconds and washed with ddH_2O for four times. Coverslips were taken out of the wells and left to air-dry for a few minutes. Meanwhile slides were prepared and a drop of 90% glycerol was put on each slide. Coverslips were placed on slides and the edges were sealed with nail polish. Slides were observed under light microscope and stored at 4ºC in dark.

CHAPTER 4. RESULTS

4.1 DUSP10 (MKP-5)

4.1.1 Bioinformatics analysis of DUSP10

4.1.1.1 Sequence and gene information

DUSP10 stands for “dual specificity phosphatase 10”. Another alias is MKP-5 which stands for “mitogen-activated protein kinase phosphatase 5”. The NCBI Gene ID for DUSP10 is 11221. The locus in which DUSP10 gene resides is named as NC_000001 (version 10) and it corresponds to a 249250621 bp linear DNA sequence. It has been mapped to the minus strand of the q arm of human chromosome 1; its exact location is 1q41 (Fig.4.1.1). Regional loss of heterozygosity is seen in this area in HCC (Jou YS et al, 2004). However contradictory results come from studies aimed at uncovering the common genomic alterations in HCC, reporting gain of 1q in 50% of HCC samples analyzed and concluding that the genes located on this chromosomal arm may be important in early stages of hepatocarcinogenesis (Tornillo L et al, 2002).

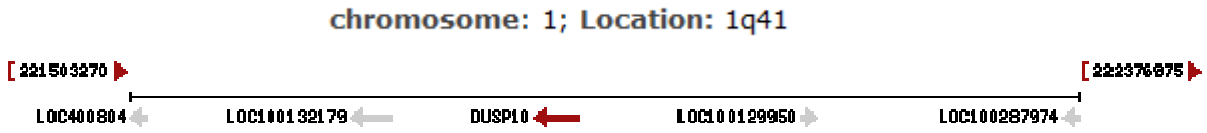

Fig.4.1.1: Genomic context of DUSP10 gene obtained from NCBI Gene.

The gene has three transcripts, coding for two protein isoforms **a** and **b**, **a** being the dominant one. Transcript variant 1 of 2619 nucleotides (NM_007207.3) codes for isoform **a** of 482 aminoacids (NP_009138.1) and has four exons. Transcript variants 2 and 3 of 2244 nucleotides and 1765 nucleotides (NM_144728.1 and NM_144729.1, respectively) code for isoform **b** of 140 aminoacids (can be accessed both by NP_653329.1 and NP_653330.1) and have three exons each. Transcript variant 2 has a unique untranslated exon that the other variants lack (Fig.4.2). Transcript variants 1 and 3 only differ in that variant 1 has an extra coding exon (Fig.4.2). The translated region of transcript variant 1 is 1449 basepairs (bp) long whereas translated regions of transcript variant 2 and 3 are 423 bp long.

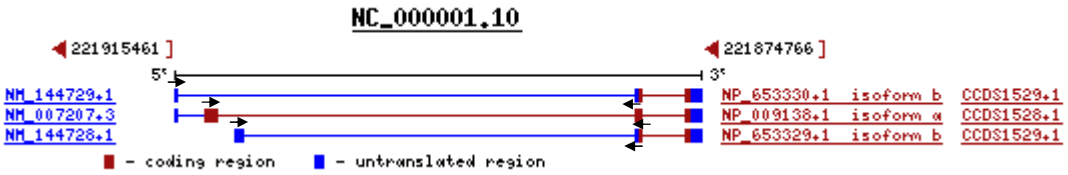

Fig.4.1.2: Locus, transcripts and protein isoforms of DUSP10 obtained from NCBI Gene: RT-PCR primers designed for different DUSP10 transcript variants are also depicted on the figure (black arrows): Second exon (forward primer) of T.V. 1 (which is specific to this variant) and third exon (reverse primer) were employed for T.V. 1-specific (shown in the middle) primer pair design. First exon (forward primer) of T.V. 2 (which is specific to this variant) and first-second exon boundary (reverse primer) were employed for T.V. 2-specific (shown in the bottom of the figure) primer pair design. First exon (forward primer) and first-second exon boundary (reverse primer) were employed for T.V. 3-specific (uppermost in the figure) primer pair design.

Additionally, 188 SNPs (single nucleotide polymorphisms) have been reported in GeneCards database so far for DUSP10 gene (Rebhan M et al, 1998). Most SNPs are intronic or located in the untranslated regions. There are three synonymous and there aren't any non-synonymous SNPs located in this gene.

4.1.1.2 Protein information

4.1.1.2.1 General information

DUSP10 isoform **a** is represented in SWISS-PROT Database by Q9Y6W6-1 symbol and it consists of 482 aminoacids, corresponding to a molecular weight of 52642 Daltons and a theoretical isoelectric point (pI) of 7.87. DUSP10 isoform **b** is represented by Q9Y6W6-2 symbol and it consists of 140 aminoacids, corresponding to a molecular weight of 16110 Daltons and a theoretical pI of 8.89.

The two protein isoforms differ at N-terminus and are identical at C-terminus. Hence the only difference between them is the extra 342 aminoacids in DUSP10 isoform **a**. DUSP10 belongs to a subfamily of phosphatases named as MAPK phosphatases which are dual specificity phosphatases that can dephosphorylate both serine-threonine and tyrosine residues on MAPKs, inactivating them. It is also highly conserved among the species that encode it (human, mouse, rat, cow, dog, chimpanzee and chicken).

4.1.1.2.2 Protein domains and motifs

DUSP10 is known to be a dual specificity phosphatase and thus contains such a catalytic domain according to Motif Scan search (Fig.4.1.3a and b). Isoform a also contains a catalytically inactive rhodanese domain which is thought to determine substrate specificity by binding the substrate and activating the C-terminal catalytic domain by inducing a conformational change. According to NCBI Conserved Domains search, putative substrate binding residues are found within this domain (Fig.4.1.4). SWISS-PROT database classifies DUSP10 as a "phosphoprotein," according to an article in which phosphoproteome of the human mitotic spindle has been analyzed by mass spectrometry. In this study, phosphorylation of DUSP10 isoform a at serine-4 has been observed (Nousiainen M et al, 2006). Interestingly, according to Motif Scan search, a possible casein kinase II phosphorylation site contains this residue. The "possible" sites given by Motif Scan search are weak matches as they are motifs that are frequently found in other proteins and may not be specific to DUSP10. However the information that Ser-4 is phosphorylated strengthens the possibility of casein kinase II phosphorylation at this residue. The Java-based online software GPS (Group-based prediction system) 2.1 from CUCKOO Workgroup predicts phosphorylation by many kinases at this residue, especially by CMGC (containing CDK, MAPK, GSK3, CLK families) kinase family (Xue Y et al, 2008).

Dual specificity phosphatase active site signature motif is [I/V]HCXAGXSR[S/T]X-TXXXAY[I/L]M, where X is any amino acid. This motif is IHCQAGVSRSA-TIVIAYLM for DUSP10. This is like an extended tyrosine phosphatase signature motif and the dash separates this motif and its extension.

Although the possible N-myristoylation sites infer a membrane-associated localization for DUSP10, its localization has been determined as "cytoplasm and nucleus" by different studies (Tanoue T et al, 1999; Theodosiou A et al, 1999).

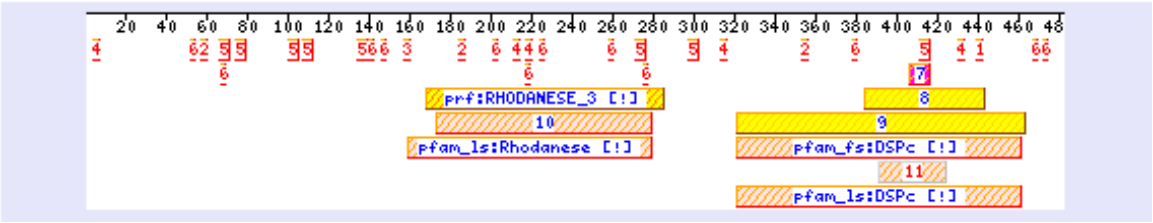

Fig.4.1.3a: Motif Scan results of DUSP10 isoform a: 1. Possible amidation site: Position 439-442, **2.** Possible N-glycosylation sites: Positions 57-60, 184-187, 353-356, **3.** Possible cAMP- and cGMP-dependent protein kinase phosphorylation site: Position 157-160, **4.** Possible casein kinase II phosphorylation sites: Positions 4-7, 211-214, 217-220, 313-316, 430-433, **5.** Possible N-myristoylation sites: Positions 66-71, 74-79, 100-105, 107-112, 134-139, 271-276, 297-302, 411-416, **6.** Possible protein kinase C phosphorylation sites: Positions 52-54, 67-69, 140-142, 146-148, 201-203, 217-219, 224-226, 258-260, 275-277, 378-380, 467-469, 472-474, **7.** Tyrosine phosphatase active site according to Prosite patterns: Position 406-416, **8.** Tyrosine phosphatase catalytic domain according to Prosite profiles: Position 384-443, **9.** Dual specificity phosphatase catalytic domain according to Prosite profiles: Position 321-463, **10.** Rhodanese homology domain according to pfam_fs: Position 173-279, **11.** Tyrosine phosphatase according to pfam_fs: Position 391-424. The number next to each site or domain indicates its position on the protein in terms of amino acid numbers. There are also un-numbered sites as can be seen on the figure: Rhodanese (rhodanese homology domain) and DSPc (dual specificity phosphatase catalytic domain).

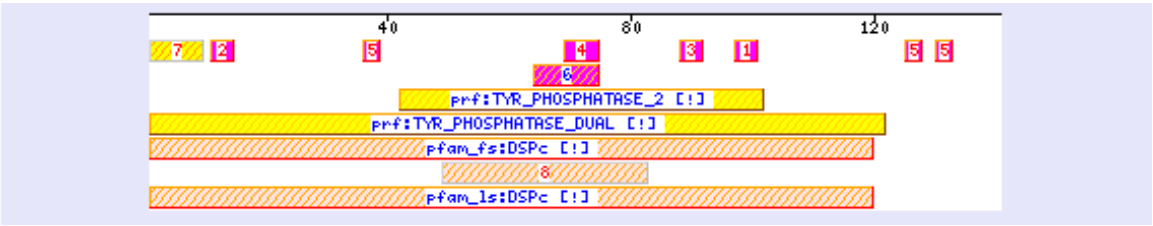

Fig.4.1.3b: Motif Scan results of DUSP10 isoform b: 1. Possible amidation site: Position 97-100, **2.** Possible N-glycosylation site: Position 11-14, **3.** Possible casein kinase II phosphorylation site: Position 88-91, **4.** Possible N-myristoylation site: Position 69-74, **5.** Possible protein kinase C phosphorylation sites: Positions 36-38, 125-127, 130-132, **6.** Tyrosine phosphatase active site according to Prosite patterns: Position 64-74, **7.** Big-1 (bacterial Ig-like domain 1) domain: Position 1-9, **8.** Tyrosine phosphatase according to pfam_fs: Position 49-82. The number next to each site or domain in the legend indicates its position on the protein in terms of amino acid numbers. There are also un-numbered sites as can be seen on the figure: DSPc (dual specificity phosphatase catalytic domain), TYR_PHOSPHATASE_2 (tyrosine phosphatase catalytic domain) and TYR_PHOSPHATASE_DUAL (dual specificity phosphatase catalytic domain).

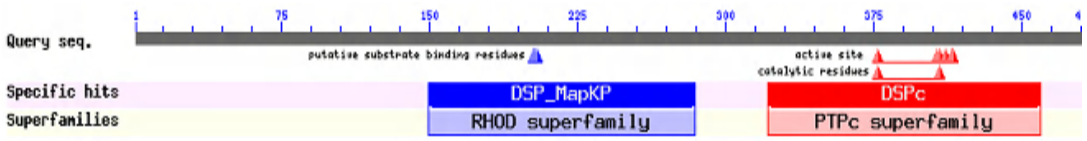

Fig.4.1.4: NCBI Conserved Domain result for DUSP10 isoform a: Putative substrate binding residues are marked with blue triangles. Active site and catalytic residues are marked with red triangles. RHOD: Rhodanese homology domain, DSPc: Dual specificity phosphatase catalytic domain.

4.1.1.2.3 Protein structure

Secondary-structure information on DUSP10 isoforms was obtained by querying at NPS (Network Protein Sequence Analysis) database using PHD (Rost B, Sander C, 1994), DSC (King RD, Stenberg MJ, 1996) and MLRC on GOR4, SIMPA96 and SOPMA (Guermeur Y et al, 1999) prediction methods. According to this, DUSP10 isoform a contains 22.2% alpha helices, 17.84% extended strands and 59.54% random coils (Fig.4.1.5a), and, DUSP10 isoform b contains 40% alpha helices, 14.29% extended strands and 45.71% random coils (Fig.4.1.5b).

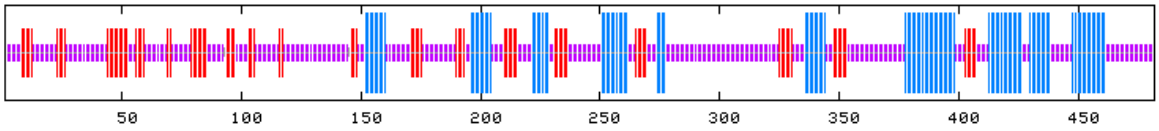

Fig.4.1.5a: NPS consensus secondary structure prediction for DUSP10 isoform a: Red parts mark the extended strands, blue parts mark the alpha helices, and purple parts mark the random coils. Alpha helices are associated with functional domains. In addition to the above figure, SWISS-PROT database predicts a turn at position 277-279.

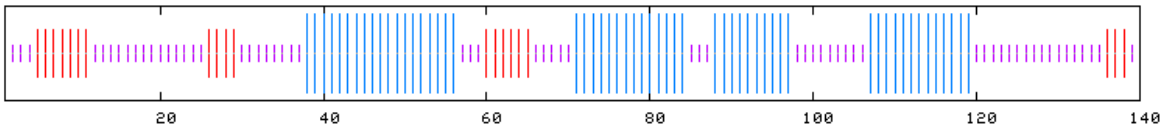

Fig.4.1.5b: NPS consensus secondary structure prediction for DUSP10 isoform b: Red parts mark the extended strands, blue parts mark the alpha helices, and purple parts mark the random coils. Alpha helices are associated with the functional domain.

In one study, tertiary structures of MAPK binding domain (also known as rhodanese domain; PDB ID: 2OUC) and catalytic domain (PDB ID: 2OUD) of DUSP10 have been determined by X-Ray diffraction (Tao X, Tong L, 2007). These are shown in Fig.4.1.6a and b, respectively.

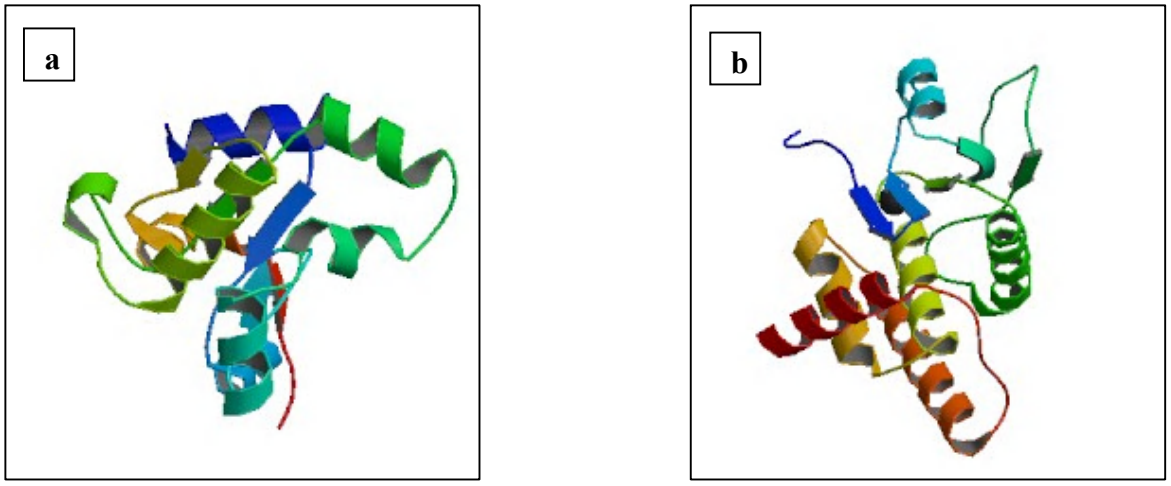

Fig.4.1.6: a. 3D structure of DUSP10 rhodanese domain, b. 3D structure of DUSP10 catalytic domain.

4.1.1.3 Gene homologs and protein sequence conservation

4.1.1.3.1 Orthologs of DUSP10

According to HomoloGene Database of NCBI, orthologs of DUSP10 exist in seven other species. This database only gives results for isoform a. These species, and the extent of identity between their DUSP10 genes/proteins and *Homo sapiens* DUSP10 gene/protein is listed in Table 4.1.1.

Gene		Identity (%)	
Species	Symbol	Protein	DNA
Homo sapiens	**DUSP10**		
vs. Pan troglodytes	DUSP10	99.8	99.7
vs. Canis lupus familiaris	DUSP10	96.3	94.3
vs. Bos taurus	DUSP10	94.8	94.7
vs. Mus musculus	Dusp10	96.7	92.3
vs. Rattus norvegicus	Dusp10	95.9	91.2
vs. Gallus gallus	DUSP10	89.5	83.8
vs. Danio rerio	LOC100007304	60.7	59.8

Table 4.1.1: Orthologs of human DUSP10 and multiple alignment pair-wise similarity scores between DUSP10 protein and DNA sequences of different species.

The multiple sequence alignment of the protein sequences of these orthologs were generated using ClustalW2 (Thompson JD et al, 1997). Fig.4.1.7 shows the conserved

residues among different species. The sequences aligned from top to bottom belong to Homo sapiens (human), Pan troglodytes (chimpanzee), Mus musculus (mouse), Rattus norvegicus (rat), Bos taurus (cow), Canis lupus familiaris (dog) and Gallus gallus (chicken), respectively. When Danio rerio is not considered the extent of conservation among the remaining species is clearly seen (Fig.4.1.7).

High conservation is seen in the N-terminus of DUSP10 orthologs (the first 30 residues are identical among all except Danio rerio), in the regulatory rhodanese domain (except Danio rerio which seems to lack this domain) and in the dual specificity phosphatase catalytic domain (in all of the species). Other short sequences of highly conserved amino acid residues may indicate important regulatory residues. The Serine residue at position 4, which has been found to be phosphorylated as already mentioned, is conserved in all species except Danio rerio (a leucine residue is found instead of serine in this species). Since Danio rerio lacks also the regulatory rhodanese domain (MAPK binding domain), the phosphorylation of this residue may be important in substrate binding and specificity.

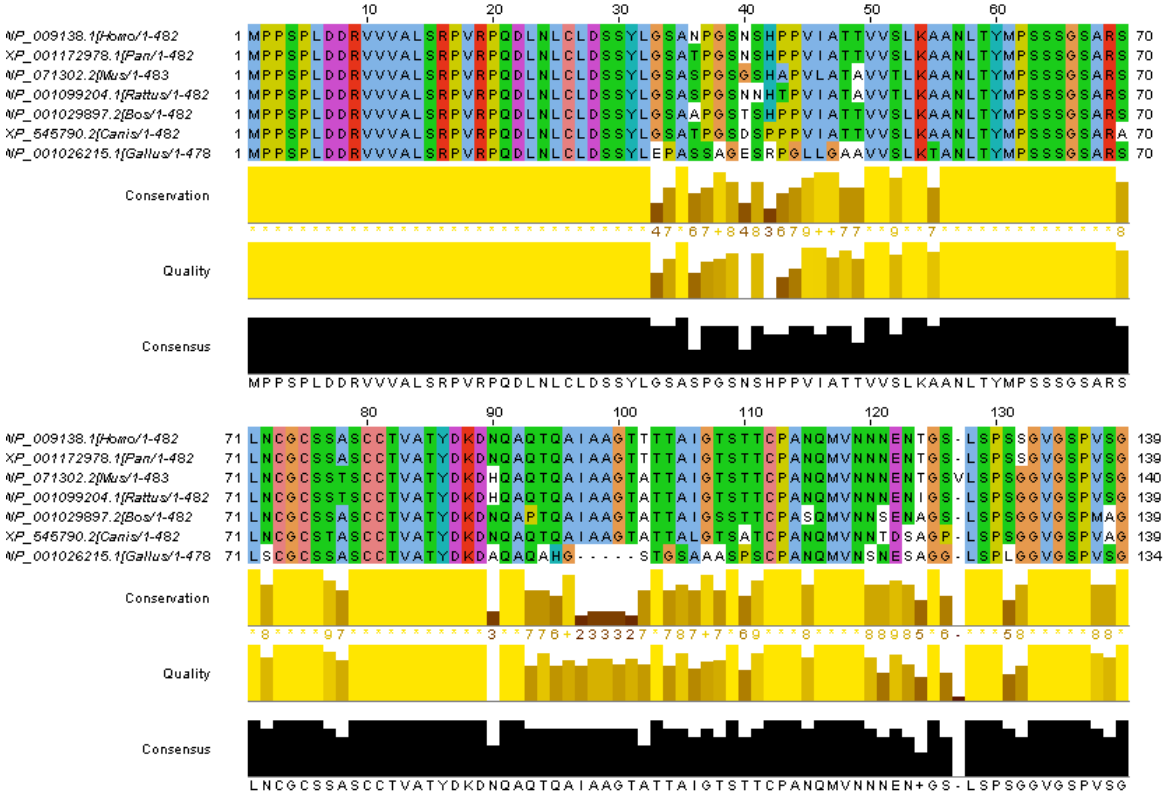

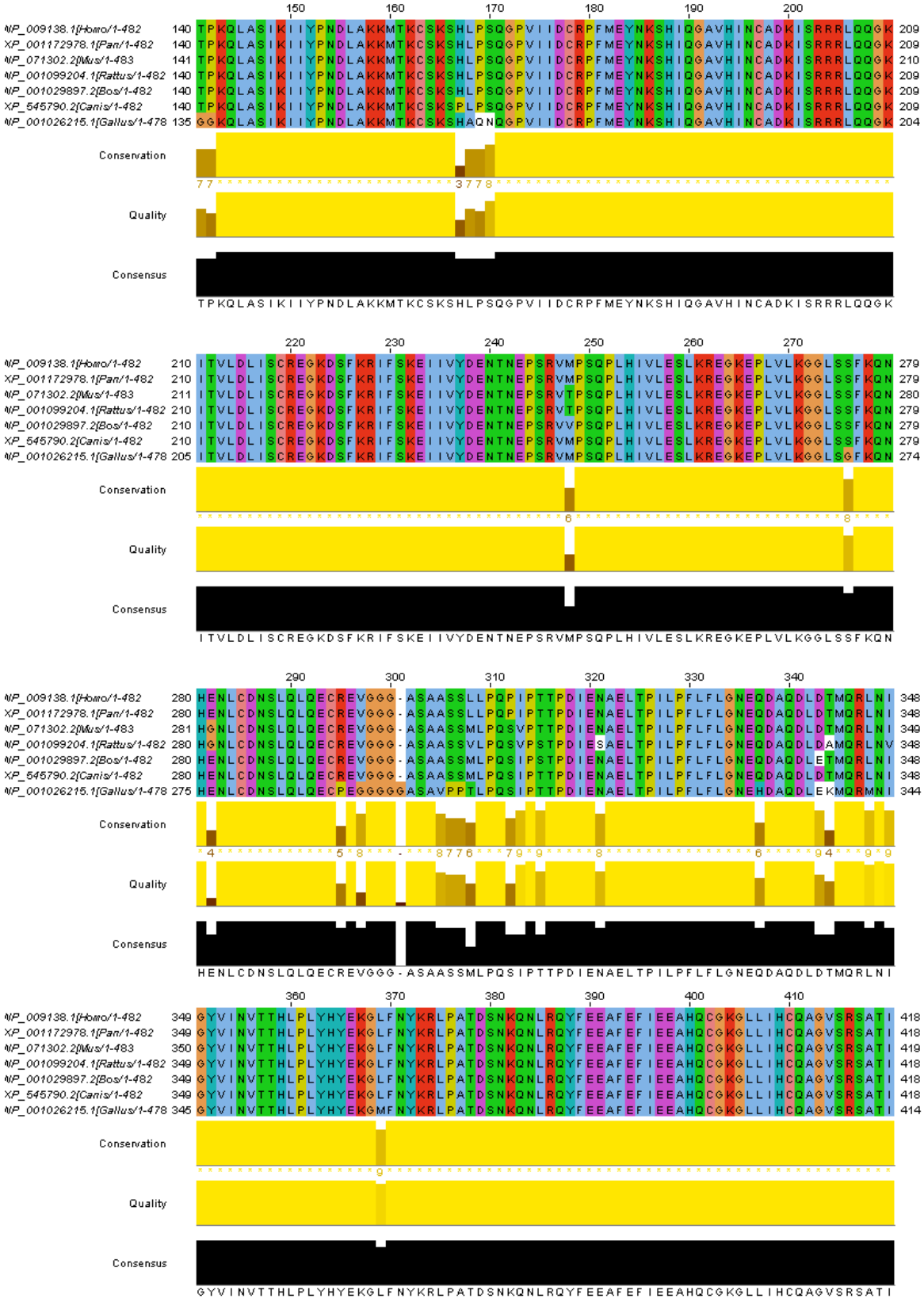
150 160 170 180 190 200
NP_009138.1[Homo/1-482 140 TPKQLASIKIIYPNDLAKKMTKCSKSHLPSQGPVIIDCRPFMEYNKSHIQGAVHINCADKISRRRLQQGK 209
XP_001172978.1[Pan/1-482 140 TPKQLASIKIIYPNDLAKKMTKCSKSHLPSQGPVIIDCRPFMEYNKSHIQGAVHINCADKISRRRLQQGK 209
NP_071302.2[Mus/1-483 141 TPKQLASIKIIYPNDLAKKMTKCSKSHLPSQGPVIIDCRPFMEYNKSHIQGAVHINCADKISRRRLQQGK 210
NP_001099204.1[Rattus/1-482 140 TPKQLASIKIIYPNDLAKKMTKCSKSHLPSQGPVIIDCRPFMEYNKSHIQGAVHINCADKISRRRLQQGK 209
NP_001029897.2[Bos/1-482 140 TPKQLASIKIIYPNDLAKKMTKCSKSHLPSQGPVIIDCRPFMEYNKSHIQGAVHINCADKISRRRLQQGK 209
XP_545790.2[Canis/1-482 140 TPKQLASIKIIYPNDLAKKMTKCSKSPLPSQGPVIIDCRPFMEYNKSHIQGAVHINCADKISRRRLQQGK 209
NP_001026215.1[Gallus/1-478 135 GGKQLASIKIIYPNDLAKKMTKCSKSHAQNQGPVIIDCRPFMEYNKSHIQGAVHINCADKISRRRLQQGK 204
Conservation
Quality
Consensus
TPKQLASIKIIYPNDLAKKMTKCSKSHLPSQGPVIIDCRPFMEYNKSHIQGAVHINCADKISRRRLQQGK
220 230 240 250 260 270
NP_009138.1[Homo/1-482 210 ITVLDLISCREGKDSFKRIFSKEIIVYDENTNEPSRVMPSQPLHIVLESLKREGKEPLVLKGGLSSFKQN 279
XP_001172978.1[Pan/1-482 210 ITVLDLISCREGKDSFKRIFSKEIIVYDENTNEPSRVMPSQPLHIVLESLKREGKEPLVLKGGLSSFKQN 279
NP_071302.2[Mus/1-483 211 ITVLDLISCREGKDSFKRIFSKEIIVYDENTNEPSRVTPSQPLHIVLESLKREGKEPLVLKGGLSSFKQN 280
NP_001099204.1[Rattus/1-482 210 ITVLDLISCREGKDSFKRIFSKEIIVYDENTNEPSRVTPSQPLHIVLESLKREGKEPLVLKGGLSSFKQN 279
NP_001029897.2[Bos/1-482 210 ITVLDLISCREGKDSFKRIFSKEIIVYDENTNEPSRVVPSQPLHIVLESLKREGKEPLVLKGGLSSFKQN 279
XP_545790.2[Canis/1-482 210 ITVLDLISCREGKDSFKRIFSKEIIVYDENTNEPSRVMPSQPLHIVLESLKREGKEPLVLKGGLSSFKQN 279
NP_001026215.1[Gallus/1-478 205 ITVLDLISCREGKDSFKRIFSKEIIVYDENTNEPSRVMPSQPLHIVLESLKREGKEPLVLKGGLSGFKQN 274
Conservation
Quality
Consensus
ITVLDLISCREGKDSFKRIFSKEIIVYDENTNEPSRVMPSQPLHIVLESLKREGKEPLVLKGGLSSFKQN
290 300 310 320 330 340
NP_009138.1[Homo/1-482 280 HENLCDNSLQLQECREVGGG-ASAASSLLPQPIPTTPDIENAELTPILPFLFLGNEQDAQDLDTMQRLNI 348
XP_001172978.1[Pan/1-482 280 HENLCDNSLQLQECREVGGG-ASAASSLLPQPIPTTPDIENAELTPILPFLFLGNEQDAQDLDTMQRLNI 348
NP_071302.2[Mus/1-483 281 HGNLCDNSLQLQECREVGGG-ASAASSMLPQSVPTTPDIENAELTPILPFLFLGNEQDAQDLDTMQRLNI 349
NP_001099204.1[Rattus/1-482 280 HGNLCDNSLQLQECREVGGG-ASAASSVLPQSVPSTPDIESAELTPILPFLFLGNEQDAQDLDAMQRLNV 348
NP_001029897.2[Bos/1-482 280 HENLCDNSLQLQECREVGGG-ASAASSMLPQSIPSTPDIENAELTPILPFLFLGNEQDAQDLETMQRLNI 348
XP_545790.2[Canis/1-482 280 HENLCDNSLQLQECREVGGG-ASAASSMLPQSIPTTPDIENAELTPILPFLFLGNEQDAQDLDTMQRLNI 348
NP_001026215.1[Gallus/1-478 275 HENLCDNSLQLQECPEGGGGGASAVPPTLPQSIPTTPDIENAELTPILPFLFLGNEHDAQDLEKMQRMNI 344
Conservation
Quality
Consensus
HENLCDNSLQLQECREVGGG-ASAASSMLPQSIPTTPDIENAELTPILPFLFLGNEQDAQDLDTMQRLNI
360 370 380 390 400 410
NP_009138.1[Homo/1-482 349 GYVINVTTHLPLYHYEKGLFNYKRLPATDSNKQNLRQYFEEAFEFIEEAHQCGKGLLIHCQAGVSRSATI 418
XP_001172978.1[Pan/1-482 349 GYVINVTTHLPLYHYEKGLFNYKRLPATDSNKQNLRQYFEEAFEFIEEAHQCGKGLLIHCQAGVSRSATI 418
NP_071302.2[Mus/1-483 350 GYVINVTTHLPLYHYEKGLFNYKRLPATDSNKQNLRQYFEEAFEFIEEAHQCGKGLLIHCQAGVSRSATI 419
NP_001099204.1[Rattus/1-482 349 GYVINVTTHLPLYHYEKGLFNYKRLPATDSNKQNLRQYFEEAFEFIEEAHQCGKGLLIHCQAGVSRSATI 418
NP_001029897.2[Bos/1-482 349 GYVINVTTHLPLYHYEKGLFNYKRLPATDSNKQNLRQYFEEAFEFIEEAHQCGKGLLIHCQAGVSRSATI 418
XP_545790.2[Canis/1-482 349 GYVINVTTHLPLYHYEKGLFNYKRLPATDSNKQNLRQYFEEAFEFIEEAHQCGKGLLIHCQAGVSRSATI 418
NP_001026215.1[Gallus/1-478 345 GYVINVTTHLPLYHYEKGMFNYKRLPATDSNKQNLRQYFEEAFEFIEEAHQCGKGLLIHCQAGVSRSATI 414
Conservation
Quality
Consensus
GYVINVTTHLPLYHYEKGLFNYKRLPATDSNKQNLRQYFEEAFEFIEEAHQCGKGLLIHCQAGVSRSATI

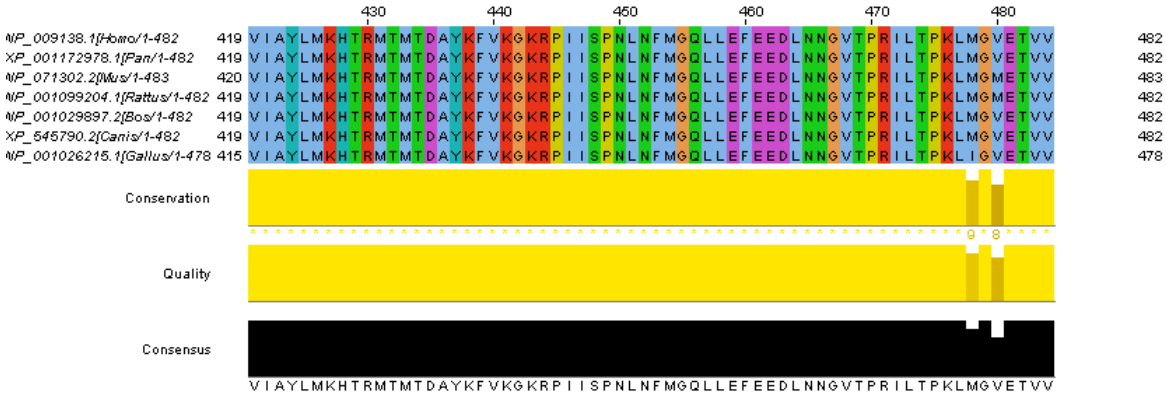

Fig.4.1.7: ClustalW2 multiple sequence alignment of DUSP10 orthologs except the Danio rerio ortholog: From top to bottom: Human, chimpanzee, mouse, rat, cow, dog and chicken orthologs are listed.

4.1.1.3.2 Paralogs of DUSP10

DUSP10 belongs to a phosphatase subfamily named as MAPK phosphatases under the family dual specificity phosphatases, as already mentioned. A dendrogram showing the relations of most DSPs are shown in Fig.4.1.8. Additional information come from studies. A tree showing the relations of most MKPs are shown in Fig.4.1.9. The conserved domains in MKP paralogs are shown in Fig.4.1.10.

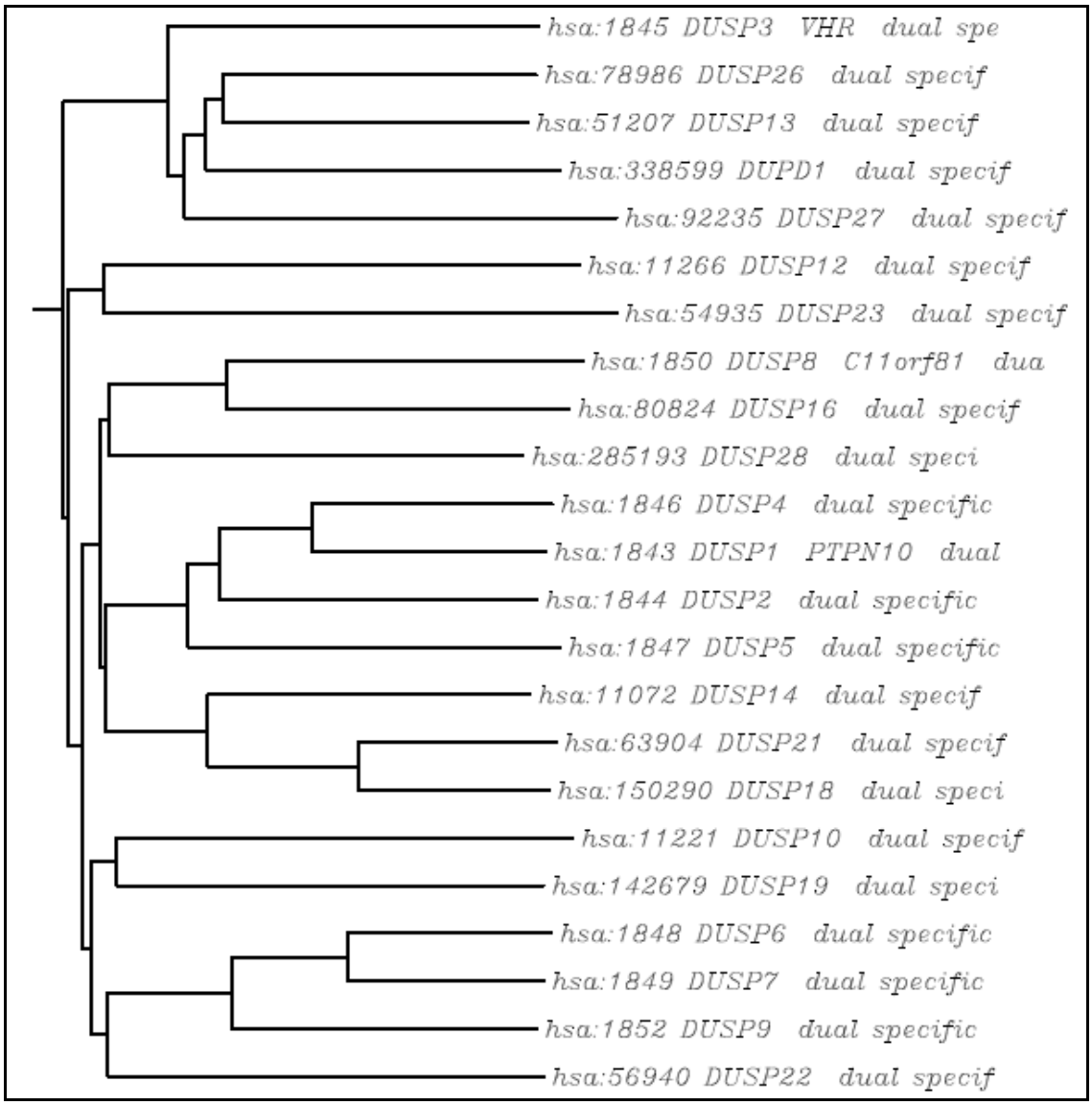

Fig.4.1.8: Phylogenetic tree of DUSP gene family with branch lengths: Includes only human genes. Paralogs are gathered by KEGG SSDB paralog search. Phylogenetic tree is generated by MAFFT sequence alignment.

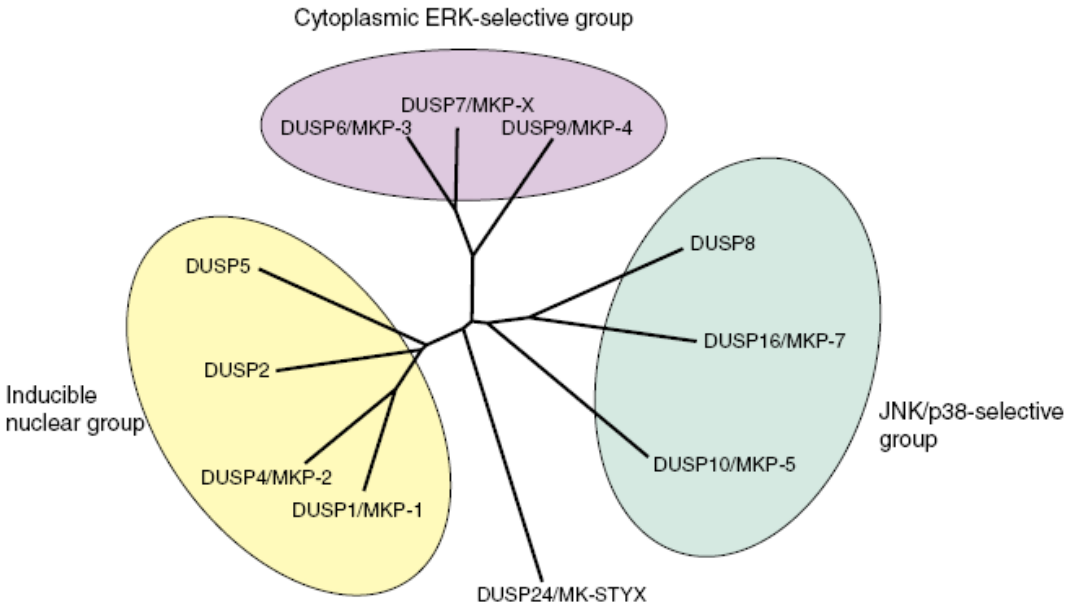

Fig.4.1.9: Cluster of MKPs according to substrate preference: Inducible nuclear group also targets ERK MAPK (Dickinson RJ, Keyse SM, 2006).

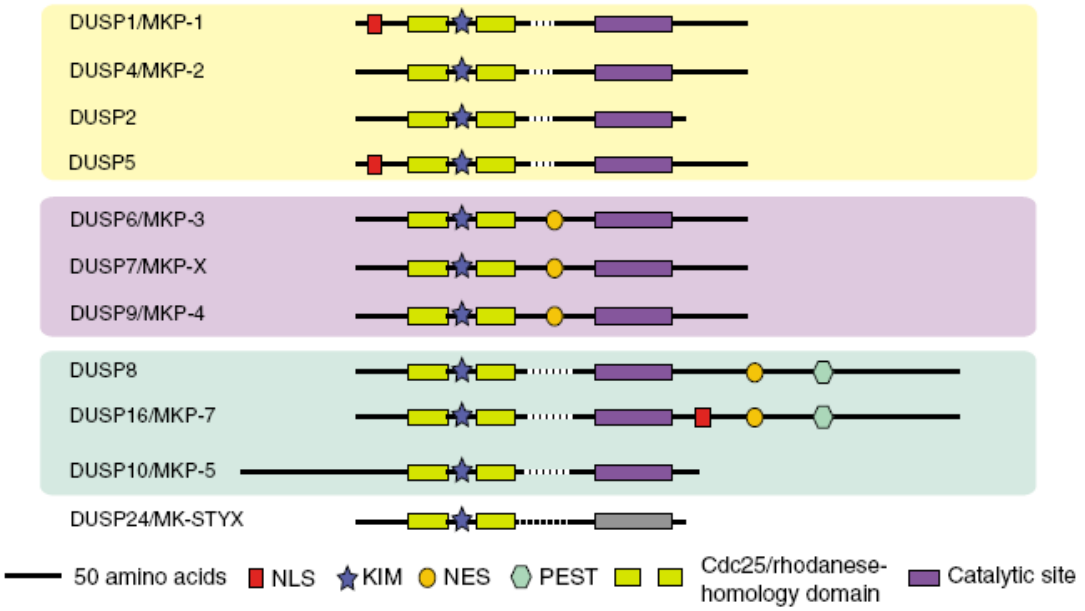

Fig.4.1.10: Conserved motifs in MKPs: Same color code is used as Fig.4.1.9 (beige marks the inducible nuclear group, light purple marks the cytoplasmic ERK-selective group, and blue marks the JNK/p38-selective group). DUS24/MK-STYX is an atypical MKP that is catalytically inactive (hence its catalytic site is shown in grey in contrast to the dark purple active catalytic sites). NLS: nuclear localization signal; NES: nuclear exclusion signal; KIM: kinase interacting motif; PEST: Proline-Glutamate-Serine-Threonine motif, associated with rapidly-degraded proteins (Dickinson RJ, Keyse SM, 2006).

As indicated in Fig.4.1.10, DUSP10 has an unusual proline-rich N-terminal sequence that is not seen in any other MKP. There are no regulatory domains associated with this sequence of about 100 amino acids yet. Since orthologous proteins from other

species also bear this unusual N-terminal sequence and is highly conserved among many of these species, important but uncharacterized motifs may be present here, such as an unknown nuclear localization signal, since generally MKPs are known to dephosphorylate MAPKs in both cytoplasm and nucleus.

4.1.1.4 DUSP10 in gene expression profiling arrays

Oncomine Cancer Profiling Database was used to check DUSP10 expression changes in different microarrays comparing HCC tissues with non-tumorous tissues. Box-plots were generated upon selection of relevant results. These are shown in Fig.4.1.11. There are two main microarray studies on HCC in Oncomine Database: Chen_Liver and Wurmbach_Liver. Chen_Liver is published by Chen X et al in 2002. This study aims at finding the gene expression patterns which distinguish between primary human liver cancers and cancers that metastasize to liver. Wurmbach_Liver is published by Wurmbach E et al in 2007. It aims at characterizing the genome-wide molecular profiles of different liver disease and cancer states, for biomarker discovery purposes. Of these two important studies, DUSP10 gave significant results in only Wurmbach_Liver (normal vs. disease state). In this study, the expression of DUSP10 was significantly reduced in HCC samples compared to normal tissues.

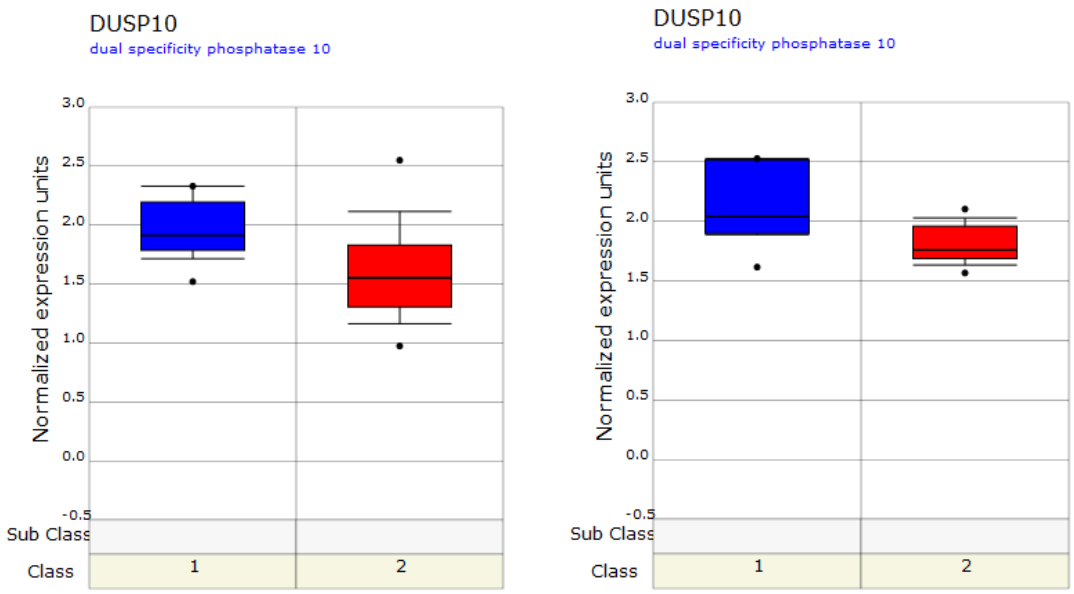

Fig.4.1.11. DUSP10 expression in Wurmbach microarray data: Left, normal (Class 1, n=10) vs HCC (Class 2, n=35), p=0.002. **Right,** normal (Class 1, n=10) vs dysplastic tissue (Class 2, n=17), p=0.01.

The fact that DUSP10 emerged as a gene downregulated in immortal clones and the above finding strengthen the possibility that a relationship between DUSP10 and hepatocarcinogenesis exists and it is possible that DUSP10 may act as a tumor suppressor in HCC.

4.1.1.5 Expression data

On the UCSC (University of California, Santa Cruz) Genome Browser website, the expression data of DUSP10 isoform **a** can be obtained from several microarray studies. The data gathered from the GNF Expression Atlas 2 human data on Affy U133A and GNF1H chips (Su AI et al, 2002), where red represents high expression level and green represents low expression level, is as follows:

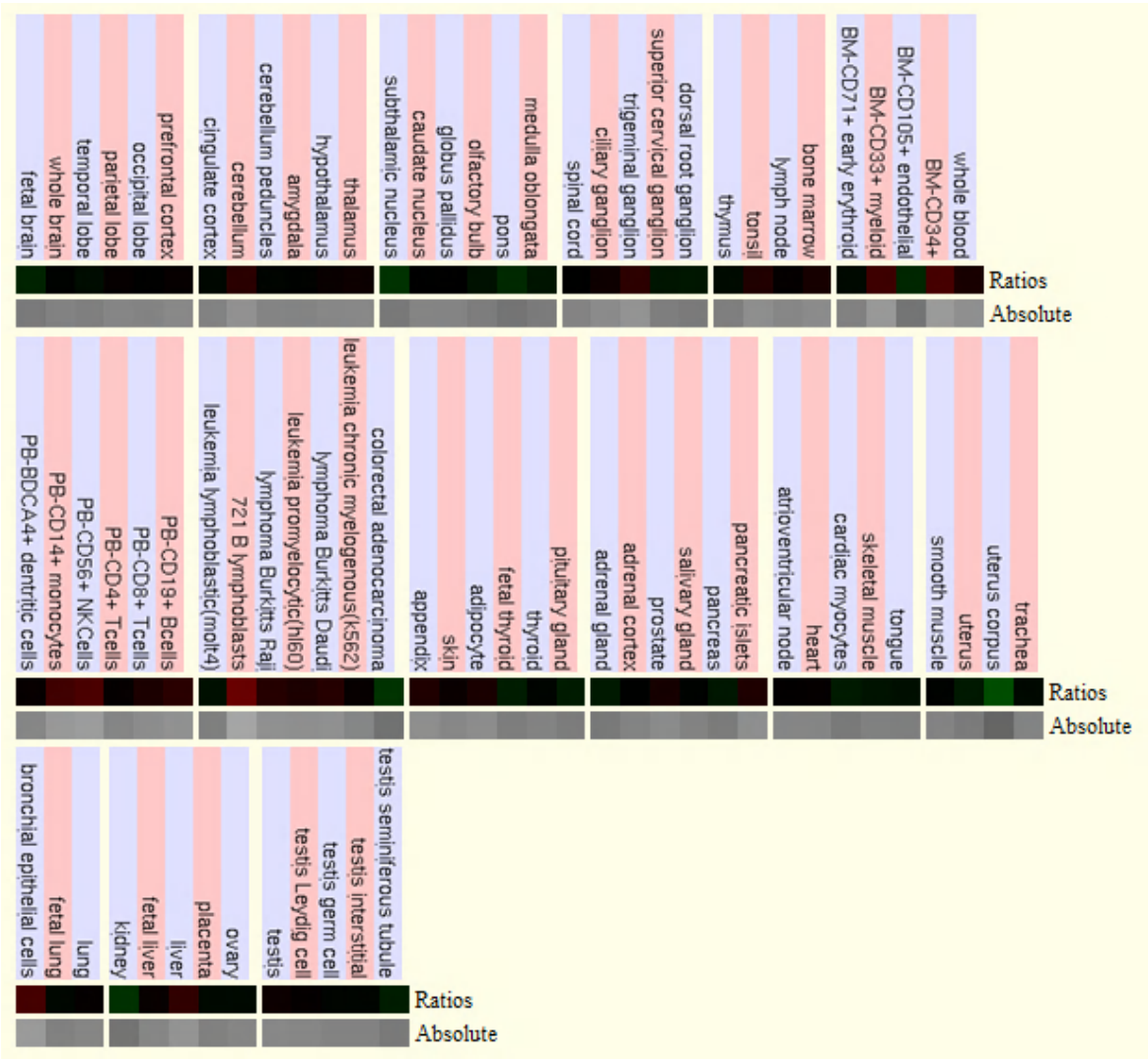

Fig.4.1.12: Expression data of DUSP10 based on the GNF Expression Atlas 2 Data from U133A

and GNF1H Chips.

According to this expression data, although generally all tissues and cells tested expressed DUSP10 to a certain level (as hinted at by the dominance of the black color), it is expressed more in a number of differentiated immune system and hematopoietic cell types, B-lymphoblasts, bronchial epithelial cells and adult liver. Relatively low levels of DUSP10 is detected in uterus corpus, kidney and colorectal adenocarcinoma.

4.1.2 Analysis of DUSP10 expression change between senescent and immortal Huh7 clones

As a first step, we performed PCR to verify DUSP10 differential expression obtained by the microarray study previously done by our group in C1, C3-Early and C3-Late clones (see Introduction chapter, section 1.5). The result of this PCR and a graph displaying the relative expression of DUSP10 in each clone are shown below:

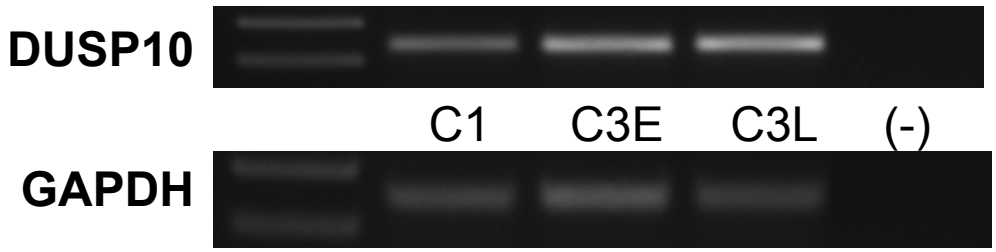

Fig.4.1.13a: DUSP10 is upregulated in senescent and revertant clones compared to the immortal clone: cDNA from C1 (immortal clone), C3-Early (revertant clone) and C3-Late (senescent clone) were used for semi-quantitative RT-PCR experiments. GAPDH: Glyceraldehyde-3-phosphate dehydrogenase was used as an internal control. (-): Negative control well to check for nucleic acid contaminants. A Western blot of these clones against DUSP10 was not done due to lack of proteins.

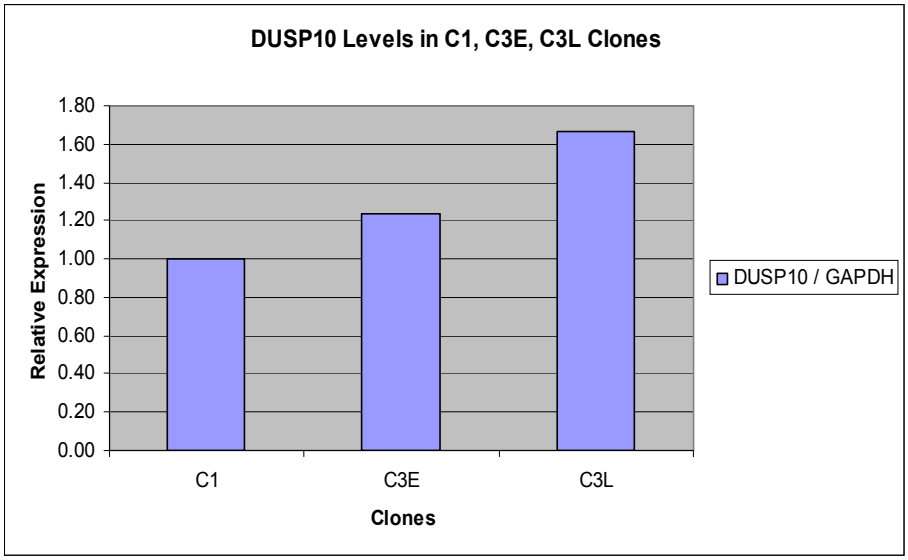

Fig.4.1.13b: DUSP10 is upregulated in senescent and revertant clones compared to the immortal clone: A graph was generated by normalization of DUSP10 band intensities according to GAPDH band intensities in Fig.4.1.13a. Intensities were quantified by Bio-1D program.

The results shown in Fig.4.1.13a and b indicate that DUSP10 expression is increased progressively from C1 immortal clone to C3 senescent clone. There is a deviation from the fold changes observed in the original microarray data (2.5 fold increase in revertant vs immortal clone and 2.6 fold increase in senescent vs immortal clone). This may be due to the method of band intensity measurement or due to the insensitivity of the semi-quantitative PCR. Still, it is clearly seen that DUSP10 is upregulated in senescent cells in contrast to immortal ones.

4.1.3 DUSP10 expression data

We then continued our analysis on DUSP10 by generating DUSP10 mRNA and protein expression data in HCC and breast cancer cell lines (Fig.4.1.14a and b). For this purpose, cDNAs from various HCC and breast cancer cell lines were extracted and used in semi-quantitative RT-PCR. Also proteins were extracted from HCC cell lines and used in Western Blot.

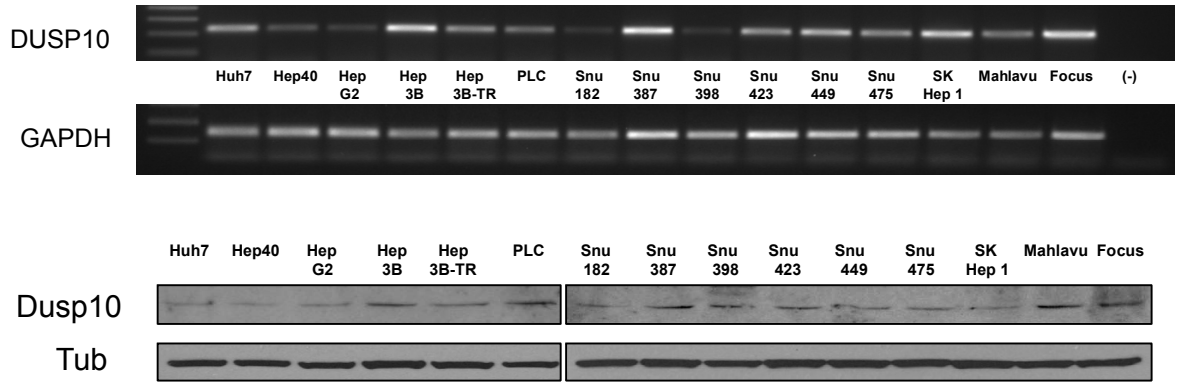

Fig.4.1.14a: Upper, DUSP10 transcript variant 1 mRNA levels in HCC cell lines: Huh7, Hep40, HepG2, Hep3B, Hep3B-TR, PLC are classified as well-differentiated cell lines. Snu182, Snu387, Snu398, Snu423, Snu449, Snu475, SK Hep1, Mahlavu and Focus are classified as poorly differentiated cell lines. GAPDH was used as an internal control. (-) well showed no contamination. **Lower, DUSP10 protein levels in HCC cell lines:** Tubulin (Tub) was used as an internal control. Western blotting was done as described in Materials and Methods.

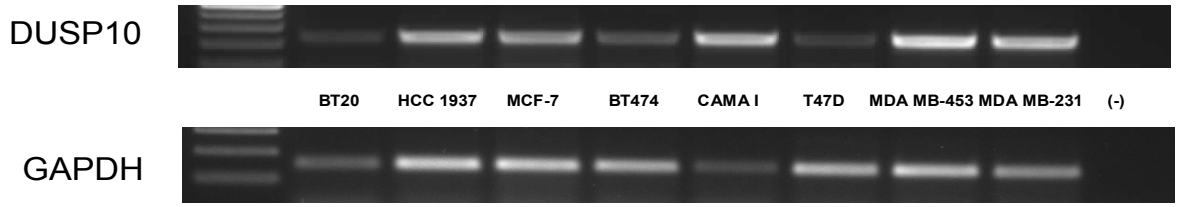

Fig.4.1.14b: DUSP10 transcript variant 1 mRNA levels in selected breast cancer cell lines: BT20 and HCC 1937 are classified as basal cell lines. MCF-7, BT474, CAMAI, T47D and MDA MB-453 are classified as luminal cell lines. MDA MB-231 is classified as a mesenchymal cell line. GAPDH was used as an internal control. (-) well showed no contamination.

These results indicate that DUSP10 transcript variant 1 is expressed in all HCC cell lines and breast cancer cell lines tested, although heterogenously. At this step, DUSP10 transcript variant 2 and 3 did not show any expression (Fig.4.1.15a and b, respectively). Since, in mice, the second transcript variant of DUSP10 (possibly representing human DUSP10 isoform **b** coding transcript variants) has been found to be specifically expressed in testis according to OMIM, this result may have been expected (Masuda K et al, 2000). Hence all the following experiments were done on DUSP10 transcript variant 1 or isoform **a**.

Fig.4.1.15a: DUSP10 transcript variant 2 is not expressed in HCC cell lines: From left to right, Huh7, Hep40, HepG2, Hep3B, PLC, Snu387, Snu475, Focus, Mahlavu and (-) control were loaded. The expected product was 197 bp long. This image shows 100-500bp region of the gel.

Fig.4.1.15b: DUSP10 transcript variant 3 is not expressed in HCC cell lines: From left to right, Huh7, HepG2, Hep3B, Snu387, Snu449, Focus, Mahlavu and (-) control were loaded. The expected product was 176 bp long. This image shows 100-500bp region of the gel.

4.1.4 Subcellular localization of DUSP10 in hepatocellular carcinoma cell lines

4.1.4.1 Localization of DUSP10 changes between different cell lines

As seen above, no significant DUSP10 expression changes are observed between well- and poorly-differentiated HCC cell lines. The morphology of well-differentiated cell lines (eg. HepG2 and Hep3B) is more similar to normal hepatocytes compared to poorly-differentiated cell lines (eg. Snu182 and Mahlavu) and they express α-fetoprotein (AFP) which is a useful marker for post-treatment monitoring of HCC patients (eg. for treatment efficacy or tumor recurrence). Well-differentiated HCC cell lines are also called as epithelial-like as opposed to mesenchymal-like poorly-differentiated cell lines, due to the epithelial/mesenchymal markers they express or do not express. Since DUSP10 is important according to our group's microarray data, we wondered if a DUSP10-related difference between these two types of cell lines is present in another aspect. One such aspect, subcellular localization, also gives substantial clues on the function of a protein. Hence we checked subcellular localization of DUSP10 in HCC by immunoperoxidase staining and by immunofluorescence. Results are shown in Fig.4.1.16 and Fig.4.1.17, respectively.

The results of immunoperoxidase staining is summarized in Table 4.1.2. Staining intensities and patterns are indicated for each cell line. Generally the cytoplasmic staining seen in cell lines were concentrated on the immediate perimeter of the nuclei.

Cell Line / Pattern	Huh 7	Hep 40	Hep G2	Hep 3B	Hep 3B-TR	PLC	Snu 182	Snu 387	Snu 398	Snu 423	Snu 449	Snu 475	Mahlavu	Focus	SK Hep1
Cytoplasmic	++	++	++	++	++	++	+	+	+++	+	++	++	+++	++	++
Nuclear	+	+/-	+	+/-	+/-	+/-	++	-	+	-	+/-	+	+	+	+/-
Peri-nuclear	+	+	-	++	+/-	+/-	-	+	++	+	++	++	+++	++	+

Table 4.1.2: DUSP10 staining patterns of 15 HCC cell lines according to immunoperoxidase staining: The number of (+)s indicates the intensity of staining. Peri-nuclear staining is positive if

some or most of the cytoplasmic staining is observed in close proximity with the nuclei compared to other parts of cytoplasm.

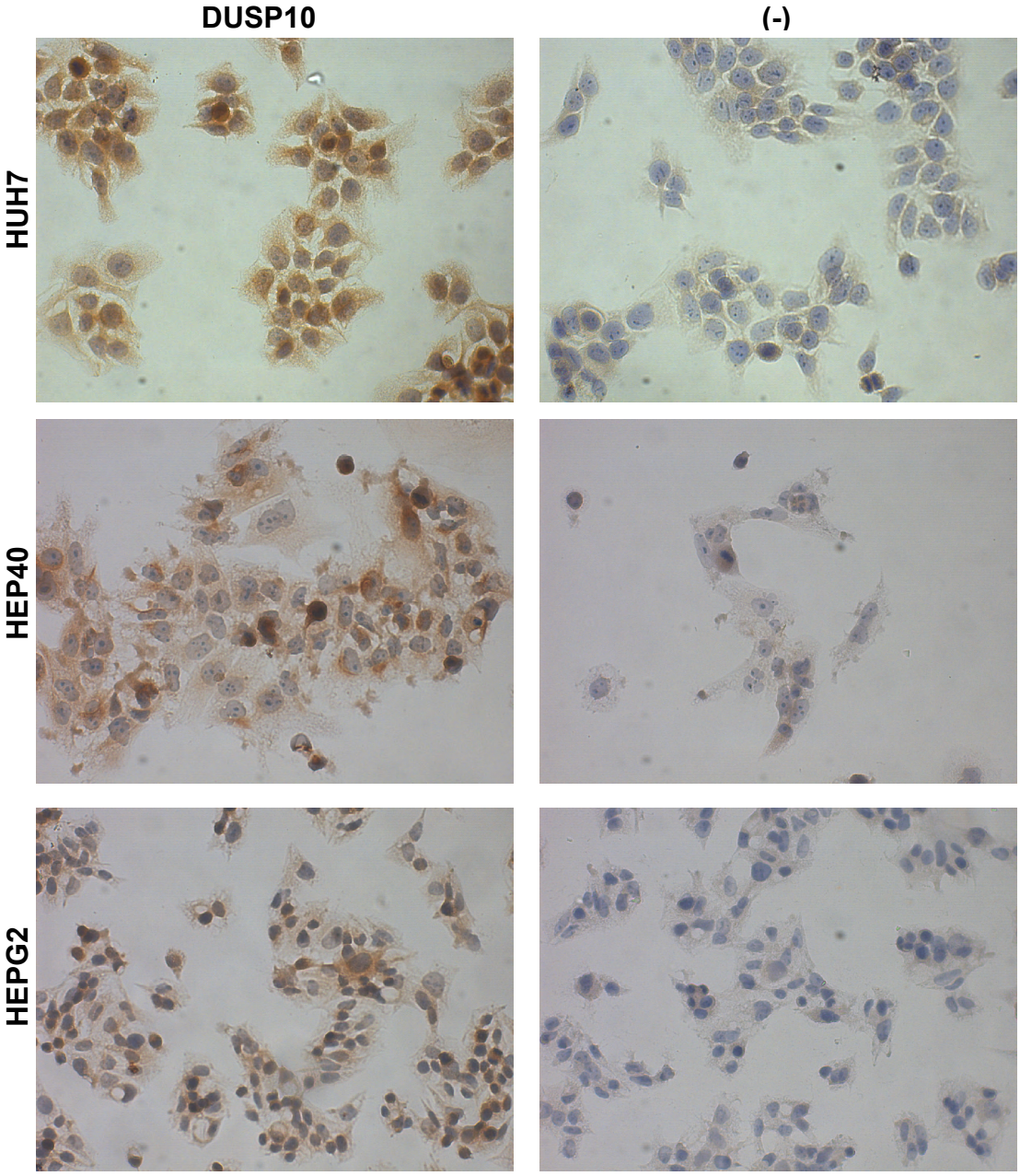

Fig.4.1.16: DUSP10 immunostaining in HCC cell lines: Cells were seeded on coverslips in 50-80% confluency and left to grow overnight at 37ºC with 5% CO_2. Immunoperoxidase staining was performed as explained in Materials and Methods. No primary antibodies were put onto (-) controls. Background staining due to the HRP-bound secondary antibody was assessed this way. All sample and negative control pairs were photographed with the same light exposure and under 40x objective, to avoid bias. The results continue in the following pages.

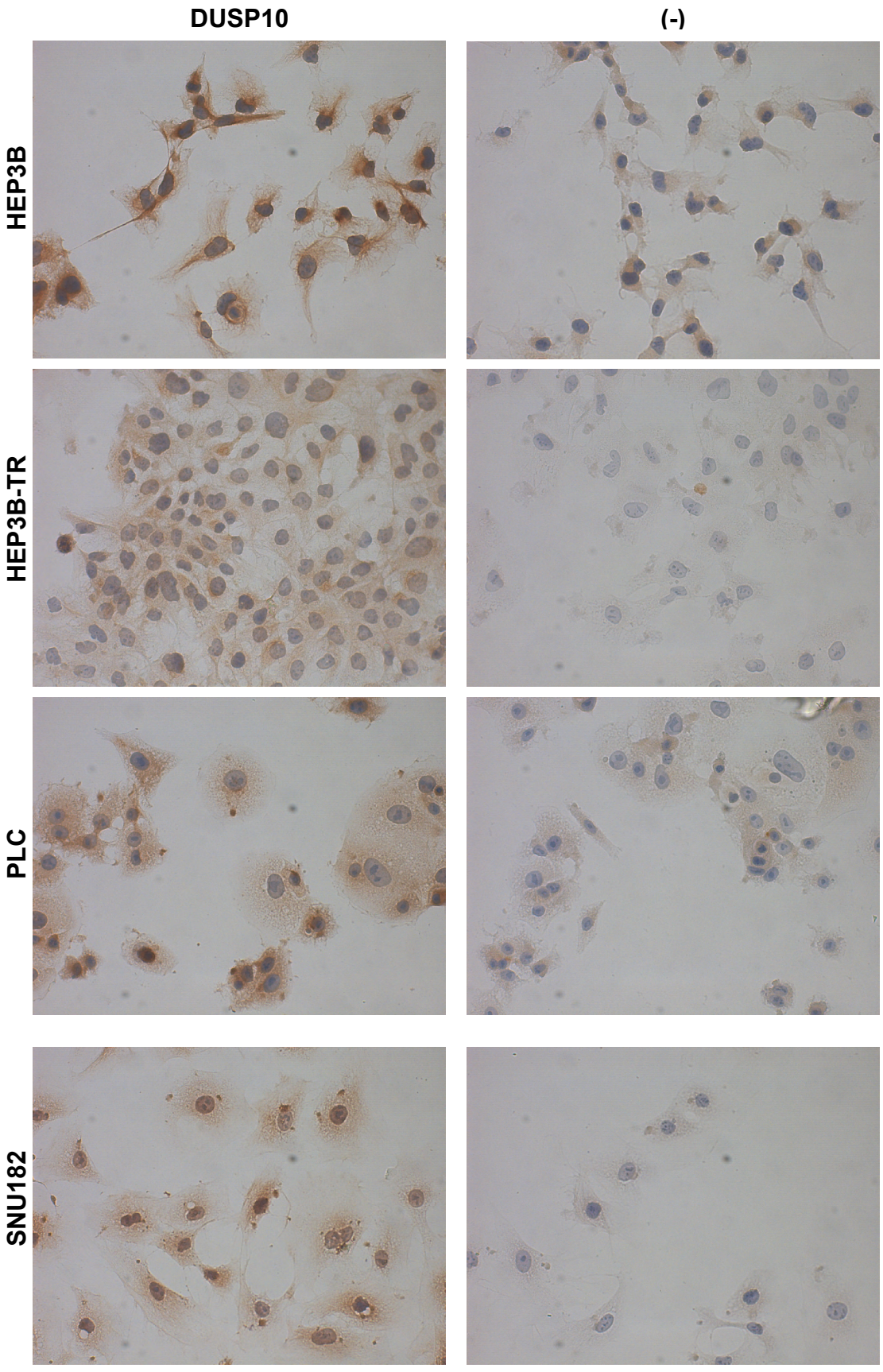
DUSP10
(-)
HEP3B
HEP3B-TR
PLC
SNU182

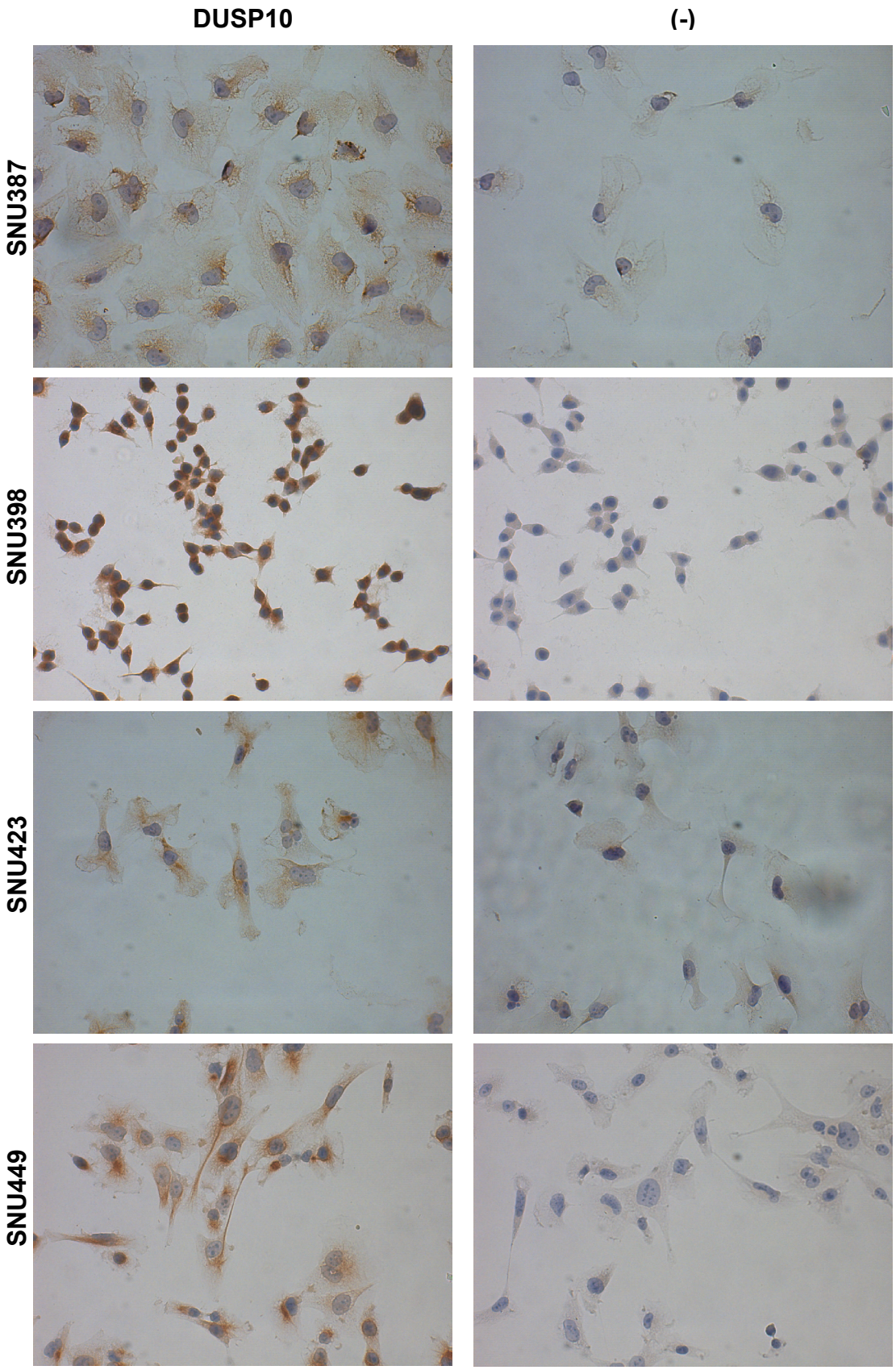
DUSP10
(-)
SNU387
SNU398
SNU423
SNU449

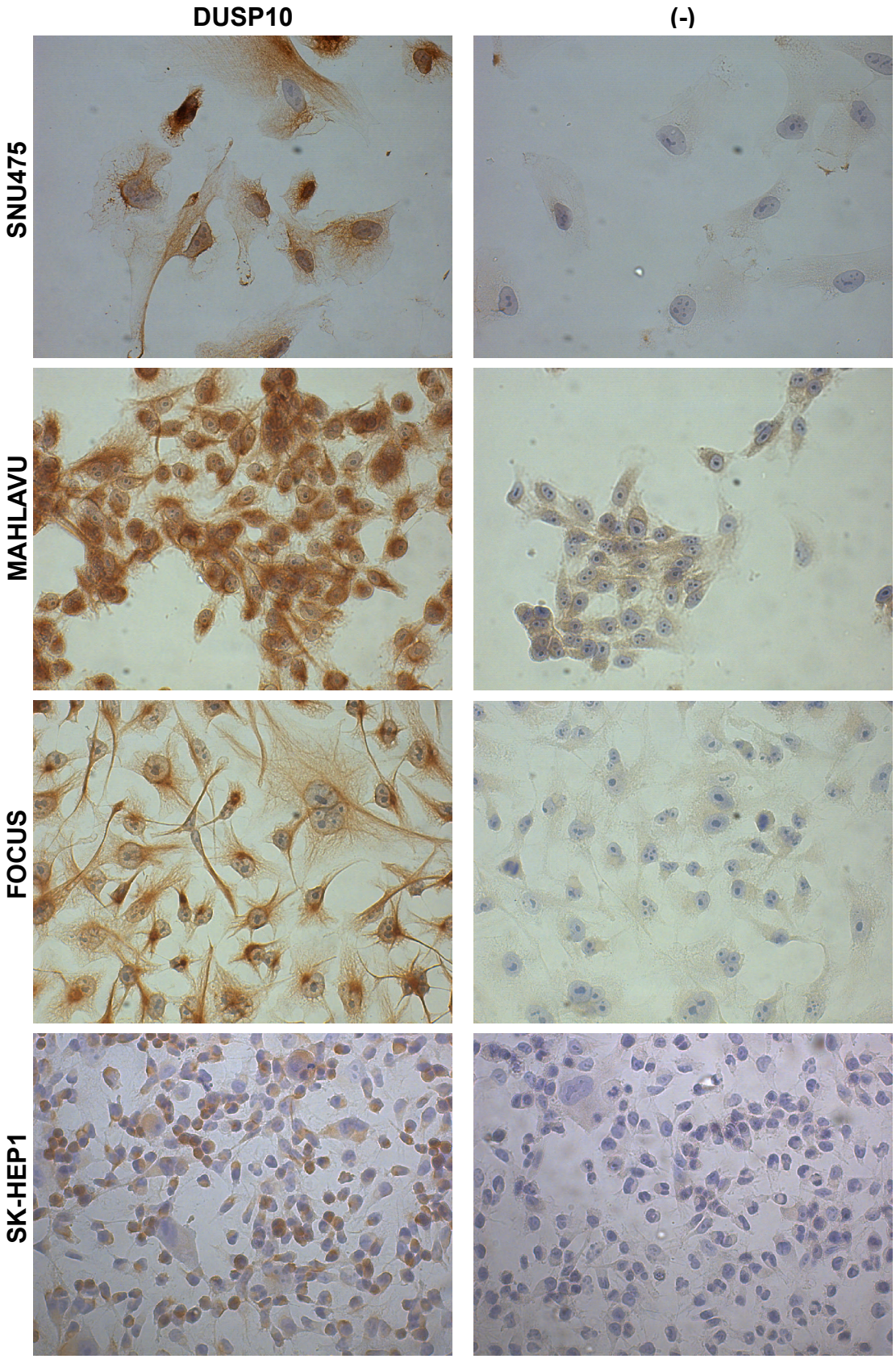

Fig.4.1.16 (continued): DUSP10 immunostaining in HCC cell lines: Cells were seeded on coverslips in 50-80% confluency and left to grow overnight at 37ºC with 5% CO_2. Immunoperoxidase staining was performed as explained in Materials and Methods. No primary antibodies were put onto (-) controls. Background staining due to the HRP-bound secondary antibody was assessed this way. All

sample and negative control pairs were photographed with the same light exposure and under 40x objective, to avoid bias.

We obtained similar results with immunofluorescence. The results of immunofluorescence is shown in Table 4.1.3. Although deviations from immunoperoxidase staining data are seen, generally both results are in correlation. Again, the cytoplasmic staining seen in cell lines mostly concentrate in the peri-nuclear region. Since this staining pattern is seen in proteins that localize to the endoplasmic reticulum (ER), we designed our next experiment as a DUSP10/Calnexin co-staining in Snu423 cell line in which peri-nuclear DUSP10 staining is clearly seen.

Cell Line / Pattern	Huh 7	Hep 40	Hep G2	Hep 3B	Hep 3B-TR	PLC	Snu 182	Snu 387	Snu 398	Snu 423	Snu 449	Snu 475	Mahlavu	Focus	SK Hep1
Cytoplasmic	+	+	+	++	+	+	+	+	++	++	++	++	+	+	++
Nuclear	+	+	++	+/-	+	++	++	++	+/-	+	+/-	+/-	++	+	+/-
Peri-nuclear	+/-	+/-	+	++	+/-	+/-	+	+/-	+	+	+	++	+	+	++

Table 4.1.3: DUSP10 staining patterns of 15 HCC cell lines according to immunofluorescence: The number of (+)s indicates the intensity of staining. Peri-nuclear staining is positive if some or most of the cytoplasmic staining is observed in close proximity with the nuclei compared to other parts of cytoplasm.

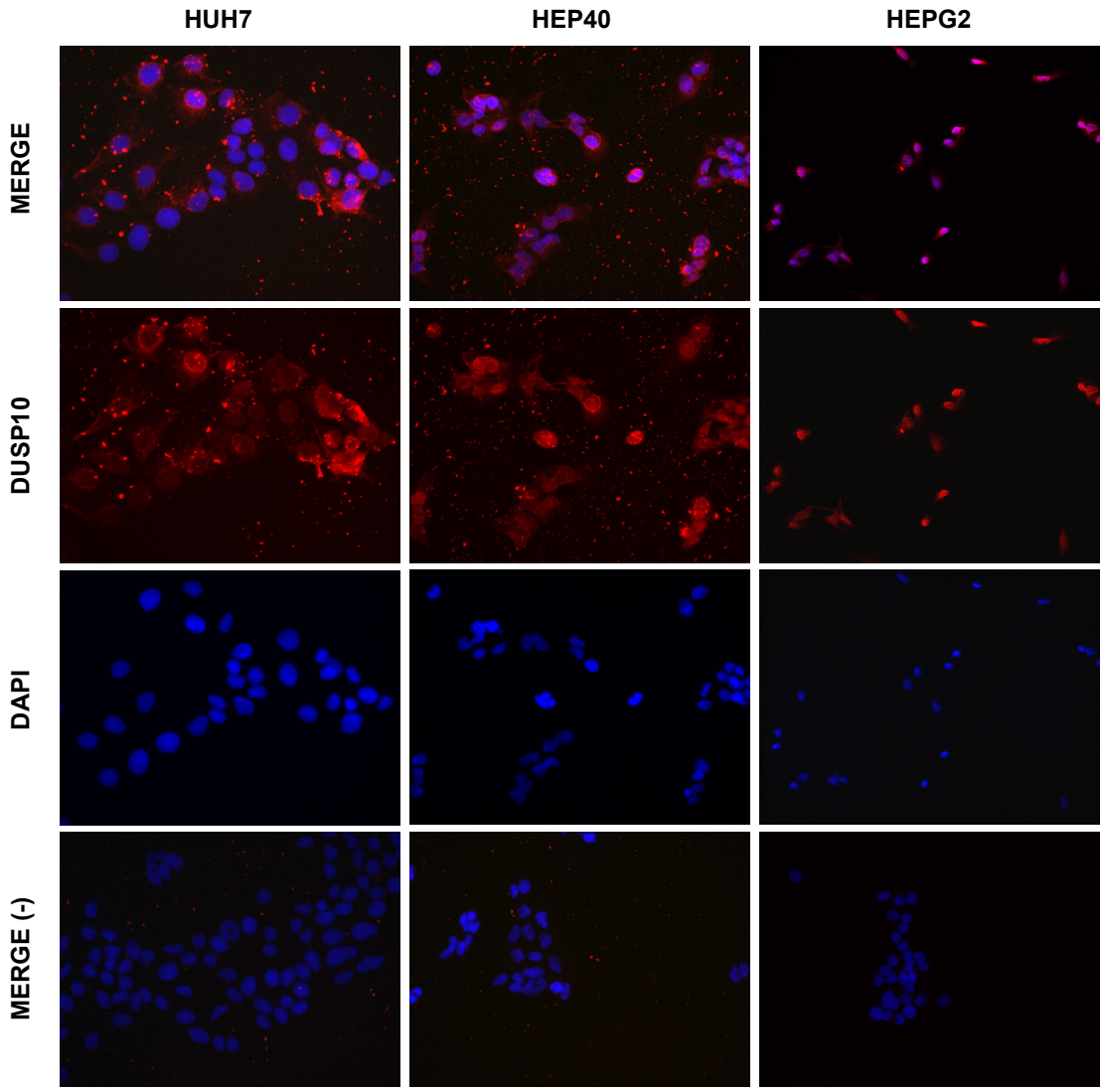

Fig.4.1.17: DUSP10 immunofluorescence in HCC cell lines: Cells were seeded on coverslips in 50-80% confluency and left to grow overnight at 37ºC with 5% CO_2. Immunofluorescence was performed as explained in Materials and Methods. Each sample has three photographs (through DAPI and Alexa Fluor 568 / TRITC filters, and the merge of these two photos). Merge (-) stands for the merged image of negative control for each sample. No primary antibodies were put onto (-) controls. Background staining due to the fluorochrome-bound secondary antibody was assessed this way. All sample and negative control pairs were photographed with the same fluorescence exposure and under 40x objective, to avoid bias. Tiny bright red dots seen in some images might be related to secondary antibody degradation. The results continue in the following pages.

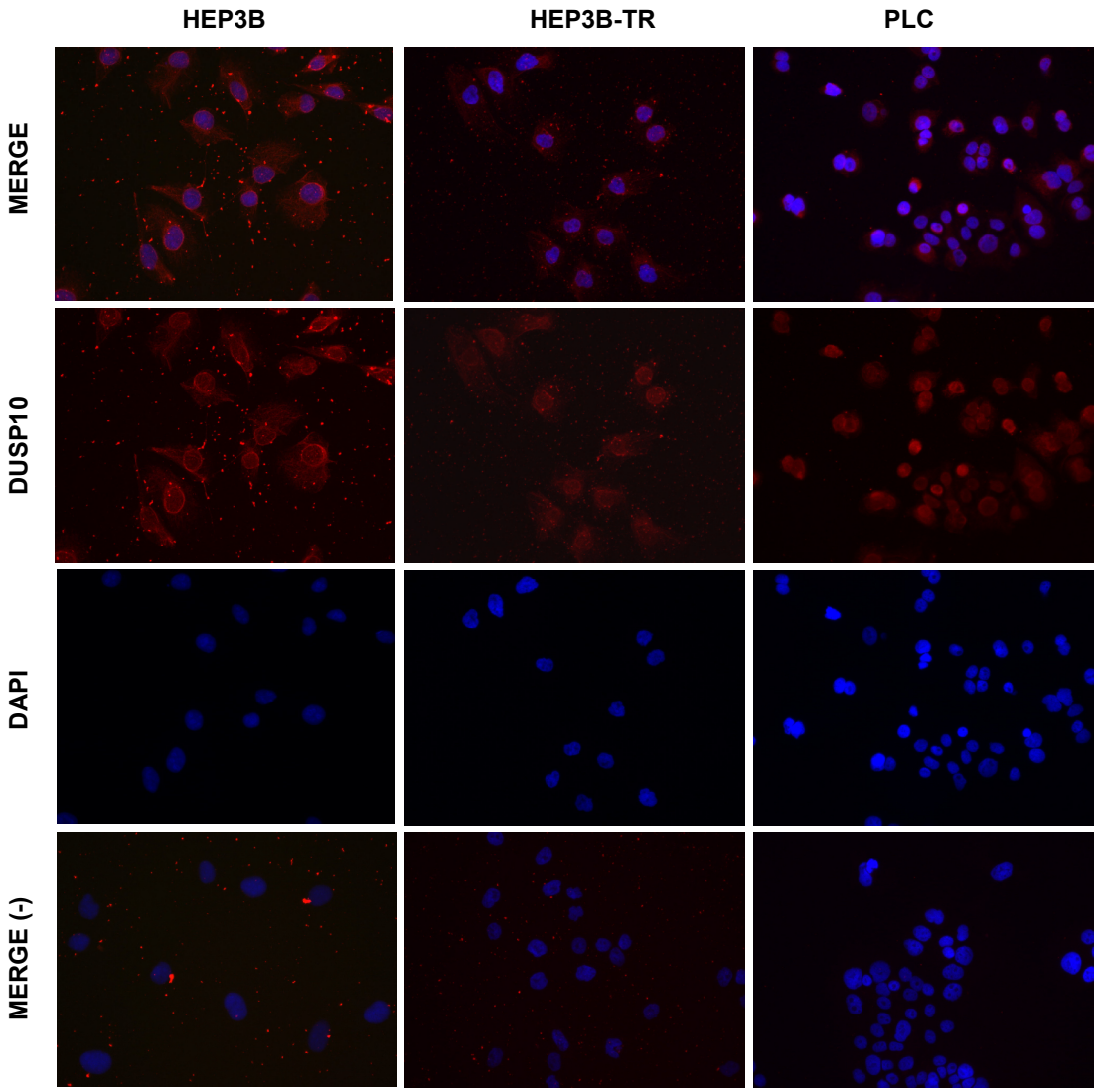

Fig.4.1.17 (Continued): DUSP10 immunofluorescence in HCC cell lines: Cells were seeded on coverslips in 50-80% confluency and grown overnight at 37ºC with 5% CO_2. Immunofluorescence was performed as explained in Materials and Methods. Each sample has three photographs (through DAPI and Alexa Fluor 568 / TRITC filters, and the merge of these two photos). Merge (-) stands for the merged image of negative control for each sample. No primary antibodies were put onto (-) controls. Background staining due to the fluorochrome-bound secondary antibody was assessed this way. All sample and negative control pairs were photographed with the same fluorescence exposure and under 40x objective, to avoid bias. Tiny bright red dots seen in some images might be related to secondary antibody degradation. The results continue in the following pages.

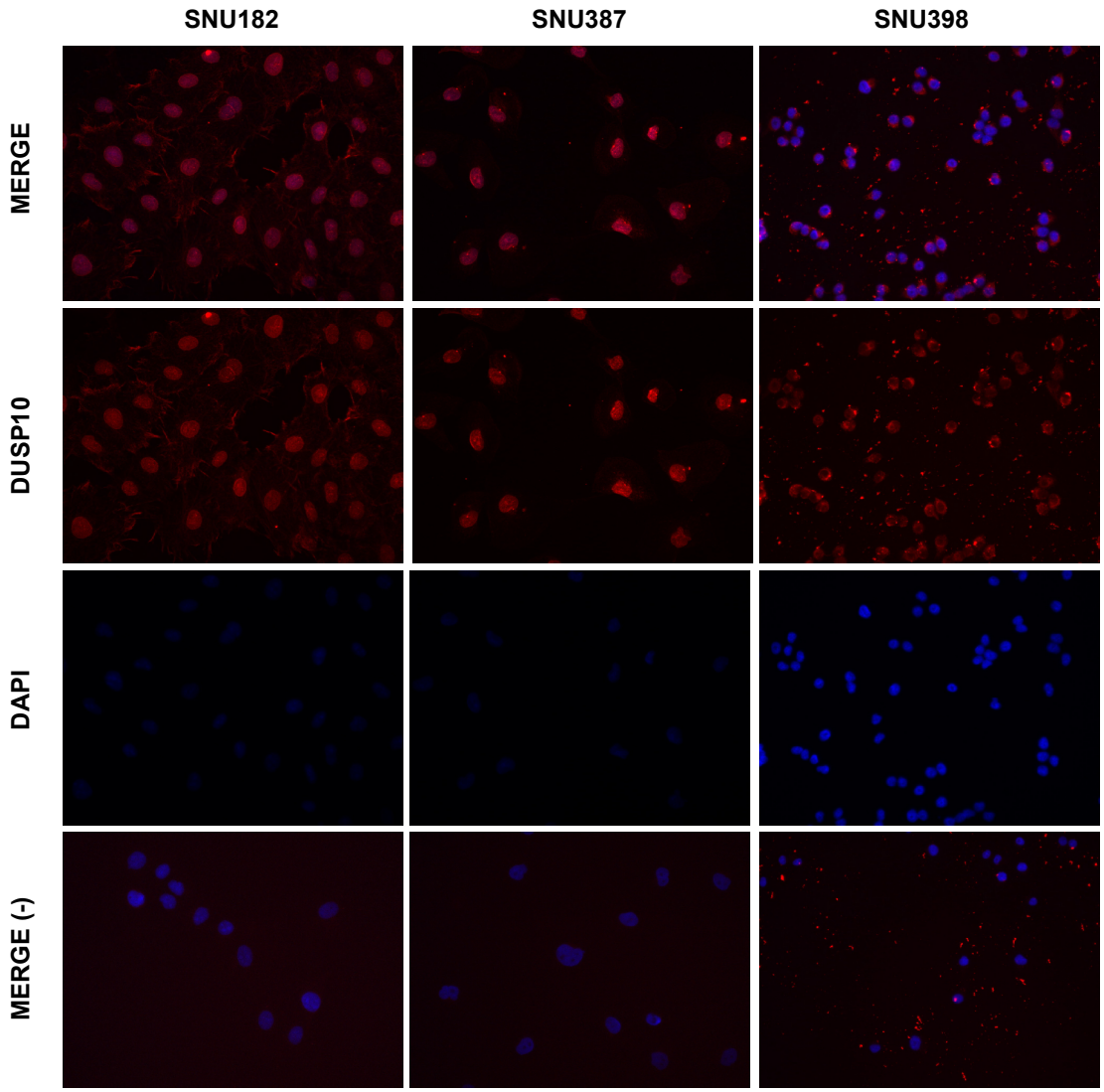

Fig.4.1.17 (Continued): DUSP10 immunofluorescence in HCC cell lines: Cells were seeded on coverslips in 50-80% confluency and grown overnight at 37ºC with 5% CO_2. Immunofluorescence was performed as explained in Materials and Methods. Each sample has three photographs (through DAPI and Alexa Fluor 568 / TRITC filters, and the merge of these two photos). Merge (-) stands for the merged image of negative control for each sample. No primary antibodies were put onto (-) controls. Background staining due to the fluorochrome-bound secondary antibody was assessed this way. All sample and negative control pairs were photographed with the same fluorescence exposure and under 40x objective, to avoid bias. Tiny bright red dots seen in some images might be related to secondary antibody degradation. The results continue in the following pages.

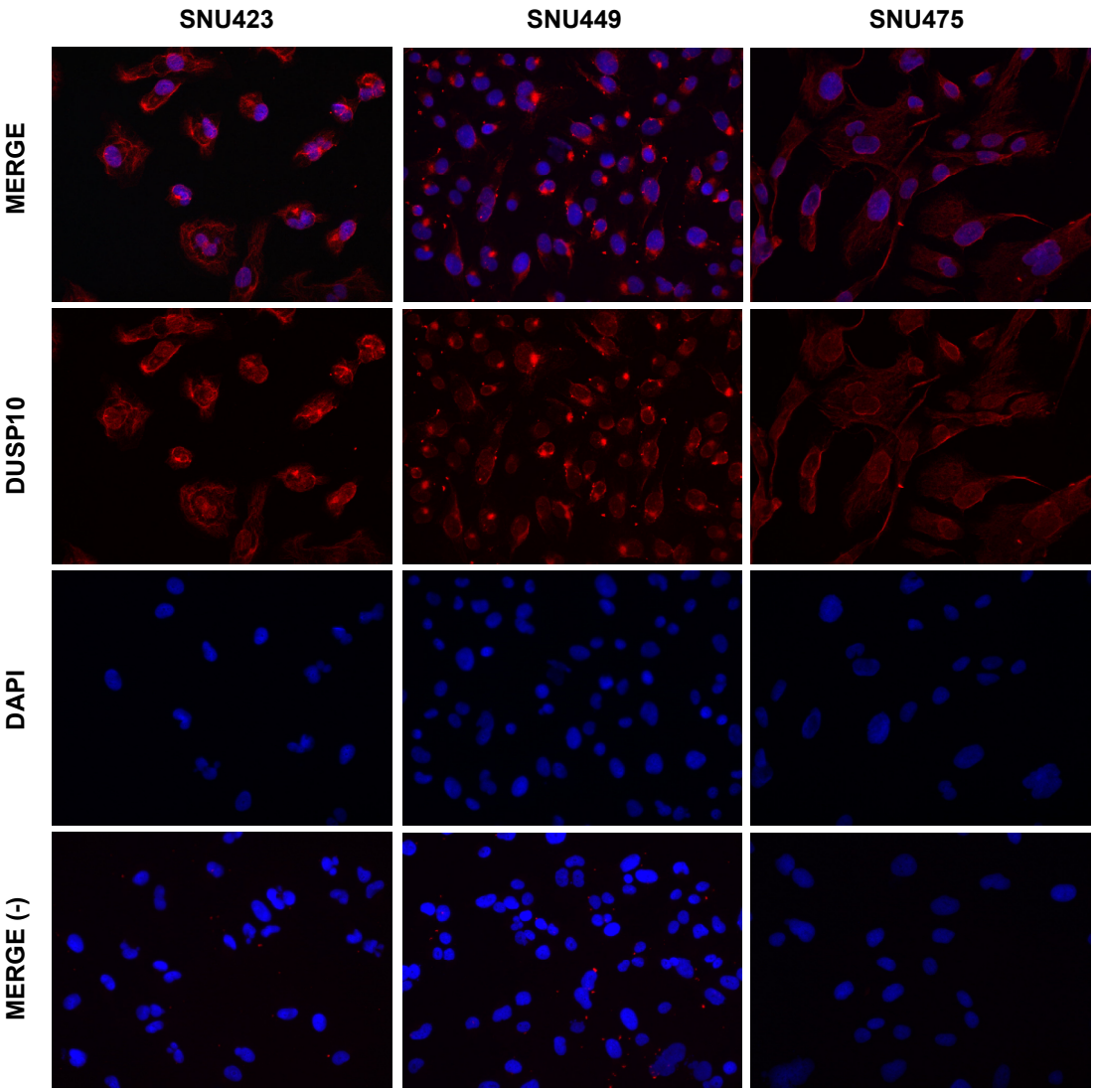

Fig.4.1.17 (Continued): DUSP10 immunofluorescence in HCC cell lines: Cells were seeded on coverslips in 50-80% confluency and grown overnight at 37ºC with 5% CO_2. Immunofluorescence was performed as explained in Materials and Methods. Each sample has three photographs (through DAPI and Alexa Fluor 568 / TRITC filters, and the merge of these two photos). Merge (-) stands for the merged image of negative control for each sample. No primary antibodies were put onto (-) controls. Background staining due to the fluorochrome-bound secondary antibody was assessed this way. All sample and negative control pairs were photographed with the same fluorescence exposure and under 40x objective, to avoid bias. Tiny bright red dots seen in some images might be related to secondary antibody degradation. The results continue in the following pages.

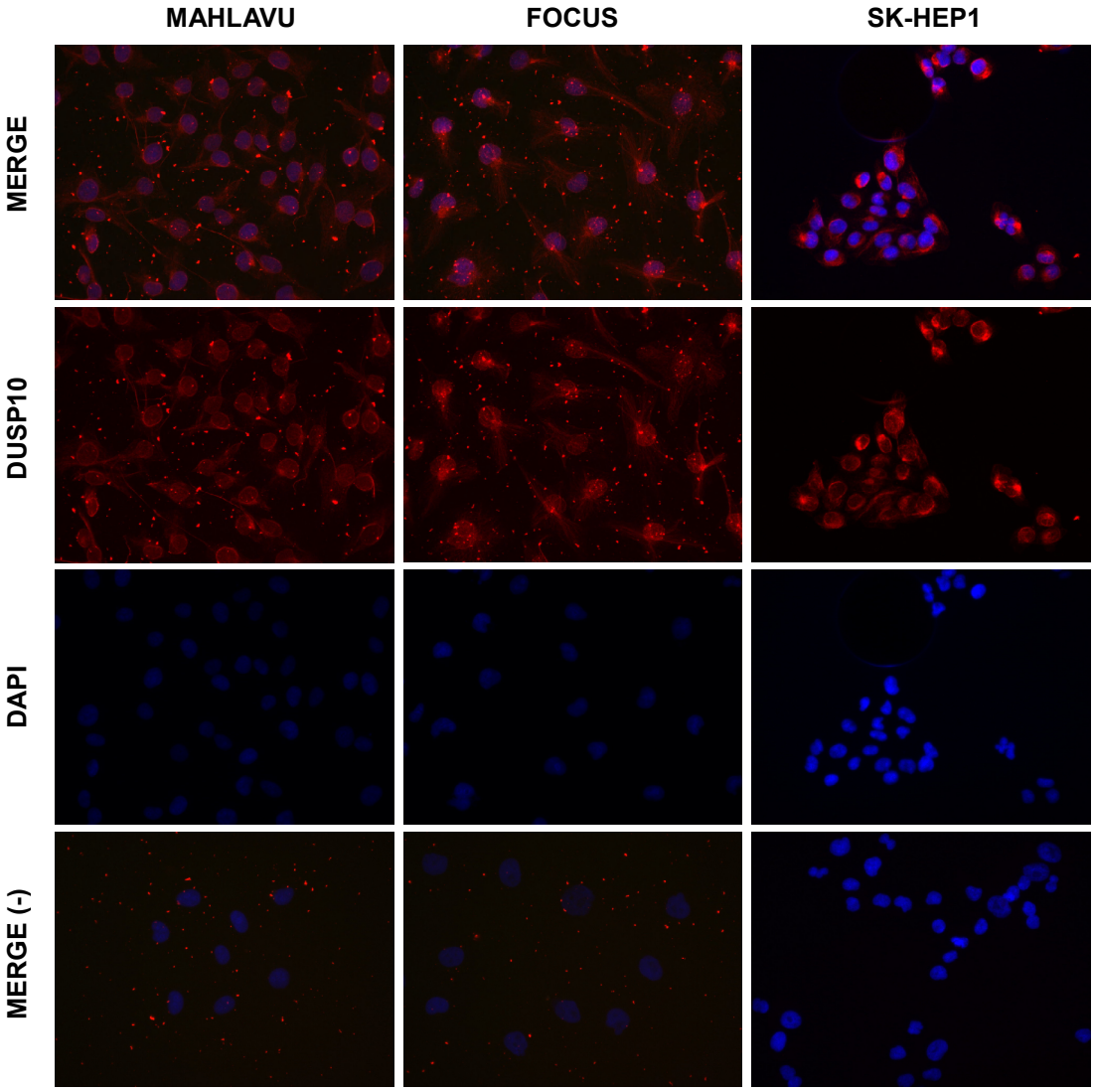

Fig.4.1.17 (Continued): DUSP10 immunofluorescence in HCC cell lines: Cells were seeded on coverslips in 50-80% confluency and grown overnight at 37ºC with 5% CO_2. Immunofluorescence was performed as explained in Materials and Methods. Each sample has three photographs (through DAPI and Alexa Fluor 568 / TRITC filters, and the merge of these two photos). Merge (-) stands for the merged image of negative control for each sample. No primary antibodies were put onto (-) controls. Background staining due to the fluorochrome-bound secondary antibody was assessed this way. All sample and negative control pairs were photographed with the same fluorescence exposure and under 40x objective, to avoid bias. Tiny bright red dots seen in some images might be related to secondary antibody degradation.

4.1.4.2 DUSP10 does not co-localize with calnexin, an ER-membrane protein, in cell lines showing peri-nuclear / cytoplasmic DUSP10 staining

Our next experiment aimed at finding if DUSP10 localized to an organelle, specifically to ER. For this purpose, we chose an HCC cell line, Snu423, in which perinuclear DUSP10 localization was clear. Results are shown in Fig.4.1.18.

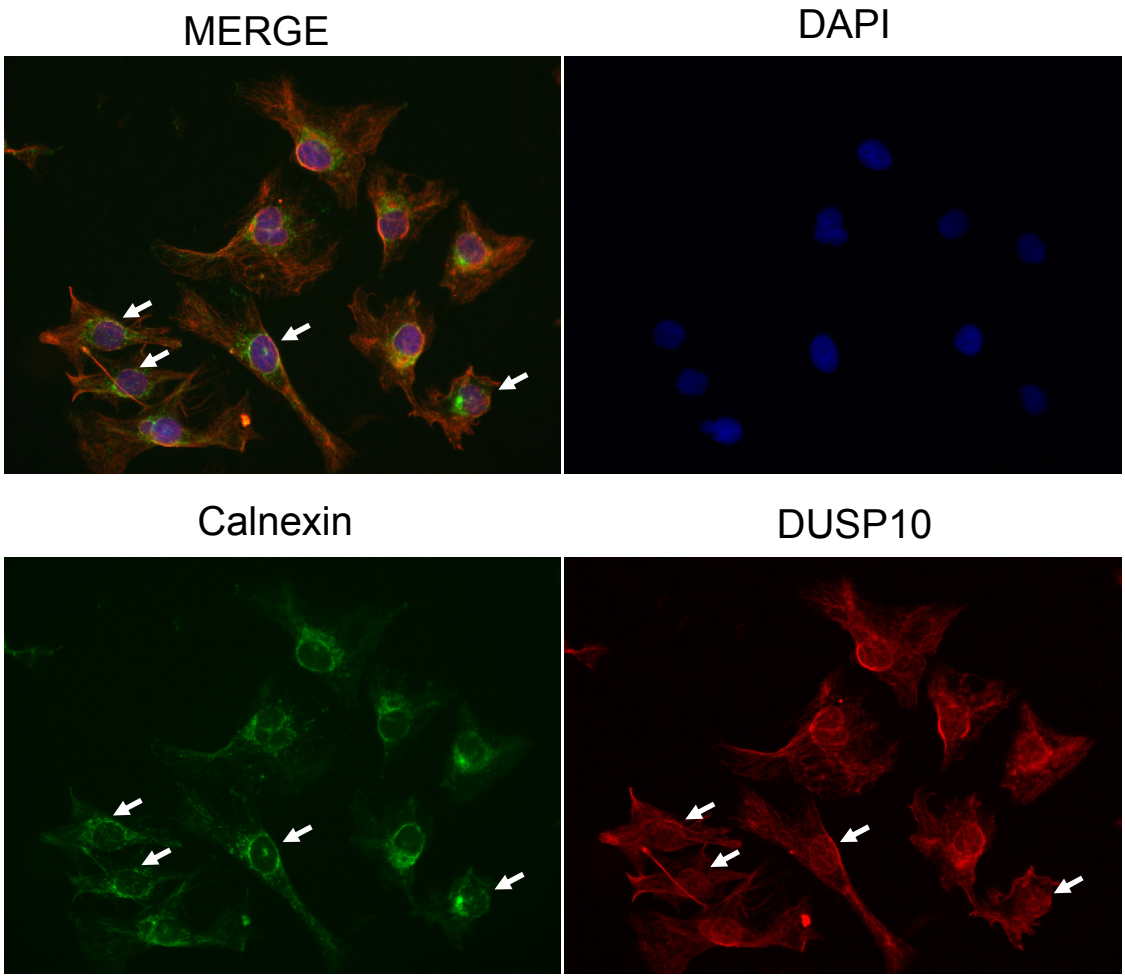

Fig.4.1.18: DUSP10 and calnexin co-staining in Snu423: Cells were seeded on coverslips in 50-80% confluency and left to grow overnight at 37ºC with 5% CO_2. Immunofluorescence was performed as explained in Materials and Methods. Although the red color generated by DUSP10 bound Alexa Fluor 568 turned to orange after merge with the green color generated by calnexin bound Alexa Fluor 488, essentially everywhere, there were extra green coloring in some places in each cell. Also some patterns of green did not match the corresponding patterns of red. These unmatching patterns of green are shown with white arrows.

Since there were regions in cells where only green staining was seen, we could say that DUSP10 is not localized to ER. The orange staining due to the faint green staining (Calnexin) coinciding with the stronger red staining (DUSP10) can be because of the channel cross-talk mediated when two fluorochromes with overlapping spectra, such as Alexa Fluor 488 (green) and 568 (red), are employed.

Next, we decided to take photographs through confocal microscopy because 3D images (images from the same z-plane) would give better information about the localization of a protein (Fig.4.1.19a, b and Fig.4.1.20a, b). Additionally, with the confocal microscope, adjustments can be made so as to overcome the channel cross-talk that is mentioned above.

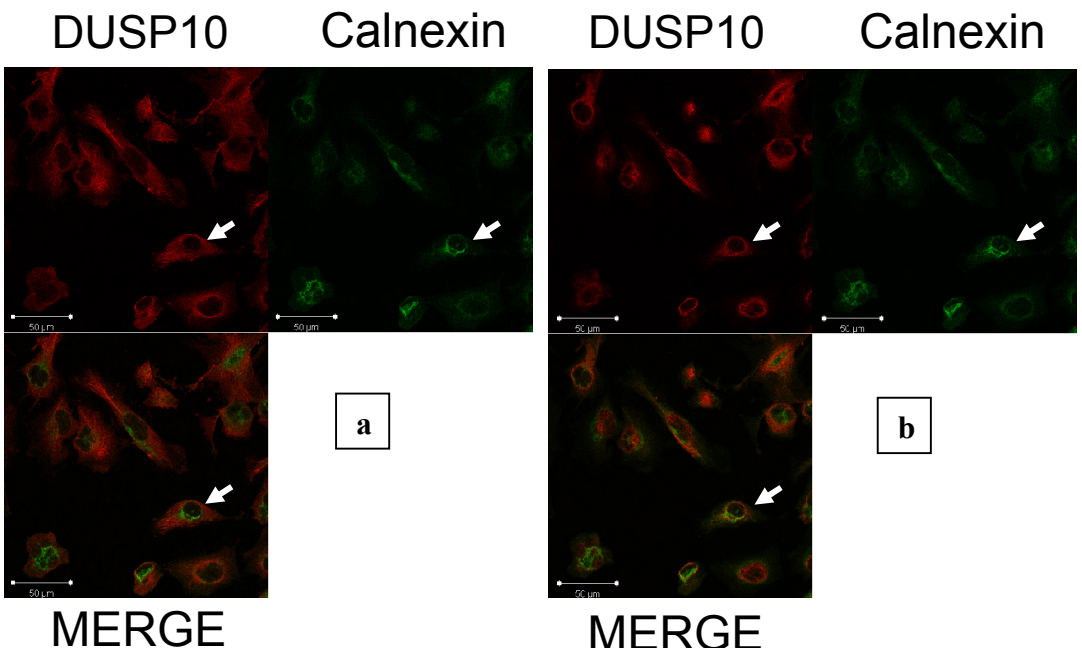

Fig.4.1.19a: Confocal image of DUSP10/Calnexin costaining, the plane where DUSP10 staining is the highest (40x), b: the plane where Calnexin staining is the highest (40x): All confocal images are taken at Zeiss LSM 510 laser scanning confocal microscope at Middle East Technical University. It is clearly seen that Calnexin and DUSP10 stainings exclude each other. The cell marked with white arrows is photographed with higher magnification in Fig.4.1.20a and b.

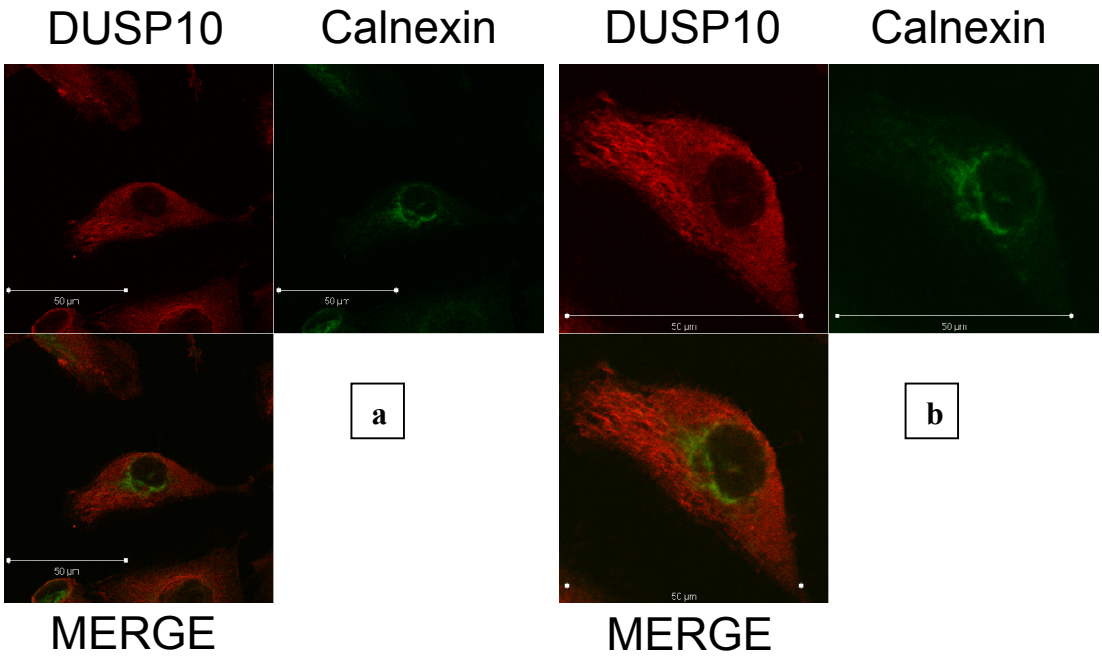

Fig.4.1.20a. Confocal image of DUSP10/Calnexin costaining, the plane where DUSP10 staining is the highest (80x), b. (160x): It is clearly seen that Calnexin and DUSP10 staining do not overlap. In b, the view was rotated so that the magnified cell fit the frame. In this specific cell, peri-nuclear DUSP10 staining is not very clear as a diffuse cytoplasmic staining is seen.

According to these results, it was verified with the confocal microscope that DUSP10 did not colocalize with Calnexin to endoplasmic reticulum.

4.1.4.3 DUSP10 co-localizes with beta-actin, a cytoskeletal protein, in cell lines showing peri-nuclear / cytoplasmic DUSP10 staining

Since DUSP10 staining was observed as a meshwork of thin lines in the cytoplasms in Fig.4.1.20a-b, we checked to see if DUSP10 colocalizes with Actin. The results showed that DUSP10 and Actin colocalize in cytoplasm (Fig.4.1.21).

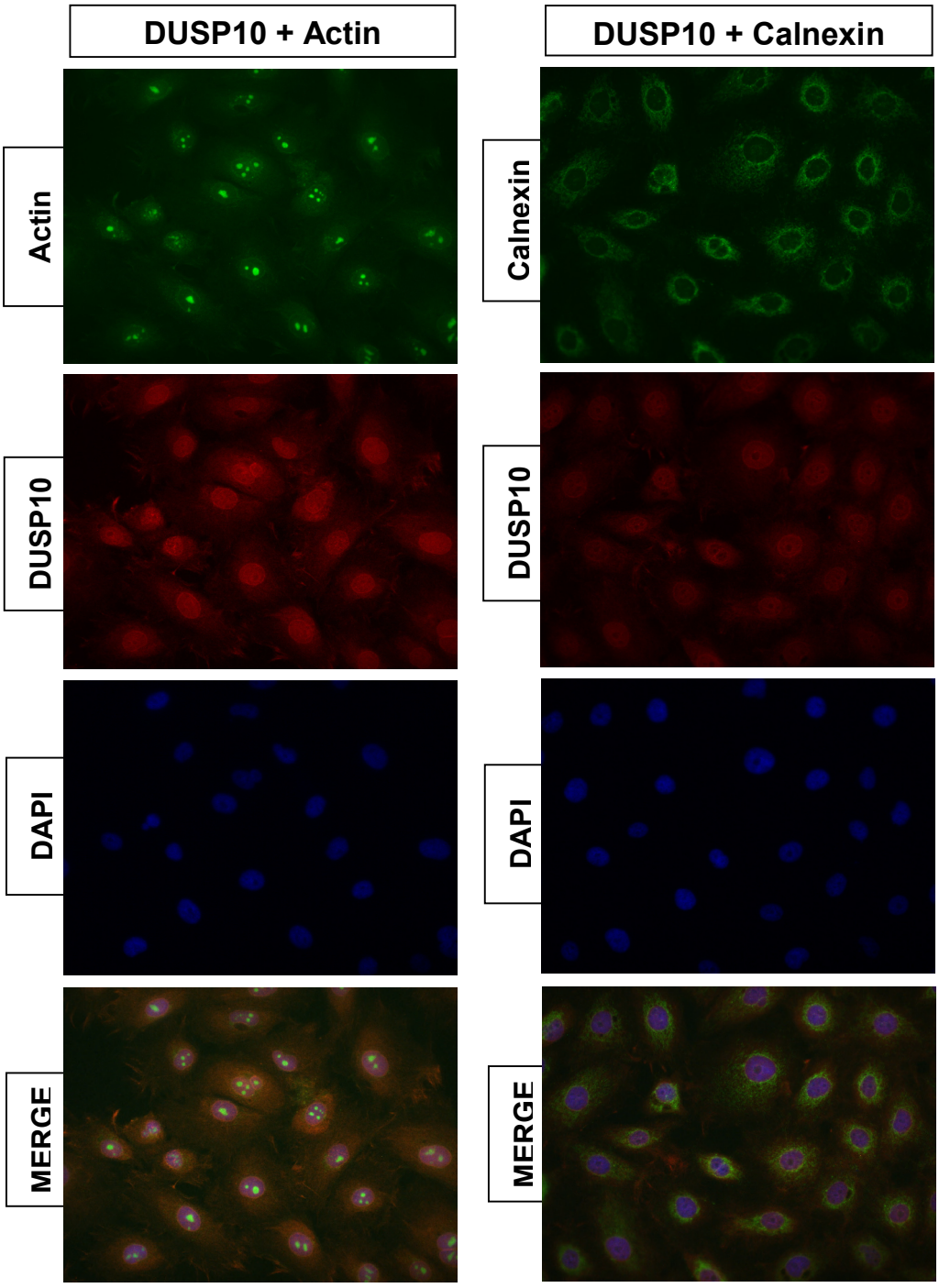

Fig.4.1.21: DUSP10/Actin and DUSP10/Calnexin staining in Snu182 cell line (40x): Actin antibody used stains the nucleoli, too, with great intensity. Except nucleoli, DUSP10 and Actin staining overlap

completely. In the group of images on the right, it can be seen that DUSP10 and Calnexin staining exclude each other completely in Snu182 cell line (which shows nuclear DUSP10 localization).

After these colocalization experiments, we concluded that DUSP10 localizes to the cytoplasm in most HCC cell lines and to the nucleus in others. The cytoplasmic DUSP10 tends to stack immediately around the nucleus in most cell lines that show cytoplasmic DUSP10 staining. In the others (Snu449 and SK-Hep1), the cytoplasmic DUSP10 tends to aggregate in bright foci. These specific clusterings of DUSP10 might be important in aiding its nuclear translocation when required.

4.1.5 Assesment of factors that may have an effect on DUSP10 localization

The observation that DUSP10 localizes to nuclei in some cell lines encouraged us to search for the factors that may be regulating and changing the subcellular localization of DUSP10.

4.1.5.1 Effect of senescence induction on DUSP10 localization

We checked if subcellular localization of DUSP10 changed in cells where senescence is induced either as a consequence of proliferative life spans of normal cells, or with senescence-inducing agents. We were especially interested in seeing if DUSP10 localization changes in replicative senescence, since DUSP10 is implicated as a senescence-associated phosphatase in our microarray data.

4.1.5.1.1 Nuclear translocation is seen in late passage MRC-5 fibroblasts compared to early passage cells

We employed MRC-5 embryonic fibroblast cell line as a non-cancerous cell line to check if DUSP10 localization changes in early passages (passage 16) compared to late passages (passage 30) of these cells.

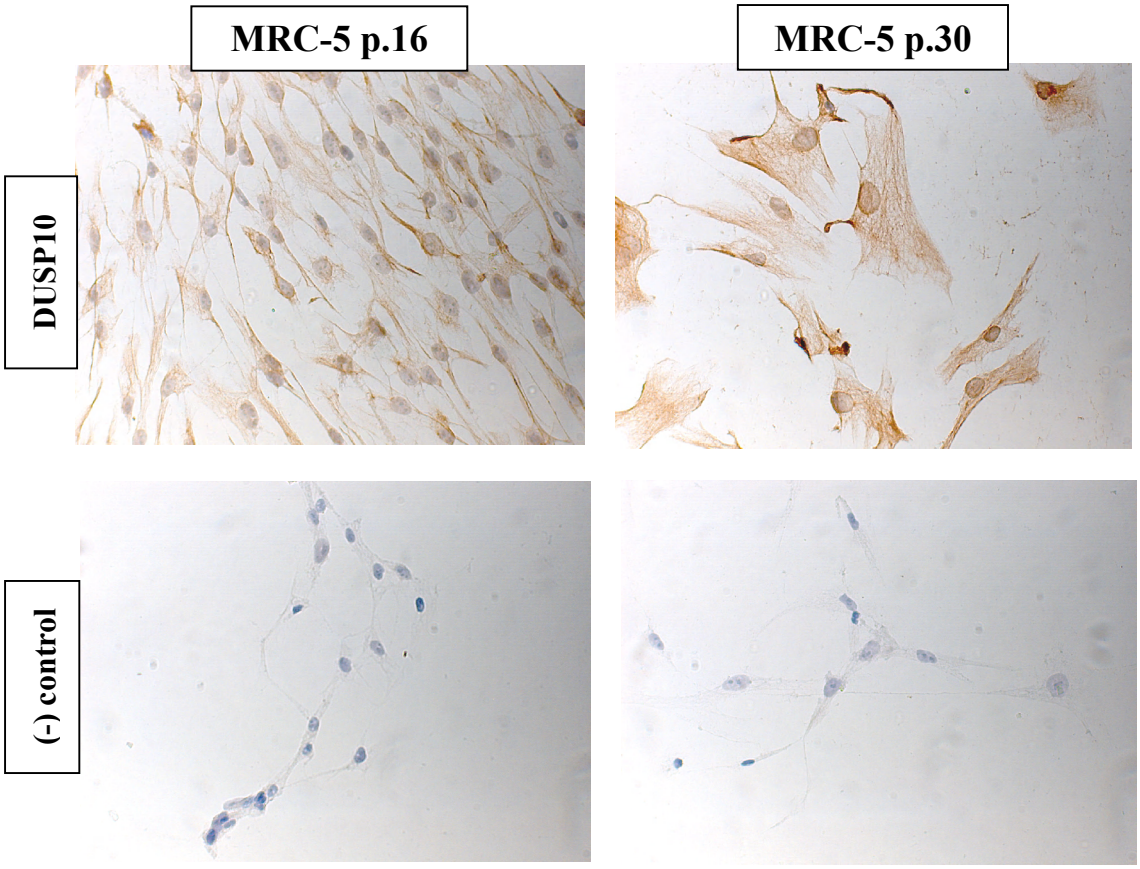

Fig.4.1.22: Effect of replicative senescence on DUSP10 subcellular localization (40x): In early passage fibroblasts (p.16) the nuclei are mostly blue due to hematoxylin counterstaining, whereas in late passage fibroblasts (p.30) the nuclei are mostly brown hinting at DUSP10 staining inside. Additionally, the enlargened morphology of late passage fibroblasts associated by senescence is clearly seen.

The result was promising, as DUSP10 localization seemed to be primarily in the cytoplasms of proliferating fibroblasts (p.16) compared to DUSP10 staining evenly in both cytoplasms and nuclei of aging cells (p.30) (Fig.4.1.22).

4.1.5.1.2 Camptothecin and TGF-β, senescence-inducing agents, do not have an effect on DUSP10 localization

We also checked if DUSP10 localization changes due to premature senescence induced by camptothecin (CPT) or TGF-β in Huh7 cell line. For this purpose, Huh7 cells were treated with 5ng/ml TGF-β, 10nM or 50nM CPT for four days before SAβG assay followed by DUSP10 immunostaining was performed. The concentrations for these reagents were determined by previous studies of our group (Şentürk Ş et al, unpublished data; Bilget-Güven E et al, unpublished data). The results are shown in Fig.4.1.23 and 4.1.24.

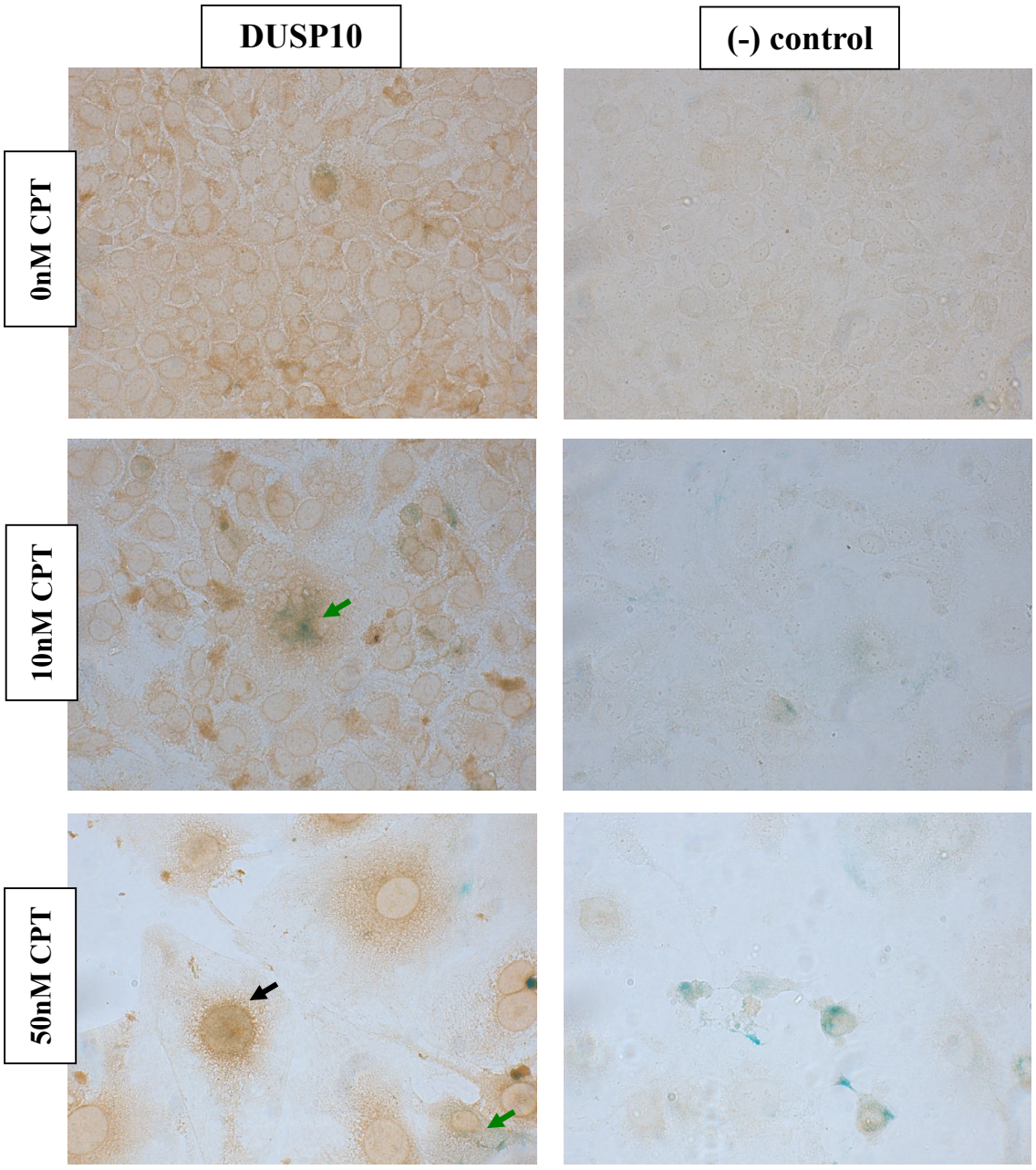

Fig.4.1.23: Effect of camptothecin on DUSP10 subcellular localization (40x): Nuclear DUSP10 (black arrow) and SAβG staining (green arrows) do not overlap. No counterstaining was done to prevent possible interference with the brown immunostaining.

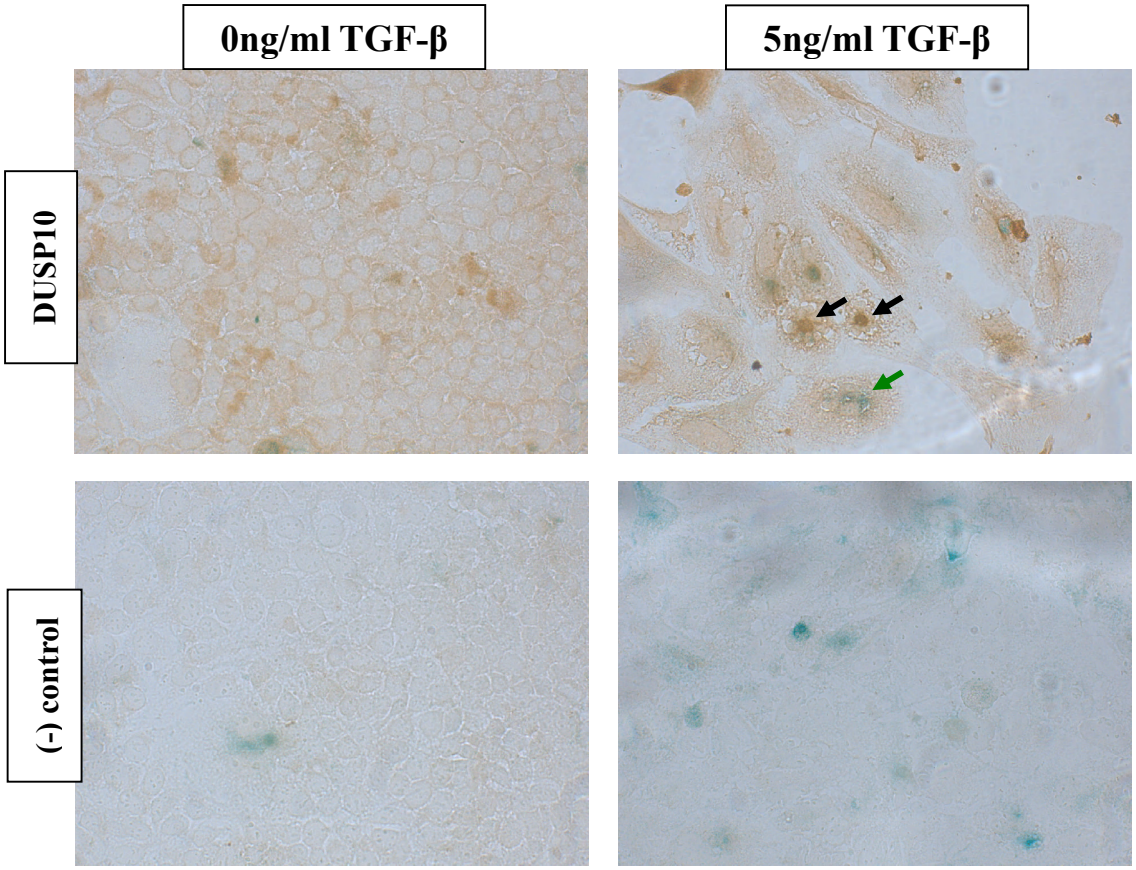

Fig.4.1.24: Effect of TGF-β on DUSP10 subcellular localization (40x): Nuclear DUSP10 (black arrows) and SAβG staining (green arrow) do not overlap. No counterstaining was done to prevent possible interference with the brown immunostaining.

These results indicate that DUSP10 localization shifts to nuclei due to replicative senescence, however it is not affected by premature senescence. We moved on to assess one more factor that may regulate the subcellular localization of DUSP10.

4.1.5.2 Effect of JNK and p38 MAPK inhibitors on the subcellular localization of DUSP10

Next, we reasoned that disruption of the pathways in which DUSP10 functions (Fig.4.1.25a-b), by kinase inhibitors, could have an effect on its subcellular localization through feedback regulation. For this purpose, we treated Hep3B and Snu182 cell lines with JNK and p38 inhibitors for three days and performed DUSP10 immunostaining. All these inhibitors are ATP-competitive, meaning they do not affect phosphorylation (and thus activation) of these kinases, but they disrupt the transmission of signal to downstream elements of the pathway by blocking phosphorylation of target proteins by the kinases.

The concentrations of inhibitors used were determined by our group's drug screening results which is also a branch of KANİLTEK project (performed on HCC cell lines to assess the cytotoxicity or proliferative arrest induced by a wide array of commercial kinase inhibitors) (Bilget-Güven E et al, unpublished).

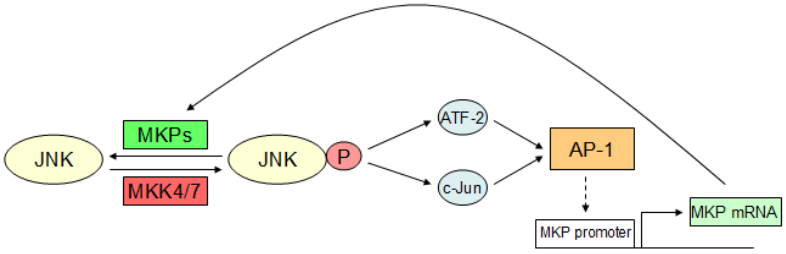

Fig.4.1.25a: Simplified JNK pathway and its possible feedback regulatory mechanism: JNK is phosphorylated at Thr-183 and Tyr-185 by MKK4/7. This is reversed by a number of phosphatases including DUSP10. Phosphorylated JNK acts on a variety of transcription factors in nucleus, such as c-Jun and ATF-2. These transcription factors form homo- or heterodimers which are collectively known as AP-1 transcription factor complexes. These complexes act on target promoters. MKP promoters are thought to be among these targets. Hence upon activation of JNK, a negative feedback loop is thought to form to control its activity (Teng CH et al, 2007).

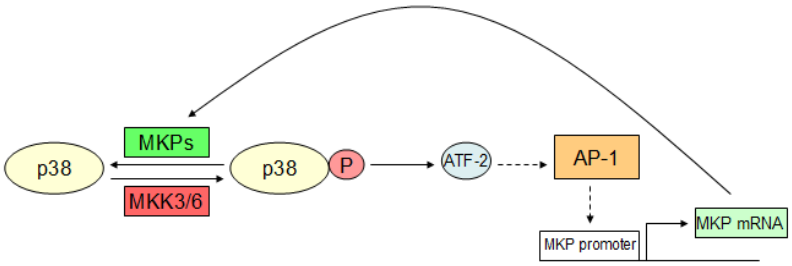

Fig.4.1.25b: Simplified p38 pathway and its possible feedback regulatory mechanism: p38 is phosphorylated at Thr-180 and Tyr-182 by MKK3/6. This is reversed by a number of phosphatases including DUSP10. Phosphorylated p38 acts on a variety of transcription factors in nucleus, such as ATF-2. This transcription factor form homodimers with another ATF-2 or heterodimers with other transcription factors, and these dimers are collectively known as AP-1 transcription factor complexes. These complexes act on target promoters. MKP promoters are thought to be among these targets. Hence upon activation of p38, a negative feedback loop may be generated to control its activity (see Krishna M, Narang H, 2008).

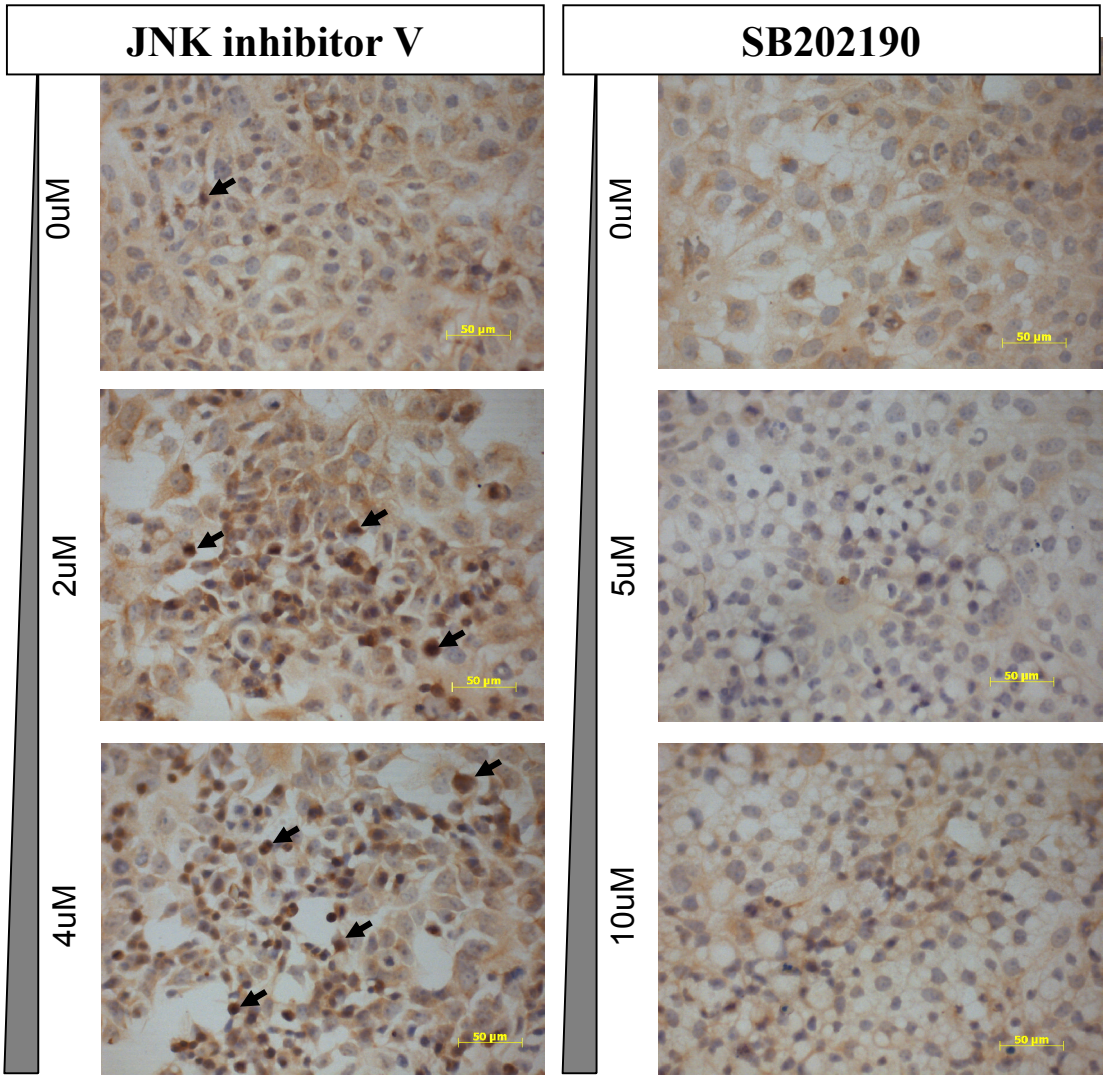

Fig.4.1.26a: Effect of JNK and p38 inhibitors on DUSP10 localization in Hep3B cell line (40x): Each inhibitor was used at its median inhibition concentration (IC50) and at the half of this concentration. To minimize the differences in staining due to procedural errors and changes, each inhibitor-treated sample is compared to its control and not to the other inhibitors' samples or controls. The arrows show examples of cells that we consider as having nuclear DUSP10. The results continue in the next page.

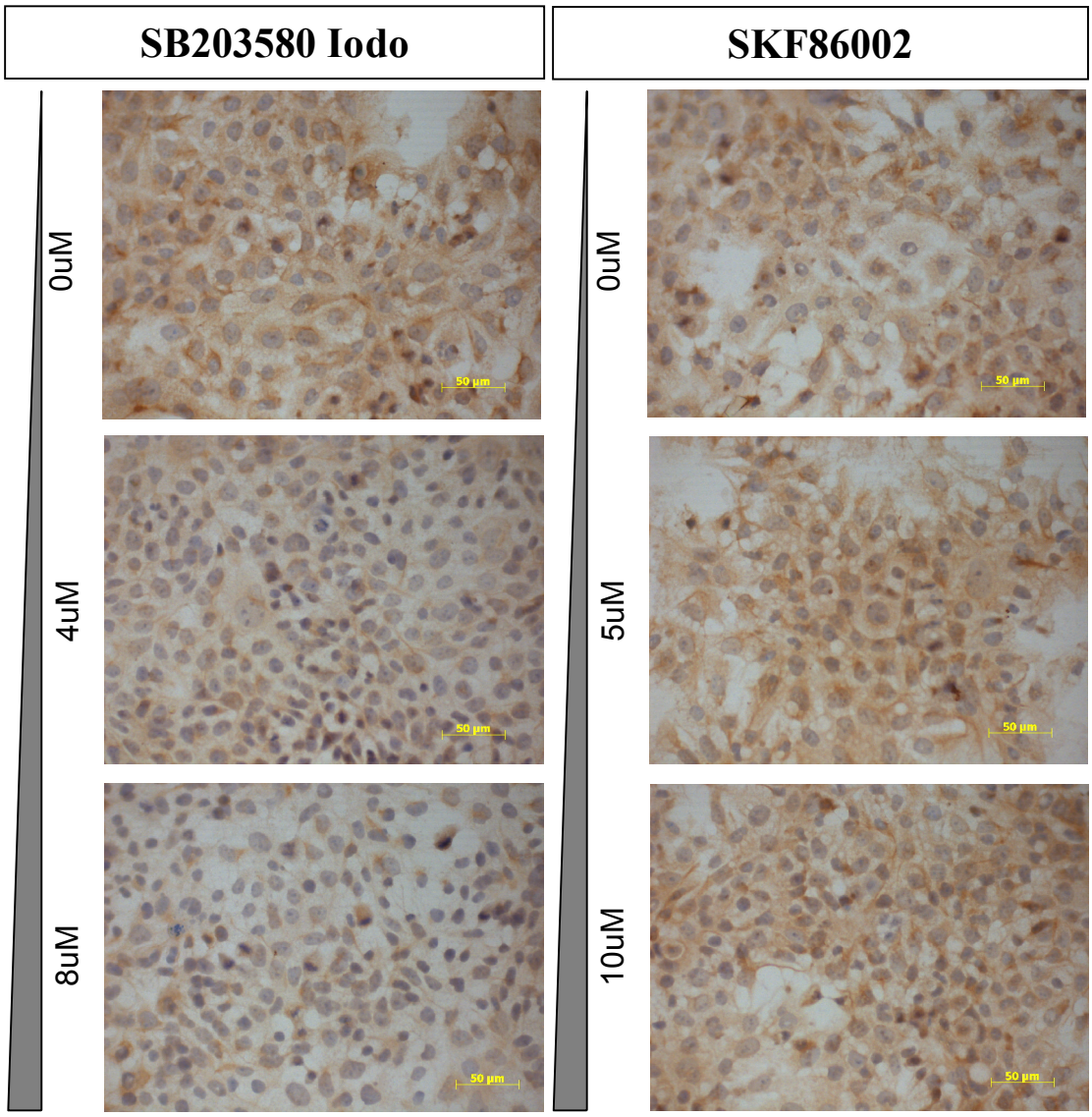

Fig.4.1.26a (continued): Effect of JNK and p38 inhibitors on DUSP10 localization in Hep3B cell line (40x): Each inhibitor was used at its median inhibition concentration (IC50) and at the half of this concentration. To minimize the differences in staining due to procedural errors and changes, each inhibitor-treated sample is compared to its control and not to the other inhibitors' samples or controls. The arrows show examples of cells that we consider as having nuclear DUSP10.

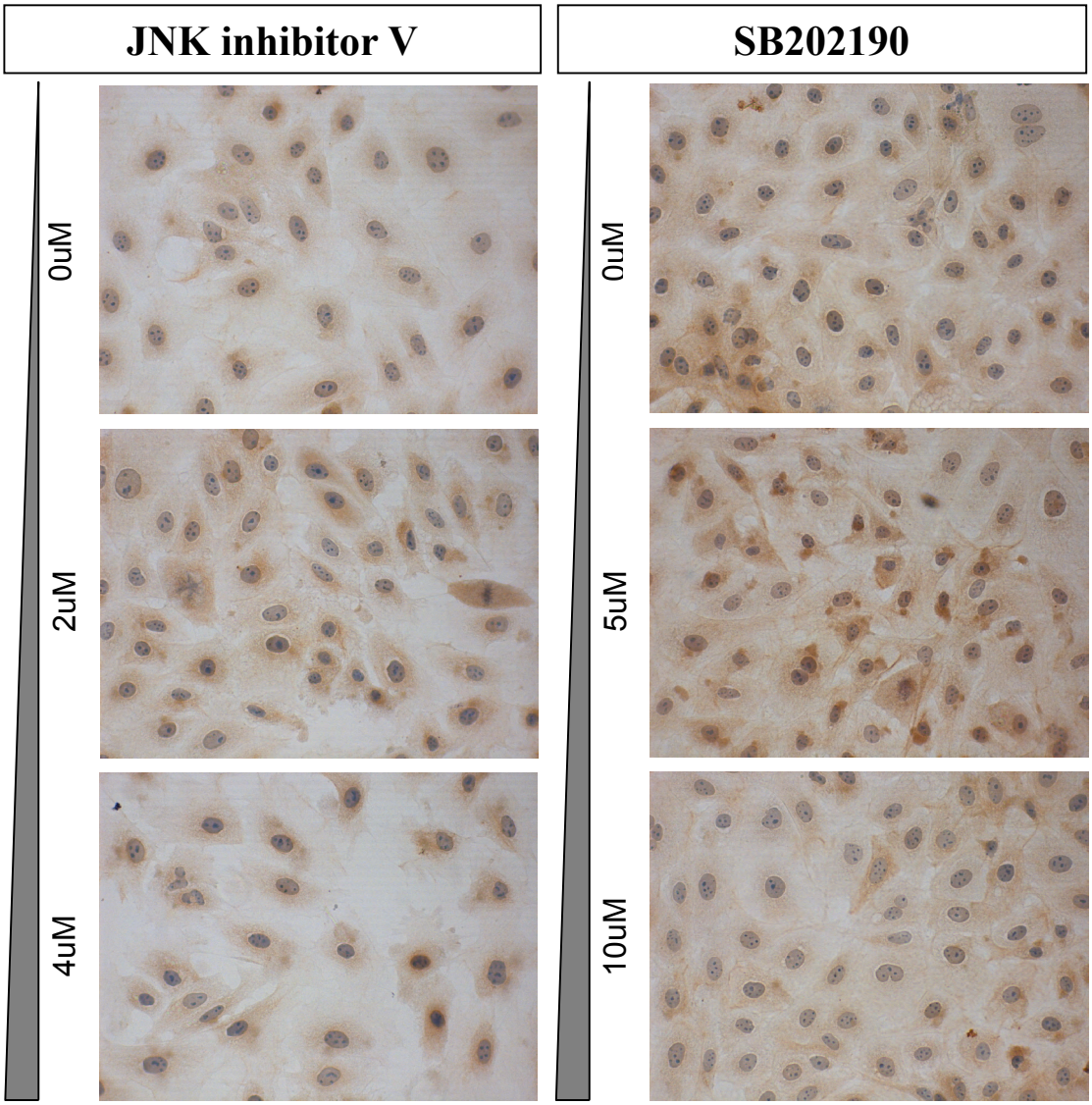

Fig.4.1.26b: Effect of JNK and p38 inhibitors on DUSP10 localization in Snu182 cell line (40x): Each inhibitor was used at its median inhibition concentration (IC50) and at the half of this concentration. To minimize the differences in staining due to procedural errors and changes, each inhibitor-treated sample is compared to its control and not to the other inhibitors' samples or controls. The results continue in the next page.

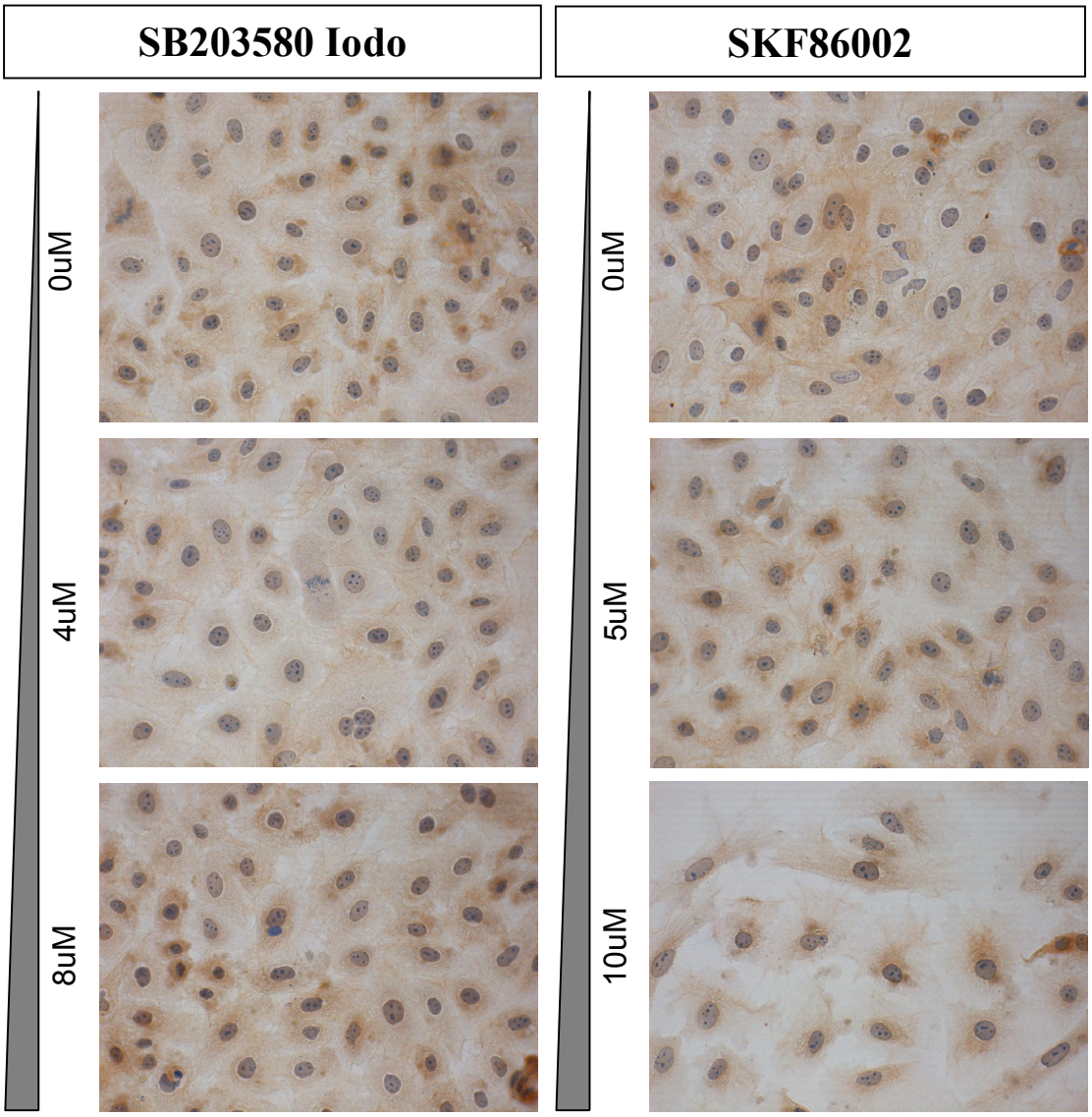

Fig.4.1.26b (continued): Effect of JNK and p38 inhibitors on DUSP10 localization in Snu182 cell line (40x): Each inhibitor was used at its median inhibition concentration (IC50) and at the half of this concentration. To minimize the differences in staining due to procedural errors and changes, each inhibitor-treated sample is compared to its control and not to the other inhibitors' samples or controls.

As can be seen in Fig.4.1.26a, JNK inhibitor V affected DUSP10 localization in Hep3B cell line where normally cytoplasmic DUSP10 is seen. The effects of p38 inhibitors were negligible. JNK inhibitor V treatment followed by DUSP10 immunostaining was also performed in Huh7, HepG2 and Mahlavu cell lines. The results are shown in Fig.4.1.27.

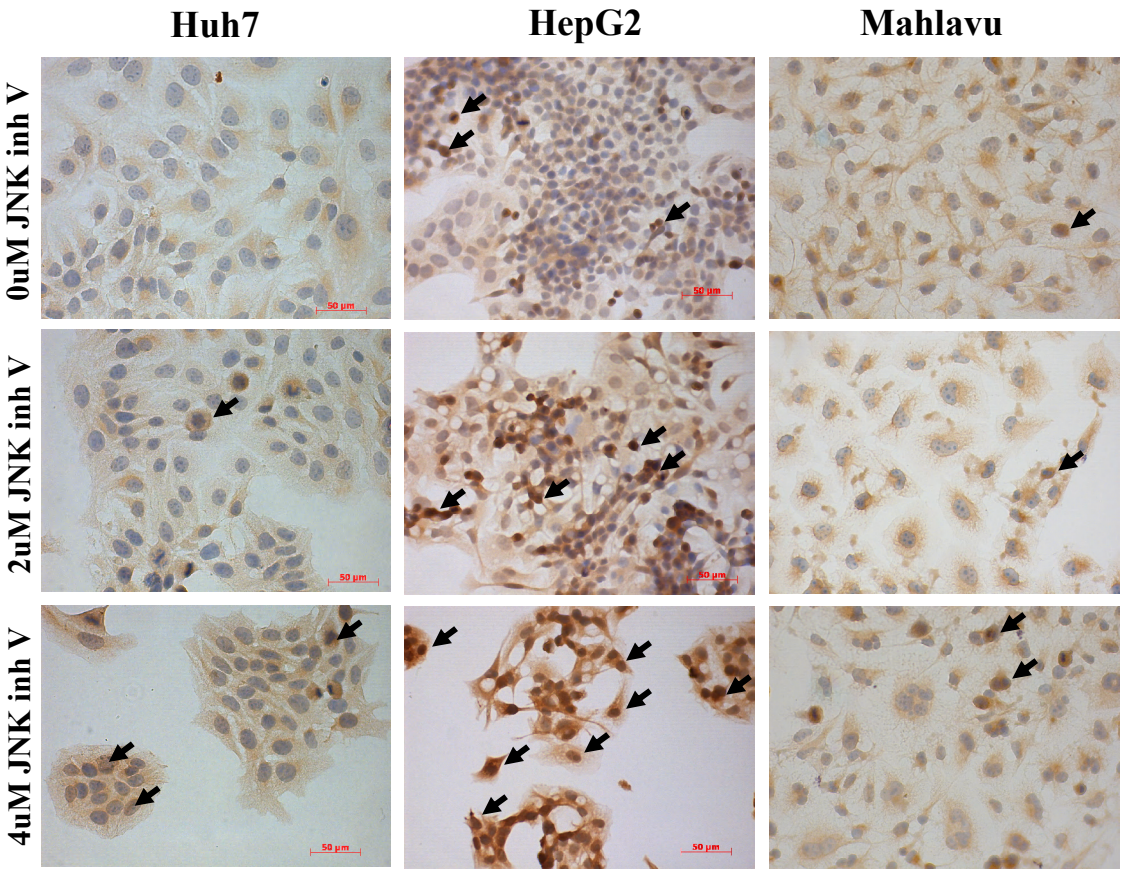

Fig.4.1.27: Effect of JNK inhibitor V on DUSP10 localization in Huh7, HepG2 and Mahlavu cell lines (40x): The arrows show examples of cells that we consider as having nuclear DUSP10.

It is seen that DUSP10 localization changed due to the inhibitor in Huh7 and HepG2 cell lines. DUSP10 amount also seemed to increase in inhibitor treated samples (IC50 concentration), although we could not detect this increase with Western blotting.

Next, quantification of nuclear DUSP10 staining was done by taking the percentages of cells similar to the ones marked with arrows in the figures in total number of cells. For this purpose, JNK inhibitor V treatment followed by DUSP10 immunostaining in Huh7, HepG2, Hep3B, Snu182 and Mahlavu cell lines were repeated twice more, completing the procedure to a triplicate. Three areas from each sample or control were counted, adding up to nine areas for each condition (0µM / 2µM / 4µM) considering a single cell line. The averages (and the standard deviations) are graphed in Fig.4.1.28a-e, and significant changes are marked.

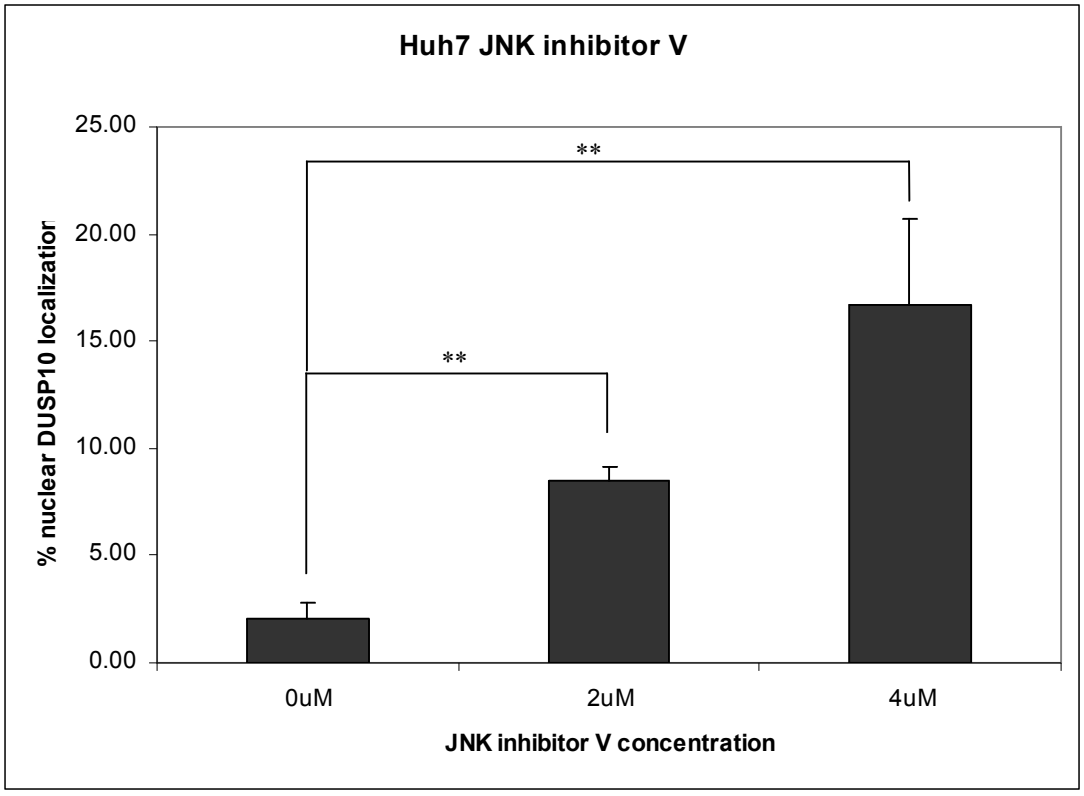

Fig.4.1.28a: Change in nuclear DUSP10 localization percentage in Huh7 cell line due to JNK inhibitor V: ** means $p < 0.001$.

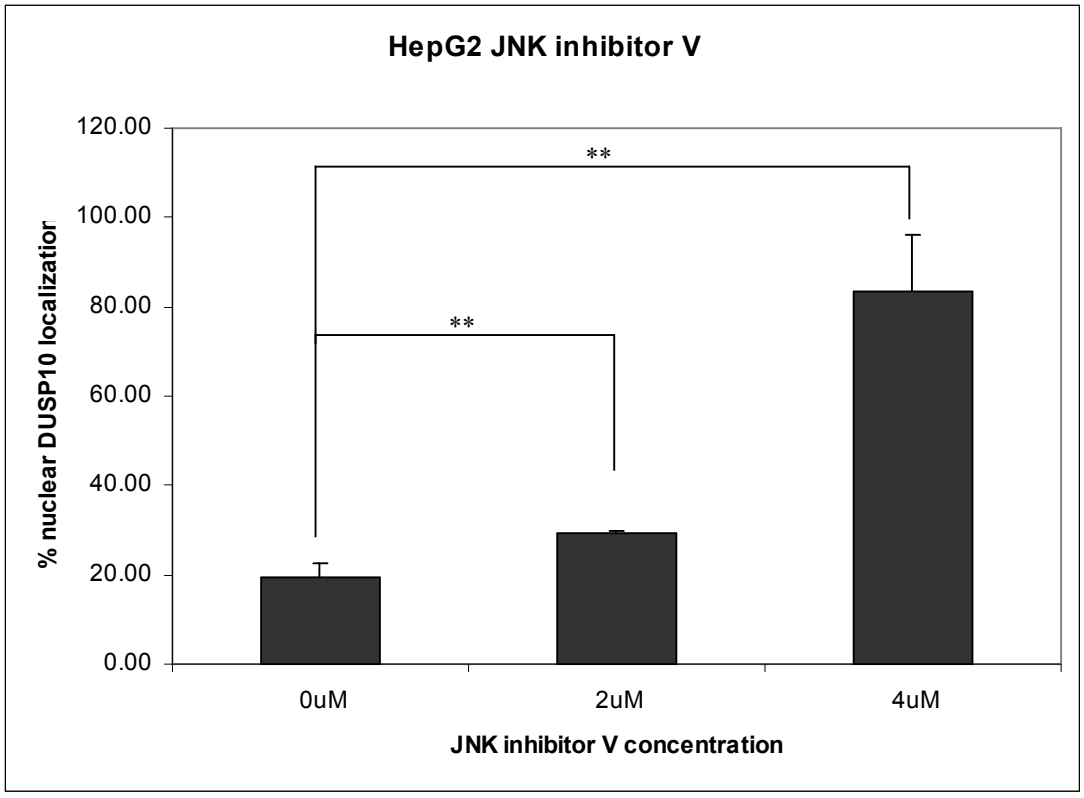

Fig.4.1.28b: Change in nuclear DUSP10 localization percentage in HepG2 cell line due to JNK inhibitor V: ** means $p < 0.001$.

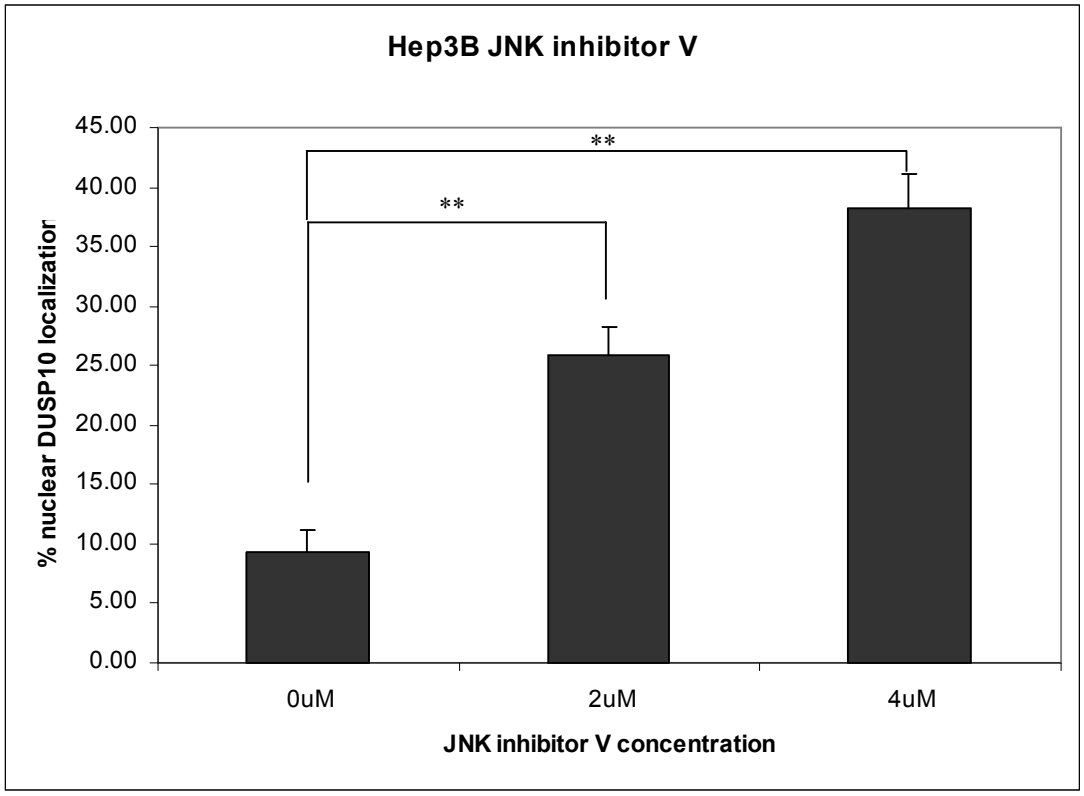

Fig.4.1.28c: Change in nuclear DUSP10 localization percentage in Hep3B cell line due to JNK inhibitor V: ** means $p < 0.001$.

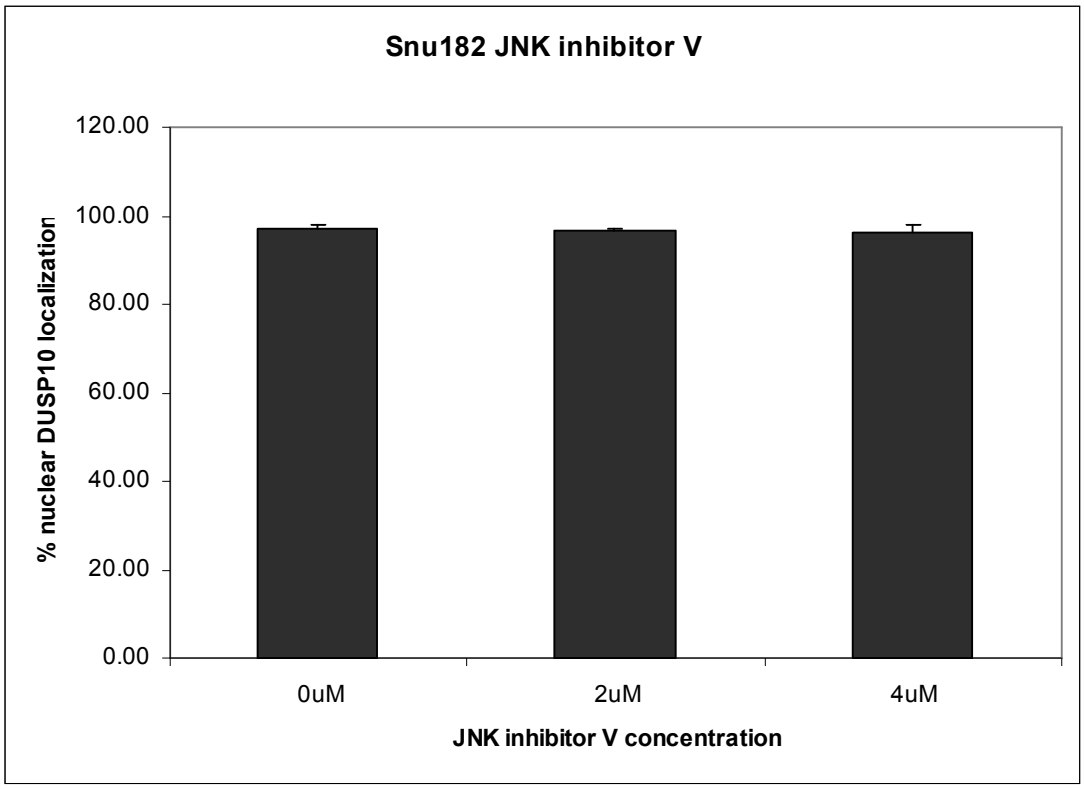

Fig.4.1.28d: Change in nuclear DUSP10 localization percentage in Snu182 cell line due to JNK inhibitor V: No significant change is observed.

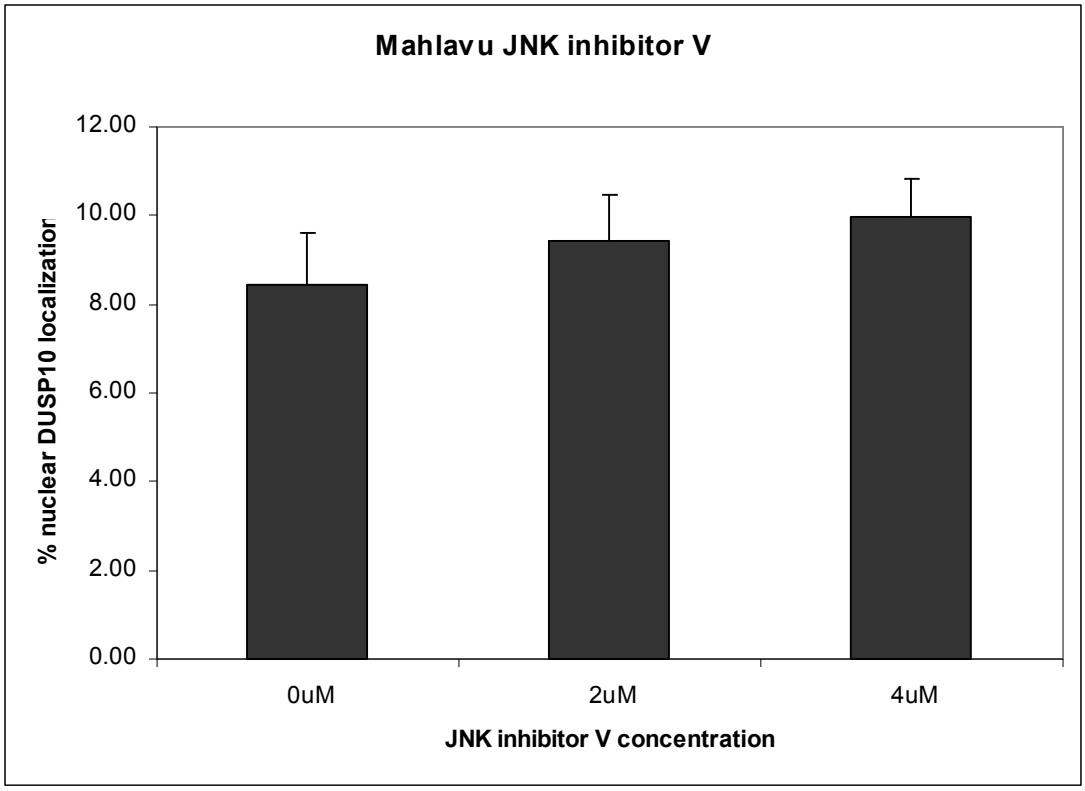

Fig.4.1.28e: Change in nuclear DUSP10 localization percentage in Mahlavu cell line due to JNK inhibitor V: No significant change is observed.

These results show that DUSP10 localization changes significantly in Huh7, Hep3B and HepG2 cell lines, which are well-differentiated HCC cell lines (see section 4.1.4.1). Hence this difference in response to JNK inhibitor V may indicate a difference in the regulation of JNK pathway in well- versus poorly-differentiated cell lines.

In the website of Calbiochem, where JNK inhibitor V was bought from, it is stated that for concentrations of JNK inhibitor V below 10μM, no inhibition of kinases other than JNK1/2/3 are seen. Although the growth-inhibitory concentration of JNK inhibitor V is known from yet unpublished results of our group, the inhibition of JNK due to this inhibitor was not yet confirmed. So our next move was to verify that the concentration of JNK inhibitor V we used efficiently inhibits JNK pathway. For this, Huh7 cells were incubated with or without 4μM JNK inhibitor V for 2 hrs. Afterwards, cells were additionally incubated with or without 300μM H_2O_2 for 2 hrs. Cell pellets were collected and after protein extraction, Western blotting was done to check for c-Jun transcription factor phosphorylation, which is the best known JNK target (hence the name; "c-Jun N-terminal kinase"). Fig.4.1.29 shows that JNK is

indeed inhibited by JNK inhibitor V in our experiments.

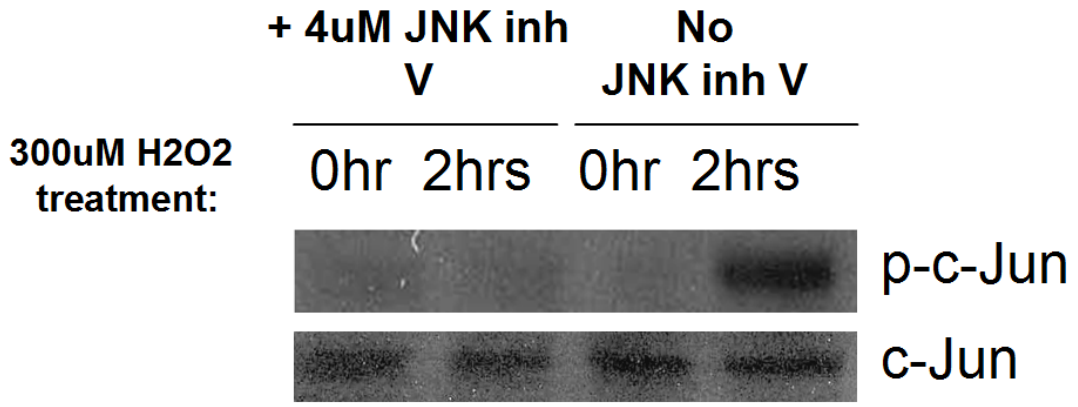

Fig.4.1.29: Effect of the used concentration of JNK inhibitor V on c-Jun phosphorylation in Huh7 cells: The effective concentration and incubation time for H_2O_2 treatment of Huh7 cells is taken from Taki K et al, 2008. Total c-Jun blotting was done to check equal protein amounts.

Since we observed a difference in DUSP10 localization between well- and poorly-differentiated HCC cell lines in response to JNK inhibitor V, we wanted to see if amounts of active JNK or p38 also differ between these cell line types, somehow rendering the poorly-differentiated cells unresponsive to the inhibitor. The results are shown below.

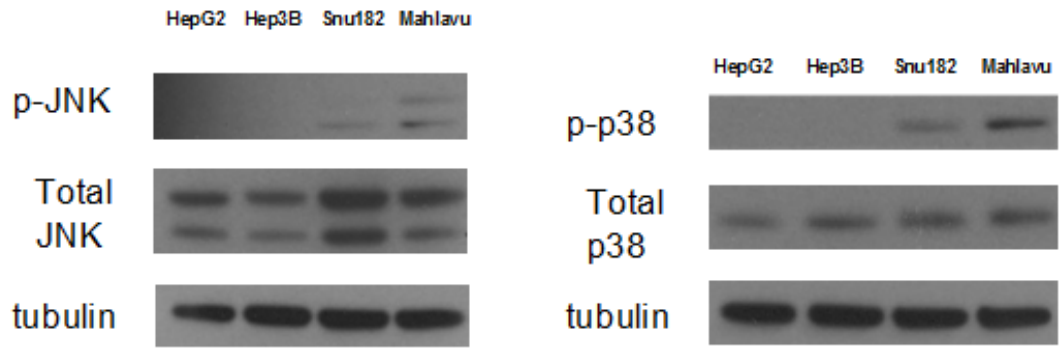

Fig.4.1.30: Phosphorylated and total JNK or p38 amounts in HepG2, Hep3B, Snu182 and Mahlavu cell lines: Both JNK1 (46 kDA) and JNK2/3 (54 kDA) are recognized by these antibodies and result in two bands on the membrane. Only p38α is recognized by these antibodies. Tubulin is used as an internal control to check for equal protein loading.

It is seen that in poorly-differentiated cell lines, but not in well-differentiated ones, JNK and p38 are phosphorylated, which probably results in constitutive activity of these MAPKs that are related to a variety of responses including apoptosis and senescence.

Additional experiments on this topic focused on confocal microscopy which we expected to give more detailed results on the change of DUSP10 localization in response to JNK inhibitor V. The results are shown below.

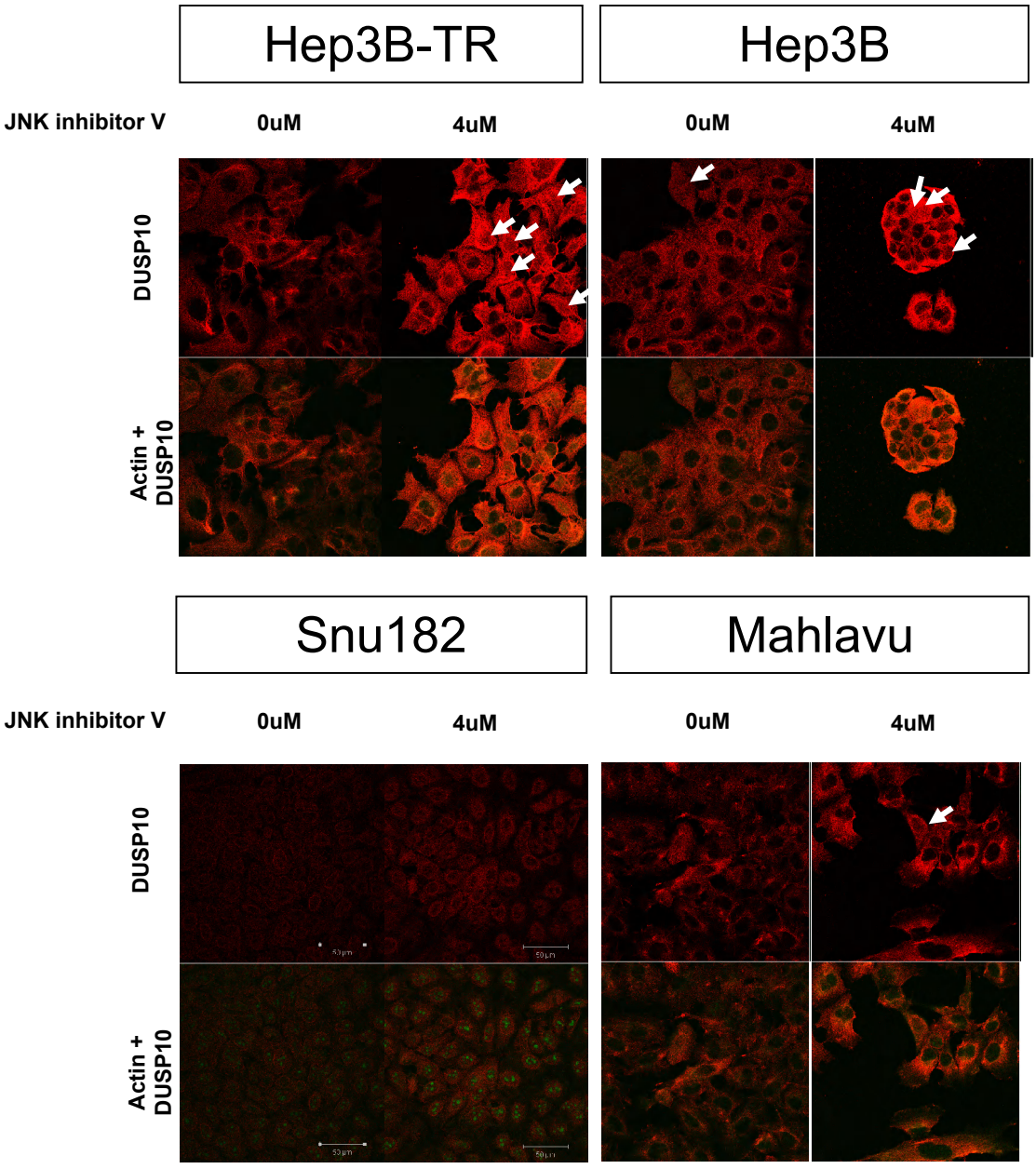

Fig.4.1.31: Confocal microscopy results on inhibitor treatment of selected HCC cell lines (40x): All images were taken at the planes where DUSP10 staining is the highest. Interestingly, DUSP10 shows high peri-nuclear staining in Snu182 cell line. Arrows are used to point out the cells that show nuclear DUSP10 staining in cell lines that normally have cytoplasmic DUSP10. Since JNK inhibitor V is a growth-inhibitory agent, the number of Hep3B and Hep3B-TR cells are observed to be decreased in response to treatment.

These results also confirm a shift from cytoplasm to nucleus for DUSP10, much better observed in well-differentiated cell lines (Hep3B and Hep3B-TR).

An increase in DUSP10 staining intensity is also observed, especially according to Figs.4.1.27 (results for HepG2) and 4.1.31 (results for Hep3B and Hep3B-TR). We tried to quantify this increase in staining intensity by Western blotting against DUSP10. However, we could not observe an increase in DUSP10 protein amount, as shown below:

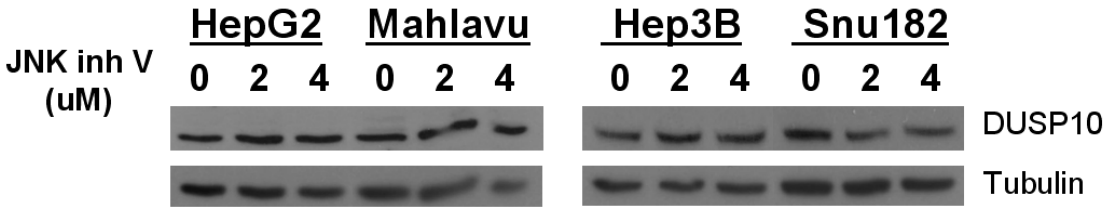

Fig.4.1.32: DUSP10 protein amounts upon JNK inhibitor V treatment in the cell lines employed: No change in DUSP10 amount could be detected. Tubulin is used as an internal control to check for equal protein loading.

Hence all of these experiments have shown that DUSP10 changes its localization upon inhibition of JNK signaling in epithelial-like HCC cell lines. Inhibition of p38 signaling does not affect DUSP10 localization. Additionally, localization change is not observed in mesenchymal-like HCC cell lines.

4.1.6 Ectopic overexpression studies for DUSP10

Expression vectors containing the coding sequence of DUSP10 isoform **a**, pEGFP-DUSP10 and pcDNA-DUSP10, were constructed, as mentioned in Methods chapter. Transient transfection of these constructs were performed in Huh7 cell line. However no significant overexpression was detected after 48 hours of transfection (Fig.4.1.33). These results may be pointing out a tight control over DUSP10 expression in Huh7.

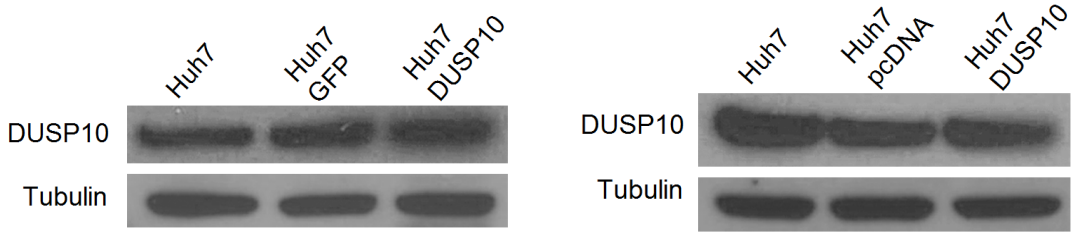

Fig.4.1.33: No significant overexpression of DUSP10 is seen upon transient transfection: Huh7 cells were transfected with empty and DUSP10-containing vectors. Proteins were were extracted 48 hours later and Western blotting was done. **Left,** transient transfection results of pEGFP-DUSP10 are seen. The empty vector is pEGFP-N2 in this case. **Right,** transient transfection results of pcDNA-DUSP10 are seen. The empty vector is pcDNA3.1/myc-His B.

4.2 MTMR11

4.2.1 Bioinformatics analysis of MTMR11

4.2.1.1 Sequence and gene information

MTMR11 stands for "myotubularin related protein 11." The NCBI Gene ID for MTMR11 is 10903. The locus in which MTMR11 gene resides is named as NC_000001 (version 10) and it corresponds to a 249250621 bp linear DNA sequence. It has been mapped to the minus strand of the q arm of human chromosome 1; its exact location is 1q12-21 according NCBI database and UCSC Human genome browser (Fig.4.2.1) (1q21.2 according to Ensembl database). Studies report gain of 1q in most of HCC samples analyzed, which implicates that the genes located on this chromosomal arm may be important in early stages of hepatocarcinogenesis (Tornillo L et al, 2002; Kitay-Cohen Y et al, 2001; Guan X-Y et al, 2000).

chromosome: 1; **Location:** 1q12-q21

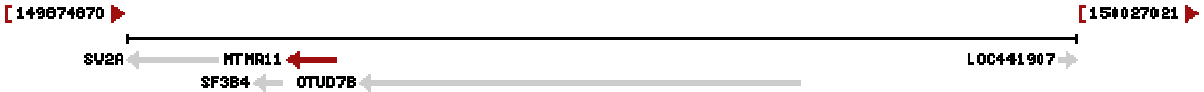

Fig.4.2.1: Genomic context of MTMR11 gene.

The gene has two transcripts, coding for two protein isoforms a and b, a being the dominant one. Transcript variant 1 of 2879 nucleotides (NM_001145862.1) codes for isoform a of 709 aminoacids (NP_001139334.1) and has 17 exons. Transcript variant 2 of 2368 nucleotides (NM_181873.3) codes for isoform b of 640 aminoacids (NP_870988.2) and also has 17 exons. The exons that MTMR11 transcript variant 1 contain are named as 1, 2b, 3a, 4-16, 17b, whereas the exons that MTMR11 transcript variant 2 contain are named as 2a, 3b, 4-16, 17a and 17c. The translated region of transcript variant 1 is 2130 basepairs (bp) long whereas translated region of transcript variant 2 is 1923 bp long.

Additionally, 29 SNPs (single nucleotide polymorphisms) have been reported in GeneCards database (Rebhan M et al, Trends in Genetics, 1997) so far for MTMR11 gene. Most SNPs are intronic. There are two non-synonymous SNPs located in this

gene. One of them is a M (methionine) to V (valine) aminoacid change at position 159 of MTMR11 isoform a (position 87 of isoform b) with minor allele frequency of 0.22. The other is a Q (glutamine) to P (proline) aminoacid change at position 531 of isoform a (position 459 of isoform b) with minor allele frequency of 0.03. These SNPs are not associated with a disease state.

4.2.1.2 Protein information

4.2.1.2.1 General information

The protein encoded by MTMR11 gene is designated as "myotubularin related protein 11." MTMR11 isoform a is represented in SWISS-PROT Database by A4FU01-1 symbol and it consists of 709 aminoacids, corresponding to a molecular weight of 79.5 kDa and a theoretical isoelectric point (pI) of 6.59. MTMR11 isoform b is represented by A4FU01-4 symbol and it consists of 640 aminoacids, corresponding to a molecular weight of 72.1 kDa and a theoretical pI of 6.98. The presence of the other isoforms listed in SWISS-PROT Database are not supported by experimental evidence, and hence are included in this section.

MTMR11 isoform b lacks residues 1-72 of isoform a. Other differences are TNF (isoform a) to MPP (isoform b) change at position 73-75 of isoform a; and RAEGDLG (isoform a) to QSHPFWITRC (isoform b) change at position 703-709 of isoform a. MTMR11 belongs to a subfamily of phosphatases named as myotubularin phosphatases which are dual specificity phosphatases that can dephosphorylate both proteins and lipids (phosphoinositides).

4.2.1.2.2 Protein domains and motifs

MTMR11 is known to be a myotubularin related protein and thus contains such a domain according to Motif Scan search (Fig.4.2.2a and b). There are also different sites that may be subject to modification associated with each different isoform. These "possible" sites given by Motif Scan search are weak matches as they are motifs that are frequently found in other proteins and may not be specific to MTMR11.

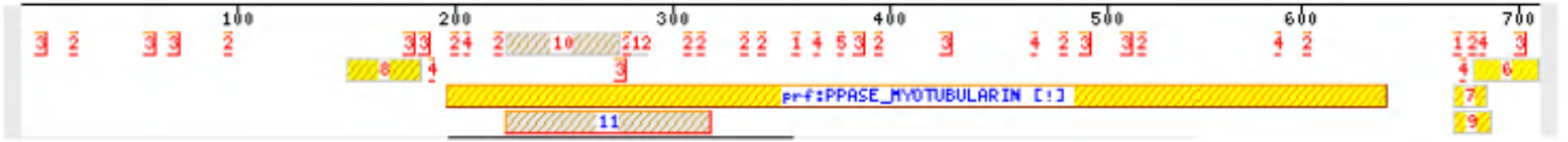

Fig.4.2.2a: Motif Scan results of MTMR11 isoform a: 1. Possible cAMP- and cGMP-dependent protein kinase phosphorylation sites: Position 355-358, 670-673, **2.** Possible casein kinase II phosphorylation sites: Positions 23-26, 94-97, 198-201, 218-221, 277-280, 305-308, 311-314, 331-334, 339-342, 393-396, 478-481, 514-517, 601-604, 677-680, **3.** Possible N-myristoylation sites: Positions 7-12, 57-62, 68-73, 176-181, 183-188, 273-278, 383-388, 423-428, 487-492, 506-511, 698-703, **4.** Possible protein kinase C phosphorylation sites: Positions 188-190, 204-206, 365-367, 465-467, 588-590, 673-675, 682-684, **5.** Possible RGD (Arg-Gly-Asp) motif (cell attachment sequence found in proteins of extracellular matrix): Position 376-378, **6.** Possible CG-1 DNA binding domain: Position 679-709, **7.** Possible bipartite nuclear localization signal: Position 670-685, **8.** Possible protein phenyltransferases alpha subunit repeat: Position 150-164, **9.** Possible bipartite nuclear localization signal: Position 670-687, **10.** Myotubularin-related domain according to pfam_fs: Position 223-275, **11.** Myotubularin-related domain according to pfam_ls: Position 223-317, **12.** Possible octapeptide repeat (found in several bacterial proteins, may be function in immunoglobulin binding): Position 281-288. The number next to each site or domain indicates its position on the protein in terms of amino acid numbers. There is also an un-numbered site as can be seen on the figure: PPASE_MYOTUBULARIN (Myotubularin phosphatase domain, position 196-639).

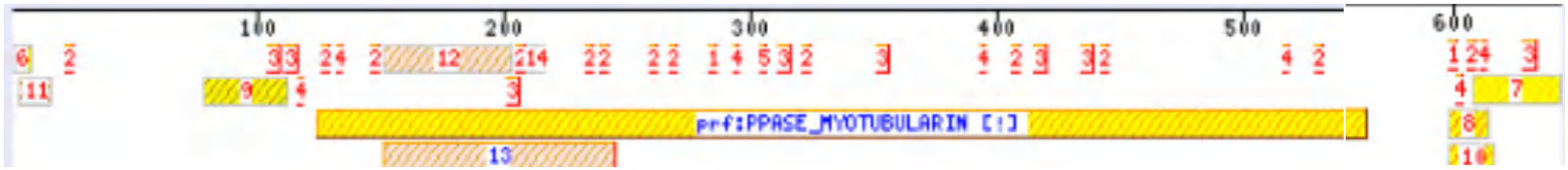

Fig.4.2.2b: Motif Scan results of MTMR11 isoform b: 1. Possible cAMP- and cGMP-dependent protein kinase phosphorylation sites: Position 283-286, 598-601, **2.** Possible casein kinase II phosphorylation sites: Positions 22-25, 126-129, 146-149, 205-208, 233-236, 239-242, 259-262, 267-270, 321-324, 406-409, 442-445, 529-532, 605-608, **3.** Possible N-myristoylation sites: Positions 104-109, 111-116, 201-206, 311-316, 351-356, 415-420, 434-439, 626-631, **4.** Possible protein kinase C phosphorylation sites: Positions 116-118, 132-134, 293-295, 393-395, 516-518, 601-603, 610-612, **5.** Possible RGD (Arg-Gly-Asp) motif (cell attachment sequence found in proteins of extracellular matrix): Position 304-306, **6.** Possible Big-1 (bacterial Ig-like domain 1) domain: Position 1-8, **7.** Possible CG-1 DNA binding domain: Position 607-640, **8.** Possible bipartite nuclear localization signal: Position 598-613, **9.** Possible protein phenyltransferases alpha subunit repeat: Position 78-112, **10.** Possible bipartite nuclear localization signal: Position 598-615, **11.** CHCH domain motif (Cys-X9-Cys motif found in some yeast proteins) : Position 3-16, **12.** Myotubularin-related domain according to pfam_fs: Position 151-203, **13.** Myotubularin-related domain according to pfam_ls: Position 151-245, **14.** Possible octapeptide repeat (found in several bacterial proteins, may be function in immunoglobulin binding): Position 209-216. The number next to each site or domain indicates its position on the protein in terms of amino acid numbers. There is also an un-numbered site as can be seen on the figure: PPASE_MYOTUBULARIN (Myotubularin phosphatase domain, position 124-567).

According to Gene Ontology (GO) Project, the molecular function terms associated with MTMR11 are DNA binding, ligand-dependent nuclear receptor activity and phosphatase activity. As seen in Fig.4.2.2a and b, MTMR11 has possible DNA binding domains and bipartite nuclear localization signals, hence these may be true sites. However SWISS-PROT lists MTMR11 as a probable pseudophosphatase since it contains a Glu residue instead of a conserved Cys residue in the catalytic loop rendering it catalytically inactive, although this information is not confirmed with experiments yet. In myotubularin related protein superfamily, there are a number of pseudophosphatases, which are thought to bind and regulate the active phosphatases. For example, pseudophosphatases MTMR5 and MTMR13 are known to be regulatory partners of MTMR2 (Kim S-A et al, 2003; Robinson FL, Dixon JE, 2005). Hence being a pseudophosphatase should not deprive MTMR11 of its value.

4.2.1.2.3 Protein structure

Secondary-structure information on MTMR11 isoforms was obtained by querying at NPS (Network Protein Sequence Analysis) database (Combet C et al, 2000), using PHD (Rost B, Sander C, 1994), DSC (King RD, Stenberg MJ, 1996) and MLRC on GOR4, SIMPA96 and SOPMA (Guermeur Y et al, 1999) prediction methods. According to this, MTMR11 isoform a contains 26.09% alpha helices, 13.54% extended strands and 58.11% random coils (Fig.4.2.3a), and, MTMR11 isoform b contains 27.81% alpha helices, 13.28% extended strands and 56.56% random coils (Fig.4.2.3b).

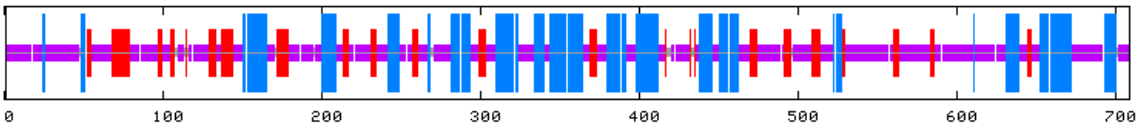

Fig.4.2.3a: NPS consensus secondary structure prediction for MTMR11 isoform a: Red parts mark the extended strands, blue parts mark the alpha helices, and purple parts mark the random coils. Alpha helices are associated with the functional domain mostly.

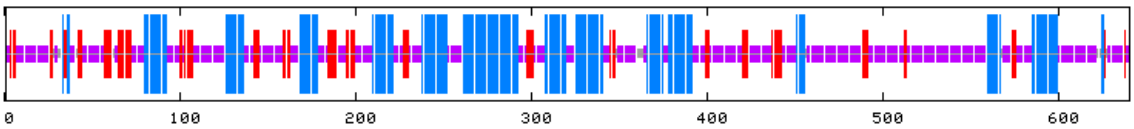

Fig.4.2.3b: NPS consensus secondary structure prediction for MTMR11 isoform b: Red parts mark the extended strands, blue parts mark the alpha helices, and purple parts mark the random coils. Alpha helices are associated with the functional domain mostly.

No three dimensional structure can be found for MTMR11 in PDB or ModBase databases.

4.2.1.3 Gene homologs and protein sequence conservation

4.2.1.3.1 Orthologs of MTMR11

According to HomoloGene Database of NCBI, orthologs of MTMR11 exist in five other species. This database only gives results for isoform b. These species, and the extent of identity between their MTMR11 genes/proteins and *Homo sapiens* MTMR11 gene/protein is listed in Table 4.2.1.

Gene		Identity (%)	
Species	Symbol	Protein	DNA
Homo sapiens	**MTMR11**		
vs. Pan troglodytes	MTMR11	99.8	99.7
vs. Canis lupus familiaris	MTMR11	91.1	91.3
vs. Bos taurus	MTMR11	91.5	92.5
vs. Mus musculus	Mtmr11	88.2	85.9
vs. Rattus norvegicus	Mtmr11	89.6	86.4

Table 4.2.1: Orthologs of human MTMR11 and multiple alignment pair-wise similarity scores between MTMR11 protein and DNA sequences of different species.

The multiple sequence alignment of the protein sequences of these orthologs were generated using ClustalW2 (Thompson JD et al, 1997). Fig.4.2.4 shows the conserved residues among different species. The sequences aligned from top to bottom belong to Homo sapiens (human), Pan troglodytes (chimpanzee), Bos taurus (cow), Canis lupus familiaris (dog), Mus musculus (mouse) and Rattus Norvegicus (rat), respectively.

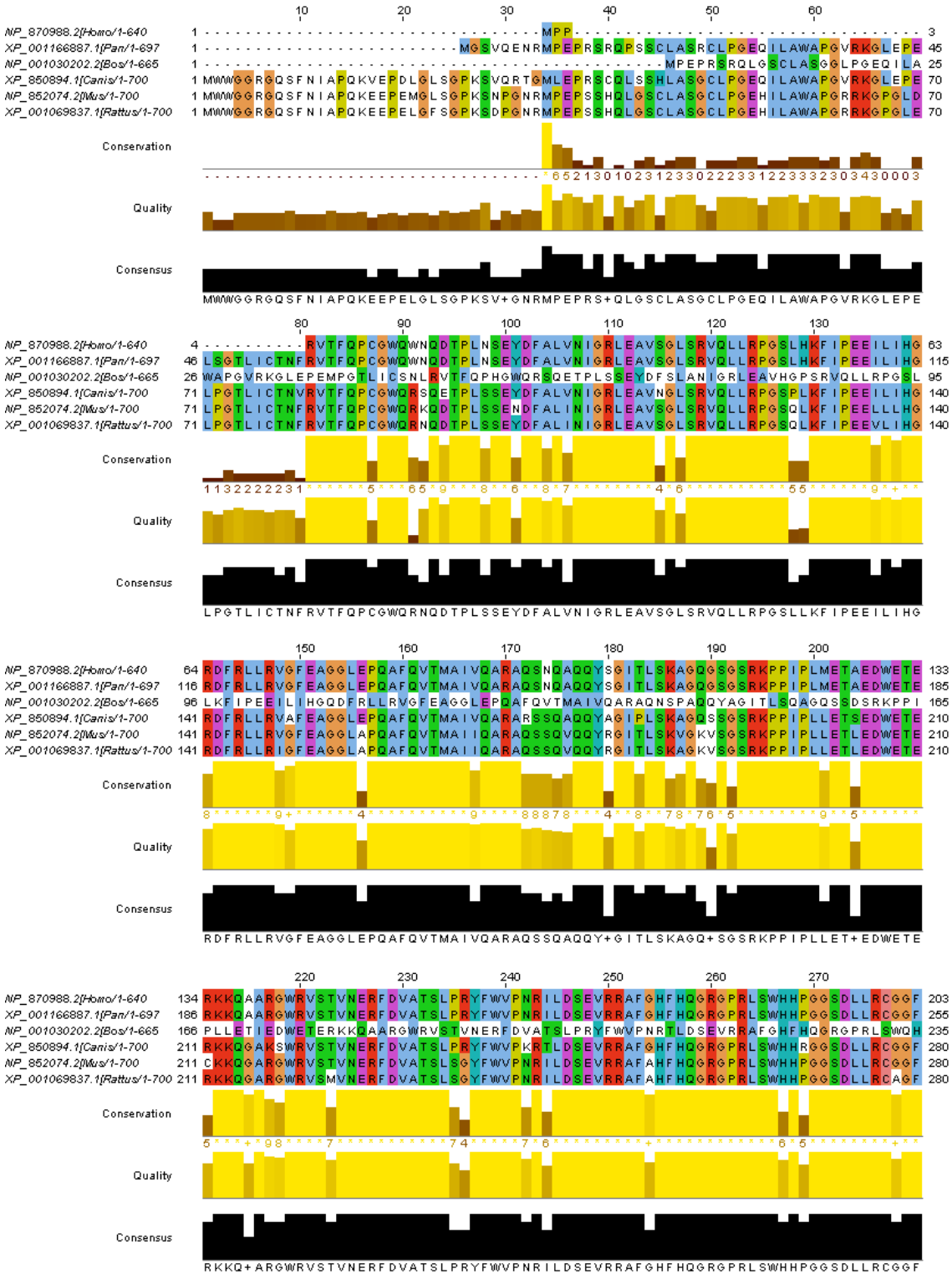

Fig.4.2.4: ClustalW2 multiple sequence alignment of MTMR11 (transcript variant 2) orthologs: From top to bottom: Human, chimpanzee, cow, dog, mouse and rat orthologs are listed. Interestingly when the beginning 72 bases of dog, mouse and rat MTMR11 orthologs are compared to the first 72 bases of MTMR11 transcript variant 1, a very high similarity is seen. The results continue in the following pages.

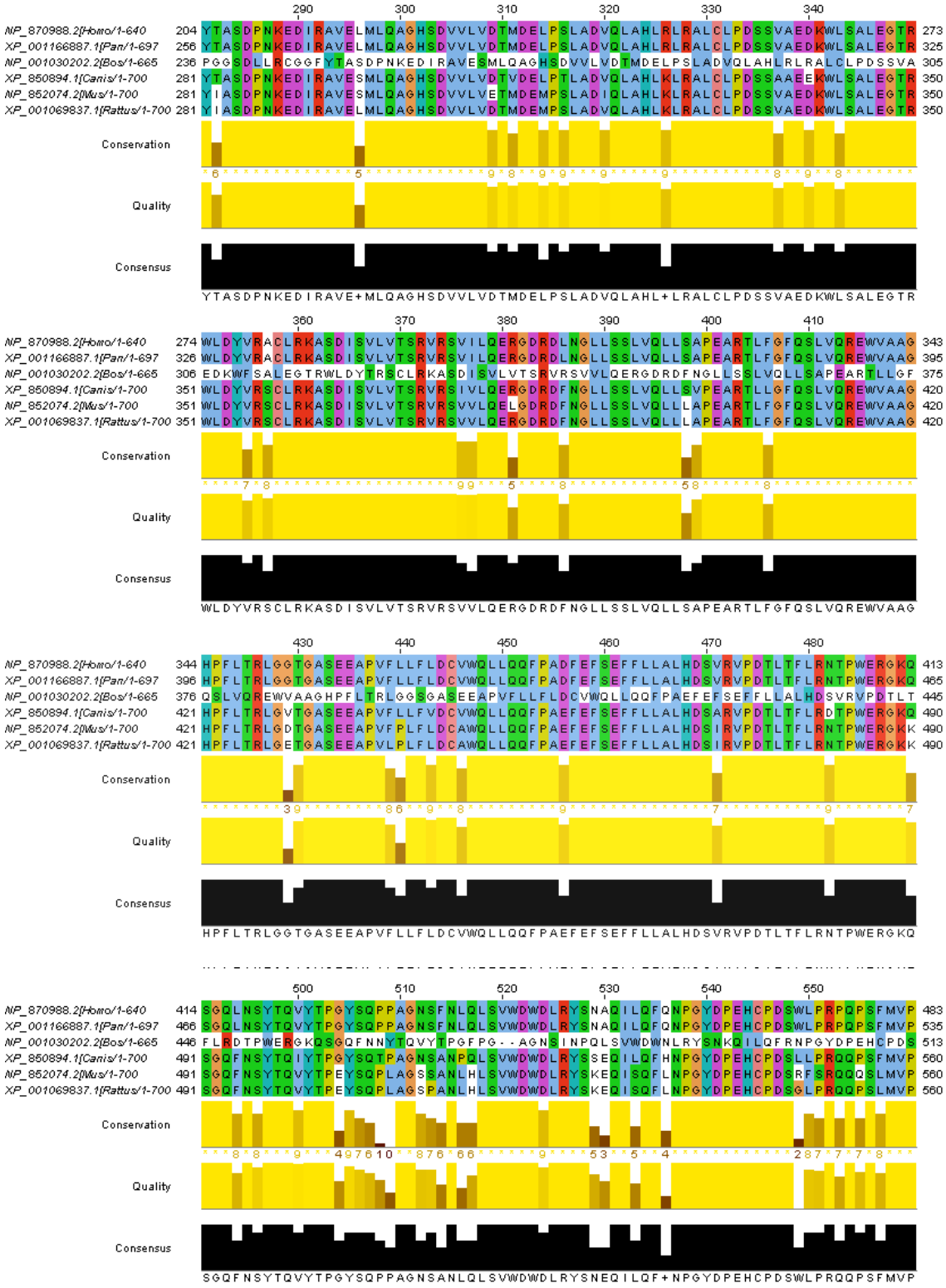

Fig.4.2.4 (continued): ClustalW2 multiple sequence alignment of MTMR11 (transcript variant 2) orthologs: From top to bottom: Human, chimpanzee, cow, dog, mouse and rat orthologs are listed. Interestingly when the beginning 72 bases of dog, mouse and rat MTMR11 orthologs are compared to the first 72 bases of MTMR11 transcript variant 1, a very high similarity is seen. The results continue in the next page.

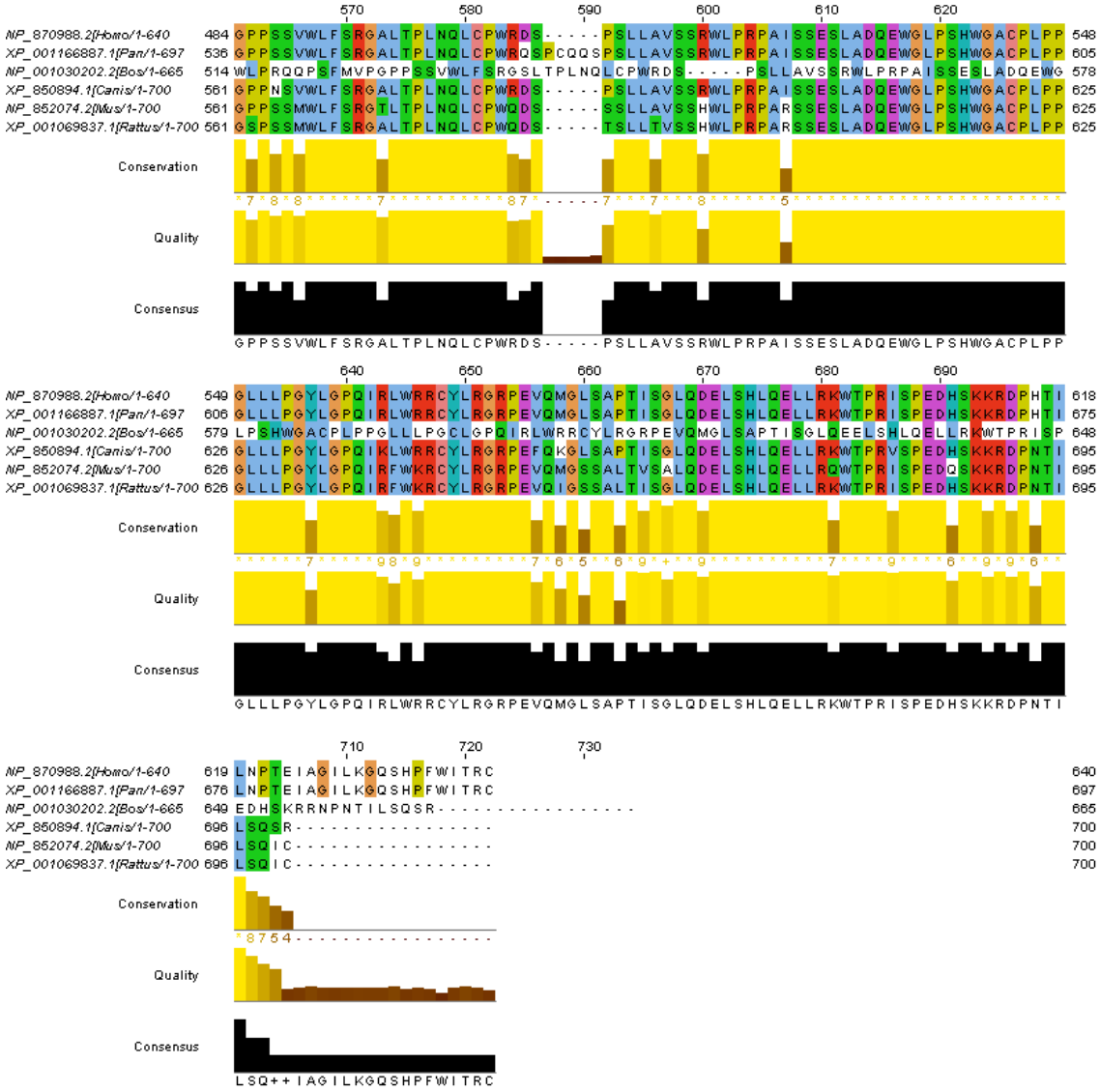

Fig.4.2.4 (continued): ClustalW2 multiple sequence alignment of MTMR11 (transcript variant 2) orthologs: From top to bottom: Human, chimpanzee, cow, dog, mouse and rat orthologs are listed. Interestingly when the beginning 72 bases of dog, mouse and rat MTMR11 orthologs are compared to the first 72 bases of MTMR11 transcript variant 1, a very high similarity is seen.

4.2.1.3.2 Paralogs of MTMR11

MTMR11 belongs to a phosphatase subfamily named as myotubularin phosphatases under the family dual specificity phosphatases, as already mentioned. A phylogenetic showing the relations of myotubularin phosphatases are shown in Fig.4.2.5. Additionally, conserved motifs found in all MTMRs are shown in Fig.4.2.6.

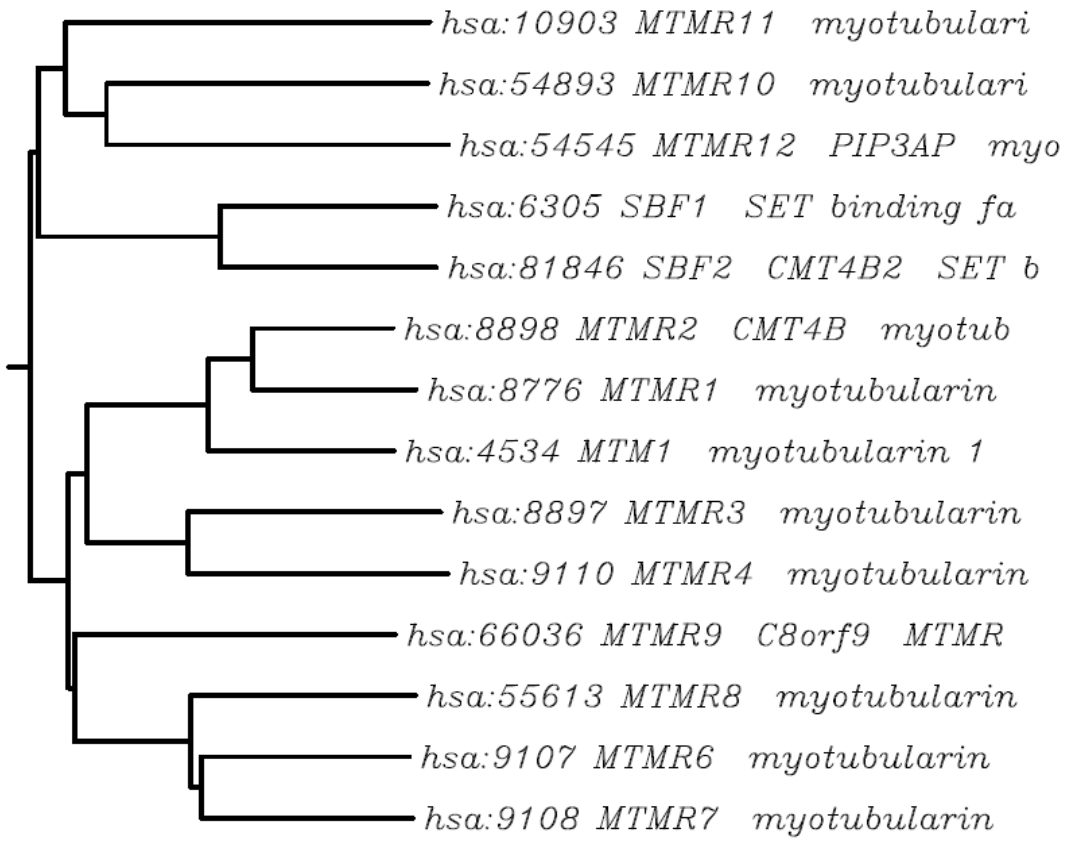

Fig.4.2.5: Phylogenetic tree of myotubularin phosphatase gene family with branch lengths: Includes only human genes. Paralogs are gathered by KEGG SSDB paralog search. Phylogenetic tree is generated by MAFFT sequence alignment.

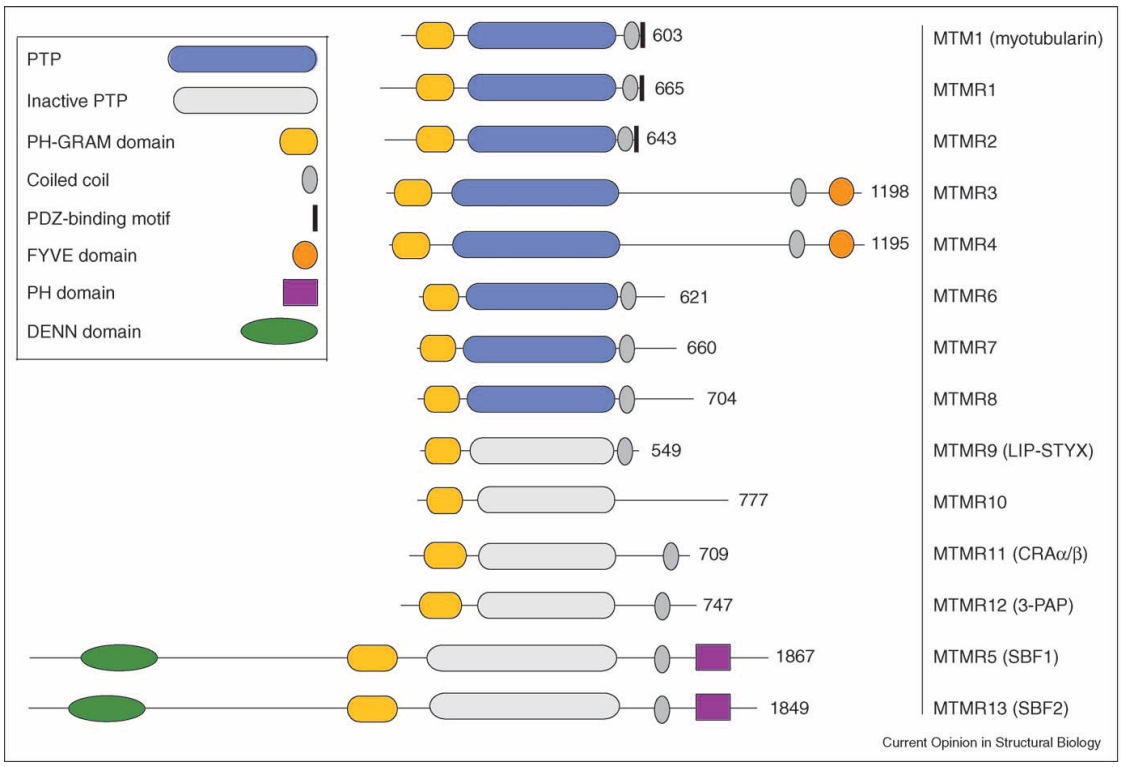

Fig.4.2.6: Conserved motifs in myotubularin phosphatases: DENN stands for "differentially expressed in neoplastic versus normal cells," and have yet to be experimentally characterized, but are proposed to function as GTPase effector domains. PH-GRAM (GRAM stands for "glucosyltransferases, Rab-like GTPase activators and myotubularins," the proteins it was first found in) domains are important in protein- or lipid-binding interactions. PH domains (stands for "pleckstrin homology") are best known as phosphoinositide-binding modules that target their host proteins to specific cell membranes. FYVE domain (stands for "FYVE finger-containing phosphoinositide kinase (Fab1), vesicle transport protein Vac 1, and EEA1," the proteins it was first found in) is a PIP-binding module known to target host proteins to endosomal membranes where PIP (inositol monophosphate) is concentrated. Coiled-coil motifs are predicted in most myotubularins and, in several cases, mediate interactions between active and inactive family members. PDZ-binding motif (stands for "postsynaptic density 95, disk large, zona occludens-1," the proteins it was first found in) is a small protein-protein interaction module that is thought to play a role in the clustering of submembranous signalling molecules. Myotubularin phosphatase domain is a type of PTP domain that is larger and contains regulatory domains. The figure is taken from Begley MJ, Dixon JE, 2005.

4.2.1.4 MTMR11 in gene expression profiling arrays

MTMR11 was searched for in Oncomine Cancer Profiling Database. Once found, differential expression data in liver tissue were searched for. The results are plotted in Fig.4.2.7a and b. MTMR11 gave significant results in both of the two important studies on liver (Wurmbach_Liver and Chen_Liver). Interestingly, this gene shows an upregulation in HCC compared to non-tumorous tissues. This may point out to the fact that MTMR11's upregulation in senescent clones according to our group's microarray data is coincidental, and it is not functionally related to the reversion of immortal phenotype seen in these clones.

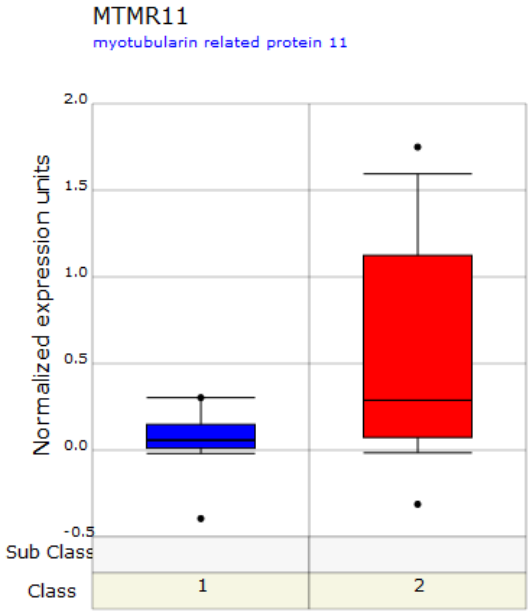

Fig.4.2.7a: MTMR11 expression in Wurmbach microarray data: Normal (Class 1, n=10) vs HCC (Class 2, n=35), p=1.5E-4.

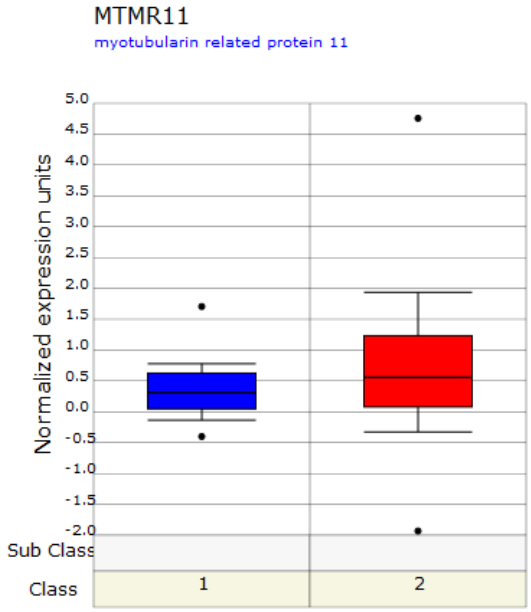

Fig.4.2.7b: MTMR11 expression in Chen microarray data: Non-tumor liver (Class 1, n=76) vs HCC (Class 2, n=104), p=0.003.

Additionally, in both microarray data, the non-tumorous expression of MTMR11 occurs in a more compact range, which means that it is expressed in similar levels in all normal samples, whereas its cancerous expression occurs in a larger range, meaning there is considerable difference in expression of this gene in different HCC samples. The grades and prognostic information of the HCC samples used could still

indicate an importance of this gene in HCC.

4.2.1.5 Expression data

On the UCSC (University of California, Santa Cruz) Genome Browser website, the expression data of MTMR11 isoform a can be obtained from several microarray studies. The data gathered from the GNF Expression Atlas 2 human data on Affy U133A and GNF1H chips (Su AI et al, 2002), where red represents high expression level and green represents low expression level, is shown in Fig.4.2.8.

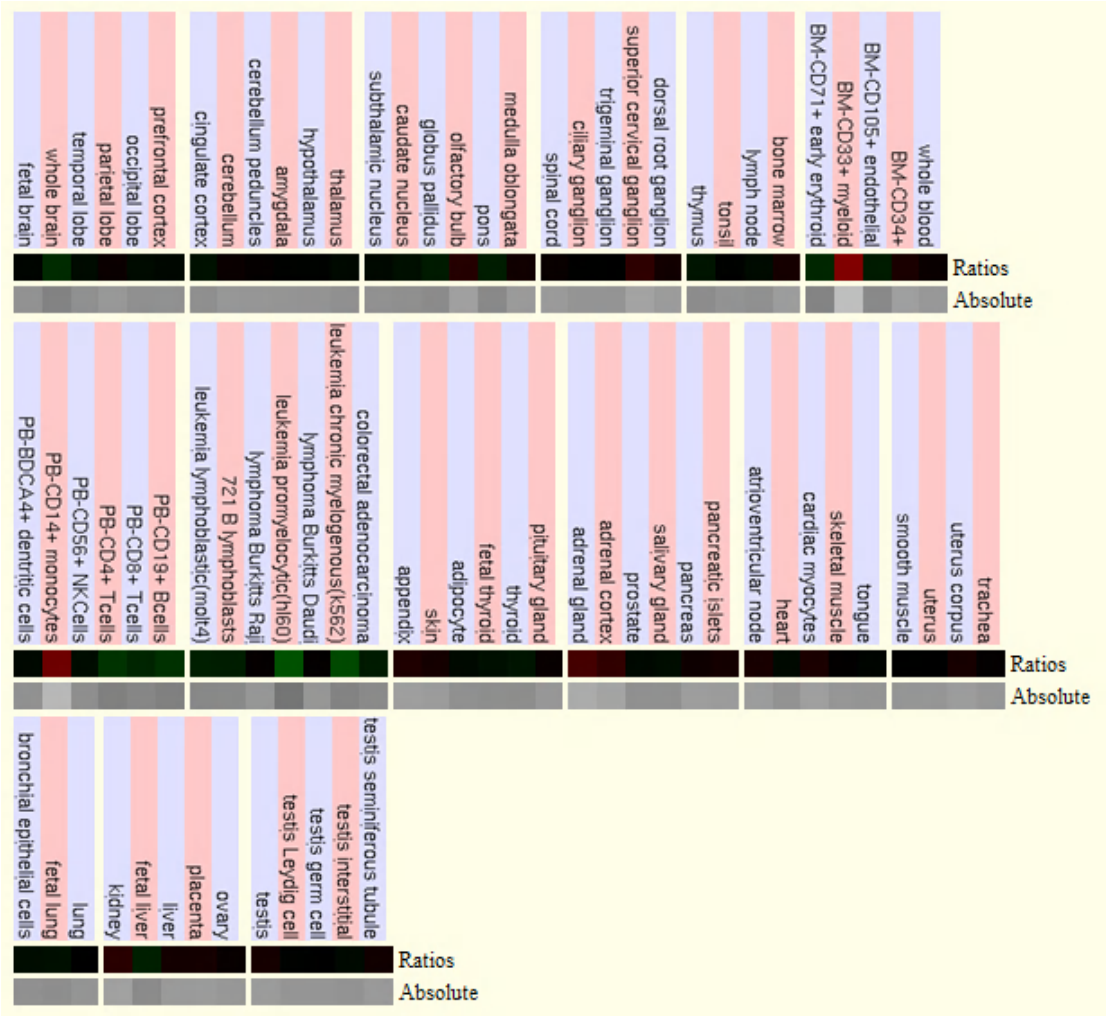

Fig.4.2.8: Expression data of DUSP10 based on the GNF Expression Atlas 2 Data from U133A and GNF1H Chips.

According to this expression data, although generally all tissues and cells tested expressed MTMR11 to a certain level (as indicated by the dominance of the black color), it is expressed more in some differentiated immune system and hematopoietic

lineage cell types, adrenal gland and adrenal cortex. Relatively low levels of MTMR11 is detected in remaining differentiated immune system and hematopoietic lineage cell types, promyelocytic leukemia, chronic myelogenous leukemia and fetal liver.

4.2.2 Analysis of MTMR11 expression change between senescent and immortal Huh7 clones

Just like DUSP10 case, as a first step, we performed PCR to verify MTMR11 differential expression in C1, C3-Early and C3-Late clones. The result of this PCR and a graph to show the relative expression of MTMR11 in each clone are shown below:

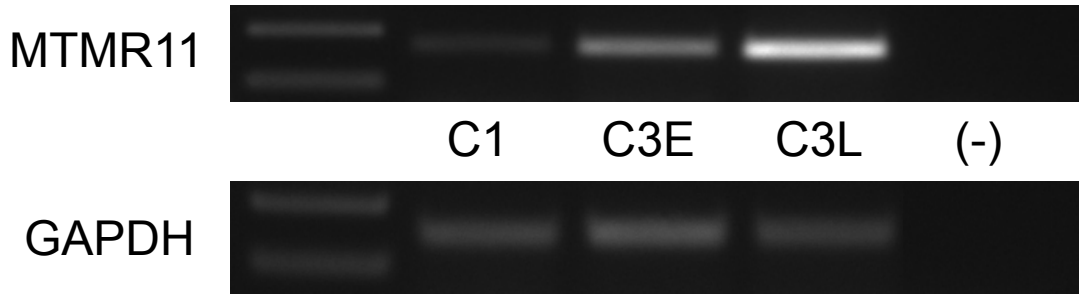

Fig.4.2.9a: MTMR11 is upregulated in senescent and revertant clones compared to the immortal clone: cDNA from C1 (immortal clone), C3-Early (revertant clone) and C3-Late (senescent clone) were used for semi-quantitative RT-PCR experiments. GAPDH: Glyceraldehyde-3-phosphate dehydrogenase was used as an internal control. (-): Negative control well to check for nucleic acid contaminants.

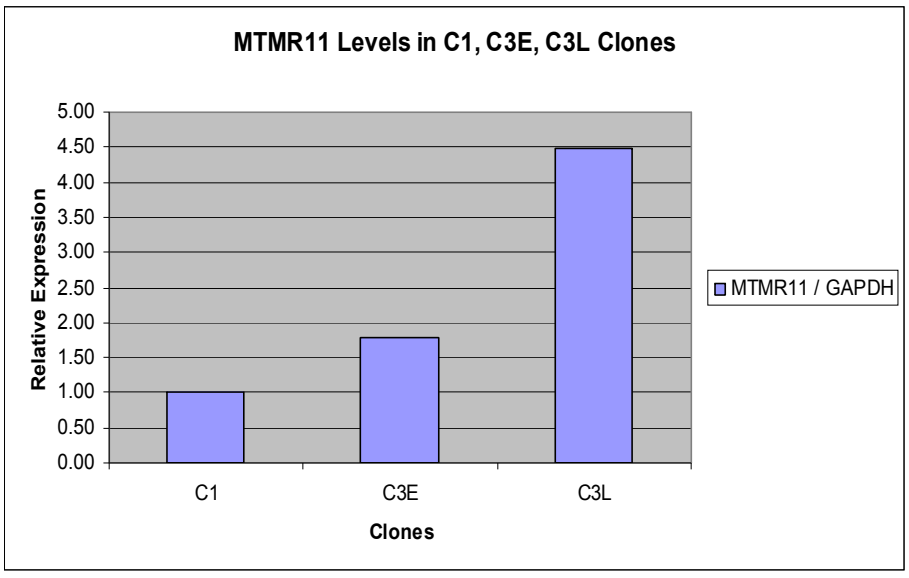

Fig.4.2.9b: MTMR11 is upregulated in senescent and revertant clones compared to the immortal

clone: A graph was generated by normalization of MTMR11 band intensities according to GAPDH band intensities in Fig.4.14a. Intensities were quantified by Bio-1D program.

The results shown in Fig.4.2.9a and b indicate that DUSP10 expression is increased progressively from C1 immortal clone to C3 senescent clone. There is a deviation from the fold changes observed in the original microarray data (2.1 fold increase in revertant vs immortal clone and 3.0 fold increase in senescent vs immortal clone). This may be due to the method of band intensity measurement or due to the insensitivity of the semi-quantitative PCR. Still, it is clearly seen that MTMR11 is upregulated in senescent cells in contrast to immortal ones.

4.2.3 MTMR11 expression data

We proceeded by gathering DUSP10 mRNA expression data in HCC cell lines (Fig.4.2.10). For this purpose, cDNAs from various HCC cell lines were extracted and used in semi-quantitative PCR.

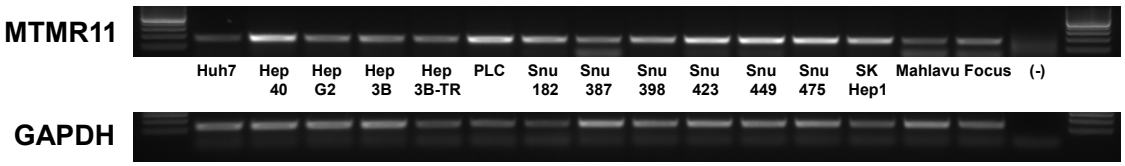

Fig.4.2.10: MTMR11 mRNA levels in HCC cell lines: Huh7, Hep40, HepG2, Hep3B, Hep3B-TR, PLC are classified as well-differentiated cell lines. Snu182, Snu387, Snu398, Snu423, Snu449, Snu475, SK Hep1, Mahlavu and Focus are classified as poorly differentiated cell lines. GAPDH was used as an internal control. (-) well showed no contamination.

4.2.4 MTMR11 transcript variants in different cell lines

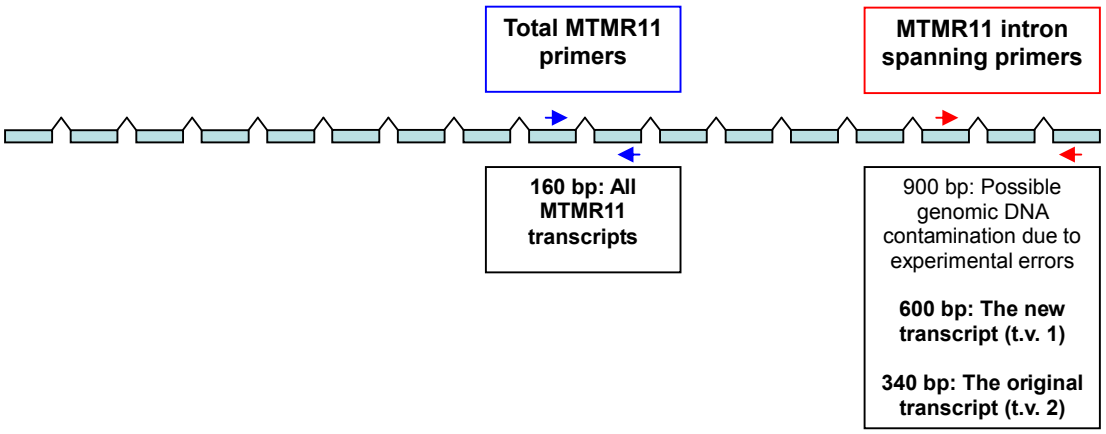

Fig.4.2.11: RT-PCR primer pairs for MTMR11 used in our studies and the lengths of the PCR products produced: MTMR11 intron spanning primer pair was employed to differentiate between the

transcript variants.

MTMR11 transcript variant 1 is a very recently discovered form of MTMR11. Before March 2009, the only MTMR11 transcript that could be found in databases was MTMR11 transcript variant 2, as it is now called. Roughly the same time, we observed the highly dominant MTMR11 transcript variant in HCC cell lines (MTMR11 transcript variant 1) while working to clone MTMR11. According to sequencing results (done at İONTEK), this variant seemed to retain the last intron (now listed as a part of exon 17b), resulting in RAEGDLG to QSHPFWITRC change in the C-terminus of the protein. Also this variant had extra 216 bases in 5'-end of the coding sequence, resulting in extra 72 residues in the N-terminus of the protein. We were immediately interested in scanning for the two different variants in HCC and breast cancer cell lines, in addition to C1, C3-Early and C3-Late clones. We designed our primers so that the pair would span the last two introns (the last intron is known as a part of exon 17b now, as already mentioned), hence both the new transcript (transcript variant 1), the original transcript (transcript variant 2) and amplification due to possible genomic DNA contamination would be detected. RT-PCR primers for MTMR11 are depicted in Fig.4.2.11.

4.2.4.1 MTMR11 transcript variants in senescent and immortal clones

We continued by checking if one or both transcript variants of MTMR11 are upregulated in senescent clones compared to immortal ones.

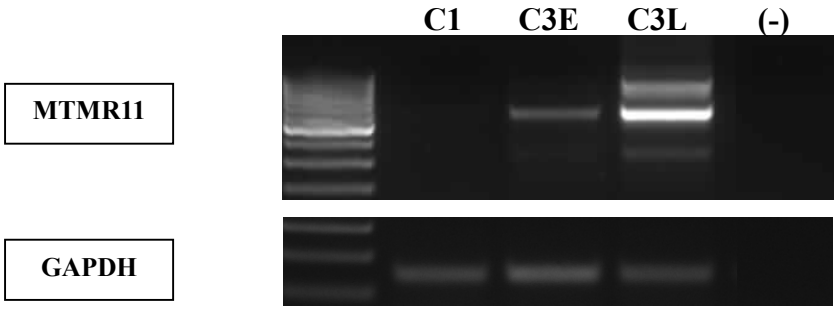

Fig.4.2.12: MTMR11 transcript variants in the established clones: cDNA from C1 (immortal clone), C3-Early (revertant clone), C3-Late (senescent clone), G11 (immortal), G12-Late (senescent) were used for this semi-quantitative RT-PCR experiment. GAPDH: Glyceraldehyde-3-phosphate dehydrogenase was used as an internal control. (-): Negative control well to check for nucleic acid contaminants.

In Fig.4.2.12, it is seen that both forms of MTMR11 are upregulated in C-clones,

whereas only transcript variant 1 is detectable in the senescent G12-Late clone. Interestingly, the above bands are also much higher in intensity in the senescent C3-Late clone compared to revertant and immortal clones. Although a 900-bp band can be the result of genomic DNA amplification, it should also have shown up in immortal and revertant clones, hence the above bands might potentially belong to other transcript variants.

4.2.4.2 MTMR11 transcript variants in HCC cell lines

MTMR11 transcript variants in HCC cell lines were also checked. The results are shown below.

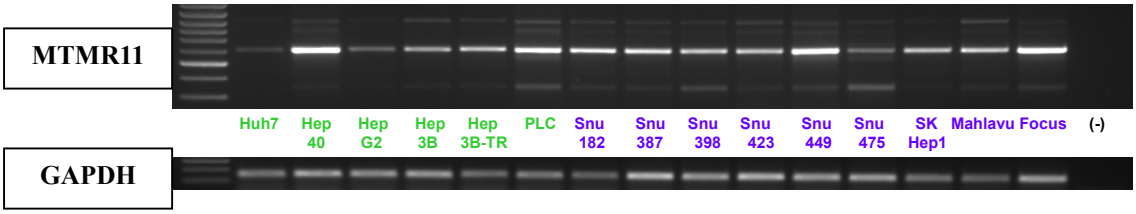

Fig.4.2.13: MTMR11 transcript variants in HCC cell lines: Some cell lines (such as PLC and Snu475) seem to have five bands instead of three, which may indicate that there are additional transcript variants of MTMR11 considering this region. Green marks the well-differentiated cell lines and dark purple marks the poorly-differentiated cell lines.

Essentially all HCC cell lines contain both transcript variants. These results also indicate the possibility of other transcript variants in this region.

4.2.4.3 MTMR11 transcript variants in breast cancer cell lines

MTMR11 transcript variants in breast cancer cell lines were also amplified. The results of a saturated RT-PCR (40 cycles of amplification) are shown in Fig.4.2.14. CAMAI and MDA MB-453 cell lines lack transcript variant 2. These results also strengthen the possibility that other transcript variants of MTMR11 might be present.

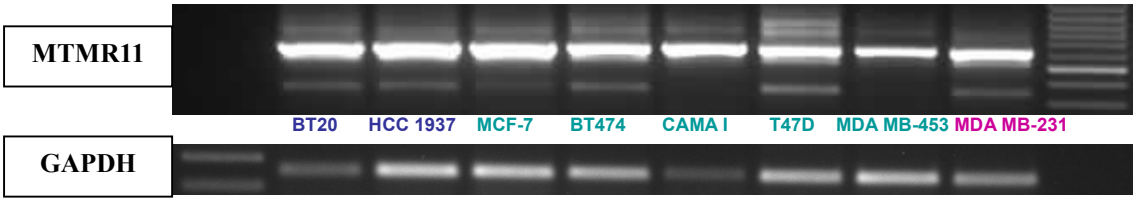

Fig.4.2.14: MTMR11 transcript variants in breast cancer cell lines: CAMAI and MDA MB-453 seem to be deficient in the shorter transcript. T47D has five bands instead of three, which may indicate

that there are additional transcript variants of MTMR11 considering this region. Dark blue marks the basal-originated cell lines, blue/green marks the luminal-originated cell lines and dark pink marks the mesenchymal-originated cell line.

4.2.5 Sequencing of the extra bands in RT-PCR experiments

Finally, we isolated the bands resulting in MTMR11 PCR, after an amplification reaction in T47D cells. We could isolate and send 340bp, 600bp, 800bp and 900bp bands for sequencing. The results for 340bp, 600bp and 900bp bands were as expected; 340bp represented MTMR11 transcript variant 2, 600bp represented MTMR11 transcript variant 1 and 900bp represented the DNA sequence bearing both introns within. Interestingly 800bp band has a 200bp insertion after the forward primer sequence, but other than that, it has the same sequence as 600bp band. However the inserted sequence came out to be simply a repeat of reverse and forward primers, which may mean that Taq DNA polymerase has erroneously amplified this region. The results of sequencing can be viewed below:

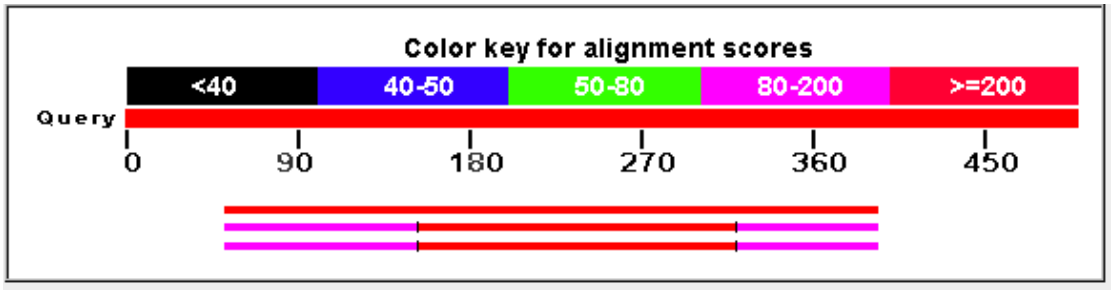

>ref|NM_181873.2| Homo sapiens myotubularin related protein 11 (MTMR11), mRNA
Length=2324

Score = 628 bits (340), Expect = 1e-177
Identities = 340/340 (100%), Gaps = 0/340 (0%)
Strand=Plus/Plus

Query	54	AGCTTGCCCTTTACCTCCAGGGCTGCTGCTGCCTGGGTATCTGGGACCCCAGATCAGGCT	113
Sbjct	1812	AGCTTGCCCTTTACCTCCAGGGCTGCTGCTGCCTGGGTATCTGGGACCCCAGATCAGGCT	1871
Query	114	CTGGAGACGCTGCTACCTGAGGGGAAGGCCTGAGGTCCAGATGGGCCTCTCAGCTCCCAC	173
Sbjct	1872	CTGGAGACGCTGCTACCTGAGGGGAAGGCCTGAGGTCCAGATGGGCCTCTCAGCTCCCAC	1931
Query	174	AATCTCTGGCCTCCAGGATGAGCTATCCCATCTTCAGGAGTTATTACGGAAATGGACACC	233
Sbjct	1932	AATCTCTGGCCTCCAGGATGAGCTATCCCATCTTCAGGAGTTATTACGGAAATGGACACC	1991
Query	234	AAGAATATCTCCTGAGGATCACTCCAAGAAAAGAGATCCACATACCATTCTCAATCCCAC	293
Sbjct	1992	AAGAATATCTCCTGAGGATCACTCCAAGAAAAGAGATCCACATACCATTCTCAATCCCAC	2051
Query	294	TGAAATTGCTGGCATTCTCAAAGGCCAATCCCATCCCTTCTGGATAACCAGATGTTAAAT	353
Sbjct	2052	TGAAATTGCTGGCATTCTCAAAGGCCAATCCCATCCCTTCTGGATAACCAGATGTTAAAT	2111
Query	354	CATGAGATCAGAGATGCTGTTCATCAGTCCCAACAAGATG 393	
Sbjct	2112	CATGAGATCAGAGATGCTGTTCATCAGTCCCAACAAGATG 2151	

Fig.4.2.15a: 340bp band sequencing results: Above, the color key for alignment scores and the representative alignment of the query sequence with the resulted sequences can be viewed. For all sequencing results, there were three results, listed from top to bottom: Homo sapiens myotubularin related protein 11 (MTMR11) - mRNA, Homo sapiens chromosome 1 genomic contig - reference

assembly, Homo sapiens chromosome 1 genomic contig - alternate assembly (based on HuRef SCAF_1103279188338). **Below,** the alignment of 340bp band query with MTMR11 mRNA. The extra sequences that did not give an alignment with any human DNA or mRNA sequence come from the pGEMT-Easy vector which was used to clone the isolated bands.

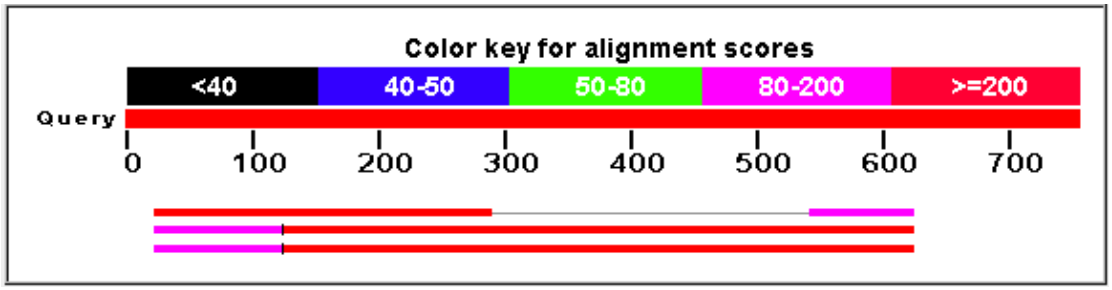

>ref|NT_004487.18|Hs1_4644 Homo sapiens chromosome 1 genomic contig, reference assembly
Length=56413061

Sort alignments for this subject sequence by:
E value Score Percent identity
Query start position Subject start position

Score = 924 bits (500), Expect = 0.0
Identities = 500/500 (100%), Gaps = 0/500 (0%)
Strand=Plus/Minus

```
Query  121     CCAGATGGGCCTCTCAGCTCCCACAATCTCTGGCCTCCAGGATGAGCTATCCCATCTTCA  180
               ||||||||||||||||||||||||||||||||||||||||||||||||||||||||||||
Sbjct  391568  CCAGATGGGCCTCTCAGCTCCCACAATCTCTGGCCTCCAGGATGAGCTATCCCATCTTCA  391509

Query  181     GGAGTTATTACGGAAATGGACACCAAGAATATCTCCTGAGGATCACTCCAAGAAAAGAGA  240
               ||||||||||||||||||||||||||||||||||||||||||||||||||||||||||||
Sbjct  391508  GGAGTTATTACGGAAATGGACACCAAGAATATCTCCTGAGGATCACTCCAAGAAAAGAGA  391449

Query  241     TCCACATACCATTCTCAATCCCACTGAAATTGCTGGCATTCTCAAAGGCAGGGCAGAGGG  300
               ||||||||||||||||||||||||||||||||||||||||||||||||||||||||||||
Sbjct  391448  TCCACATACCATTCTCAATCCCACTGAAATTGCTGGCATTCTCAAAGGCAGGGCAGAGGG  391389

Query  301     GGATCTGGGGTAGAGGAGGGTTCTGTCTAATCTTTTTTTTTTTTTTTTGTATCTGCACTT  360
               ||||||||||||||||||||||||||||||||||||||||||||||||||||||||||||
Sbjct  391388  GGATCTGGGGTAGAGGAGGGTTCTGTCTAATCTTTTTTTTTTTTTTTTGTATCTGCACTT  391329

Query  361     GCAGCCTCAGCTTTCACACTTCAGCCCTTAAGTTCACTAAGAAGGTCTGAGTTTCTGCTG  420
               ||||||||||||||||||||||||||||||||||||||||||||||||||||||||||||
Sbjct  391328  GCAGCCTCAGCTTTCACACTTCAGCCCTTAAGTTCACTAAGAAGGTCTGAGTTTCTGCTG  391269

Query  421     CAGATAGTGGTGTTAACTGCTCCAACTCTTGTCTTGCTTAGTTTCTACAAATATTTTTGC  480
               ||||||||||||||||||||||||||||||||||||||||||||||||||||||||||||
Sbjct  391268  CAGATAGTGGTGTTAACTGCTCCAACTCTTGTCTTGCTTAGTTTCTACAAATATTTTTGC  391209

Query  481     TTCTTGTCATTTGAAGGATTAAGAAACAAAAACAATCCAGAAATTGATCGGTTTTTTTAG  540
               ||||||||||||||||||||||||||||||||||||||||||||||||||||||||||||
Sbjct  391208  TTCTTGTCATTTGAAGGATTAAGAAACAAAAACAATCCAGAAATTGATCGGTTTTTTTAG  391149

Query  541     GCCAATCCCATCCCTTCTGGATAACCAGATGTTAAATCATGAGATCAGAGATGCTGTTCA  600
               ||||||||||||||||||||||||||||||||||||||||||||||||||||||||||||
Sbjct  391148  GCCAATCCCATCCCTTCTGGATAACCAGATGTTAAATCATGAGATCAGAGATGCTGTTCA  391089

Query  601     TCAGTCCCAACAAGATGGCC  620
               ||||||||||||||||||||
Sbjct  391088  TCAGTCCCAACAAGATGGCC  391069
```

Score = 185 bits (100), Expect = 5e-44
Identities = 100/100 (100%), Gaps = 0/100 (0%)
Strand=Plus/Minus

```
Query  25      AGCTTGCCCTTTACCTCCAGGGCTGCTGCTGCCTGGGTATCTGGGACCCCAGATCAGGCT  84
               ||||||||||||||||||||||||||||||||||||||||||||||||||||||||||||
Sbjct  391969  AGCTTGCCCTTTACCTCCAGGGCTGCTGCTGCCTGGGTATCTGGGACCCCAGATCAGGCT  391910

Query  85      CTGGAGACGCTGCTACCTGAGGGGAAGGCCTGAGGTCCAG  124
               ||||||||||||||||||||||||||||||||||||||||
Sbjct  391909  CTGGAGACGCTGCTACCTGAGGGGAAGGCCTGAGGTCCAG  391870
```

Fig.4.2.15b: 600bp band sequencing results: Above, the color key for alignment scores and the representative alignment of the query sequence with the resulted sequences can be viewed. For all sequencing results, there were three results, listed from top to bottom: Homo sapiens myotubularin related protein 11 (MTMR11) - mRNA, Homo sapiens chromosome 1 genomic contig - reference assembly, Homo sapiens chromosome 1 genomic contig - alternate assembly (based on HuRef SCAF_1103279188338). **Below,** the alignment of 600bp band query with human chromosome 1 genomic contig (reference assembly). An intron is retained in this sequence compared to the 340bp band. The extra sequences that did not give an alignment with any human DNA or mRNA sequence come from the pGEMT-Easy vector which was used to clone the isolated bands.

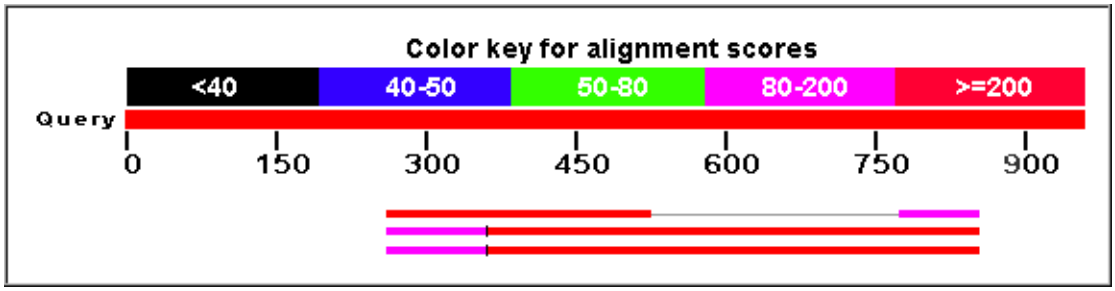

>ref|NW_001838529.1|Hs1_WGA125_36 Homo sapiens chromosome 1 genomic contig, alternate assembly (based on HuRef SCAF_1103279188338)
Length=4867057

Sort alignments for this subject sequence by:
E value Score Percent identity
Query start position Subject start position

Features in this part of subject sequence:
Myotubularin related protein 11 isoform b

Score = 913 bits (494), Expect = 0.0
Identities = 496/497 (99%), Gaps = 0/497 (0%)
Strand=Plus/Minus

```
Query  358    CCAGATGGGCCTCTCAGCTCCCACAATCTCTGGCCTCCAGGATGAGCTATCCCATCTTCA  417
              ||||||||||||||||||||||||||||||||||||||||||||||||||||||||||||
Sbjct  99528  CCAGATGGGCCTCTCAGCTCCCACAATCTCTGGCCTCCAGGATGAGCTATCCCATCTTCA  99469

Query  418    GGAGTTATTACGGAAATGGACACCAAGAATATCTCCTGAGGATCACTCCAAGAAAAGAGA  477
              ||||||||||||||||||||||||||||||||||||||||||||||||||||||||||||
Sbjct  99468  GGAGTTATTACGGAAATGGACACCAAGAATATCTCCTGAGGATCACTCCAAGAAAAGAGA  99409

Query  478    TCCACATACCATTCTCAATCCCACTGAAATTGCTGGCATTCTCAAAGGCAGGGCAGAGGG  537
              ||||||||||||||||||||||||||||||||||||||||||||||||||||||||||||
Sbjct  99408  TCCACATACCATTCTCAATCCCACTGAAATTGCTGGCATTCTCAAAGGCAGGGCAGAGGG  99349

Query  538    GGATCTGGGGTAGAGGAGGGTTCTGTCTAATCTTTTTTTTTTTTTTTTGTATCTGCACTT  597
              ||||||||||||||||||||||||||||||||||||||||||||||||||||||||||||
Sbjct  99348  GGATCTGGGGTAGAGGAGGGTTCTGTCTAATCTTTTTTTTTTTTTTTTGTATCTGCACTT  99289

Query  598    GCAGCCTCAGCTTTCACACTTCAGCCCTTAAGTTCACTAAGAAGGTCTGAGTTTCTGCTG  657
              ||||||||||||||||||||||||||||||||||||||||||||||||||||||||||||
Sbjct  99288  GCAGCCTCAGCTTTCACACTTCAGCCCTTAAGTTCACTAAGAAGGTCTGAGTTTCTGCTG  99229

Query  658    CAGATAGTGGTGTTAACTGCTCCAACTCTTGTCTTGCTTAGTTTCTACAAATATTTTTGC  717
              ||||||||||||||||||||||||||||||||||||||||||||||||||||||||||||
Sbjct  99228  CAGATAGTGGTGTTAACTGCTCCAACTCTTGTCTTGCTTAGTTTCTACAAATATTTTTGC  99169

Query  718    TTCTTGTCATTCGAAGGATTAAGAAACAAAAACAATCCAGAAATTGATCGGTTTTTTTAG  777
              |||||||||||| ||||||||||||||||||||||||||||||||||||||||||||||
Sbjct  99168  TTCTTGTCATTTGAAGGATTAAGAAACAAAAACAATCCAGAAATTGATCGGTTTTTTTAG  99109

Query  778    GCCAATCCCATCCCTTCTGGATAACCAGATGTTAAATCATGAGATCAGAGATGCTGTTCA  837
              ||||||||||||||||||||||||||||||||||||||||||||||||||||||||||||
Sbjct  99108  GCCAATCCCATCCCTTCTGGATAACCAGATGTTAAATCATGAGATCAGAGATGCTGTTCA  99049

Query  838    TCAGTCCCAACAAGATG  854
              |||||||||||||||||
Sbjct  99048  TCAGTCCCAACAAGATG  99032
```

Features in this part of subject sequence:
Myotubularin related protein 11 isoform b

Score = 185 bits (100), Expect = 6e-44
Identities = 100/100 (100%), Gaps = 0/100 (0%)
Strand=Plus/Minus

```
Query  262    AGCTTGCCCTTTACCTCCAGGGCTGCTGCTGCCTGGGTATCTGGGACCCCAGATCAGGCT  321
              ||||||||||||||||||||||||||||||||||||||||||||||||||||||||||||
Sbjct  99929  AGCTTGCCCTTTACCTCCAGGGCTGCTGCTGCCTGGGTATCTGGGACCCCAGATCAGGCT  99870

Query  322    CTGGAGACGCTGCTACCTGAGGGGAAGGCCTGAGGTCCAG  361
              ||||||||||||||||||||||||||||||||||||||||
Sbjct  99869  CTGGAGACGCTGCTACCTGAGGGGAAGGCCTGAGGTCCAG  99830
```

Fig.4.2.15c: 800bp band sequencing results: Above, the color key for alignment scores and the representative alignment of the query sequence with the resulted sequences can be viewed. For all sequencing results, there were three results, listed from top to bottom: Homo sapiens myotubularin related protein 11 (MTMR11) - mRNA, Homo sapiens chromosome 1 genomic contig - reference assembly, Homo sapiens chromosome 1 genomic contig - alternate assembly (based on HuRef SCAF_1103279188338). **Below,** the alignment of 800bp band query with human chromosome 1 genomic contig (reference assembly). After a thorough analysis of this sequence, it was understood that a 200bp sequence of primer repeats were inserted. Other than that, the sequence is the same as the 600bp sequence. The extra sequences that did not give an alignment with any human DNA or mRNA sequence come from the pGEMT-Easy vector which was used to clone the isolated bands.

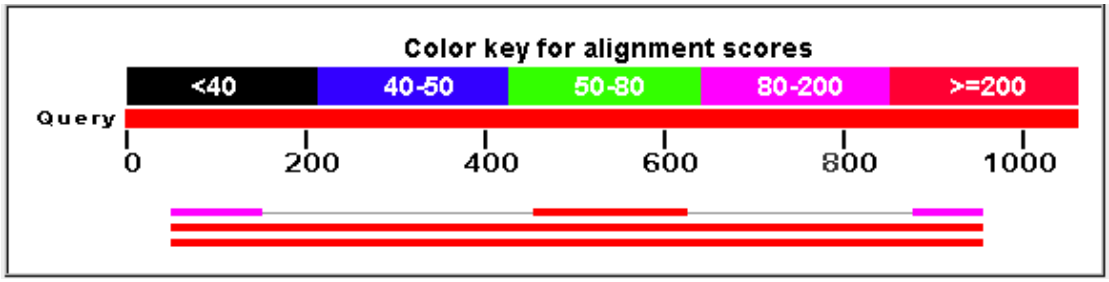

>ref|NT_004487.18|Hs1_4644 Homo sapiens chromosome 1 genomic contig, reference assembly
Length=56413061

```
 Score = 1659 bits (898),  Expect = 0.0
 Identities = 898/898 (100%), Gaps = 0/898 (0%)
 Strand=Plus/Minus

Query  54      AGCTTGCCCTTTACCTCCAGGGCTGCTGCTGCCTGGGTATCTGGGACCCCAGATCAGGCT  113
               ||||||||||||||||||||||||||||||||||||||||||||||||||||||||||||
Sbjct  391969  AGCTTGCCCTTTACCTCCAGGGCTGCTGCTGCCTGGGTATCTGGGACCCCAGATCAGGCT  391910

Query  114     CTGGAGACGCTGCTACCTGAGGGGAAGGCCTGAGGTCCAGGTAAGAAGGGAAAATAGACT  173
               ||||||||||||||||||||||||||||||||||||||||||||||||||||||||||||
Sbjct  391909  CTGGAGACGCTGCTACCTGAGGGGAAGGCCTGAGGTCCAGGTAAGAAGGGAAAATAGACT  391850

Query  174     GGGAGTGGGACAAGGGACTTGACTCTGCTGAACCAGATGAACAGGAGCTGGAAAGGCAAG  233
               ||||||||||||||||||||||||||||||||||||||||||||||||||||||||||||
Sbjct  391849  GGGAGTGGGACAAGGGACTTGACTCTGCTGAACCAGATGAACAGGAGCTGGAAAGGCAAG  391790

Query  234     GAGCTGAAGCCTCTGGGAGTCTGGGAAGTGAAGTTCTACTCCTCTTGGCATCAAACAAGG  293
               ||||||||||||||||||||||||||||||||||||||||||||||||||||||||||||
Sbjct  391789  GAGCTGAAGCCTCTGGGAGTCTGGGAAGTGAAGTTCTACTCCTCTTGGCATCAAACAAGG  391730

Query  294     TTTGGGAGTGTAGGAGGTGCGGGAAAGTGCTTGTGGCTTAGATTAAGTGGAATTTAGGGC  353
               ||||||||||||||||||||||||||||||||||||||||||||||||||||||||||||
Sbjct  391729  TTTGGGAGTGTAGGAGGTGCGGGAAAGTGCTTGTGGCTTAGATTAAGTGGAATTTAGGGC  391670

Query  354     ATAGCTGAAAGGGGAAACAGAATTAAAGACACCAGAAGTAGCAGAGAAGCAGGGGGCCAG  413
               ||||||||||||||||||||||||||||||||||||||||||||||||||||||||||||
Sbjct  391669  ATAGCTGAAAGGGGAAACAGAATTAAAGACACCAGAAGTAGCAGAGAAGCAGGGGGCCAG  391610

Query  414     AGCTACAACAGTATTCTTCTCTGTTCCTCTTTGCCTCCTCCCCAGATGGGCCTCTCAGCT  473
               ||||||||||||||||||||||||||||||||||||||||||||||||||||||||||||
Sbjct  391609  AGCTACAACAGTATTCTTCTCTGTTCCTCTTTGCCTCCTCCCCAGATGGGCCTCTCAGCT  391550

Query  474     CCCACAATCTCTGGCCTCCAGGATGAGCTATCCCATCTTCAGGAGTTATTACGGAAATGG  533
               ||||||||||||||||||||||||||||||||||||||||||||||||||||||||||||
Sbjct  391549  CCCACAATCTCTGGCCTCCAGGATGAGCTATCCCATCTTCAGGAGTTATTACGGAAATGG  391490

Query  534     ACACCAAGAATATCTCCTGAGGATCACTCCAAGAAAAGAGATCCACATACCATTCTCAAT  593
               ||||||||||||||||||||||||||||||||||||||||||||||||||||||||||||
Sbjct  391489  ACACCAAGAATATCTCCTGAGGATCACTCCAAGAAAAGAGATCCACATACCATTCTCAAT  391430

Query  594     CCCACTGAAATTGCTGGCATTCTCAAAGGCAGGGCAGAGGGGGATCTGGGGTAGAGGAGG  653
               ||||||||||||||||||||||||||||||||||||||||||||||||||||||||||||
Sbjct  391429  CCCACTGAAATTGCTGGCATTCTCAAAGGCAGGGCAGAGGGGGATCTGGGGTAGAGGAGG  391370

Query  654     GTTCTGTCTAATCTTTTTTTTTTTTTTTTGTATCTGCACTTGCAGCCTCAGCTTTCACAC  713
               ||||||||||||||||||||||||||||||||||||||||||||||||||||||||||||
Sbjct  391369  GTTCTGTCTAATCTTTTTTTTTTTTTTTTGTATCTGCACTTGCAGCCTCAGCTTTCACAC  391310

Query  714     TTCAGCCCTTAAGTTCACTAAGAAGGTCTGAGTTTCTGCTGCAGATAGTGGTGTTAACTG  773
               ||||||||||||||||||||||||||||||||||||||||||||||||||||||||||||
Sbjct  391309  TTCAGCCCTTAAGTTCACTAAGAAGGTCTGAGTTTCTGCTGCAGATAGTGGTGTTAACTG  391250

Query  774     CTCCAACTCTTGTCTTGCTTAGTTTCTACAAATATTTTTGCTTCTTGTCATTTGAAGGAT  833
               ||||||||||||||||||||||||||||||||||||||||||||||||||||||||||||
Sbjct  391249  CTCCAACTCTTGTCTTGCTTAGTTTCTACAAATATTTTTGCTTCTTGTCATTTGAAGGAT  391190

Query  834     TAAGAAACAAAAACAATCCAGAAATTGATCGGTTTTTTTAGGCCAATCCCATCCCTTCTG  893
               ||||||||||||||||||||||||||||||||||||||||||||||||||||||||||||
Sbjct  391189  TAAGAAACAAAAACAATCCAGAAATTGATCGGTTTTTTTAGGCCAATCCCATCCCTTCTG  391130

Query  894     GATAACCAGATGTTAAATCATGAGATCAGAGATGCTGTTCATCAGTCCCAACAAGATG  951
               ||||||||||||||||||||||||||||||||||||||||||||||||||||||||
Sbjct  391129  GATAACCAGATGTTAAATCATGAGATCAGAGATGCTGTTCATCAGTCCCAACAAGATG  391072
```

Fig.4.2.15d: 900bp band sequencing results: Above, the color key for alignment scores and the representative alignment of the query sequence with the resulted sequences can be viewed. For all sequencing results, there were three results, listed from top to bottom: Homo sapiens myotubularin related protein 11 (MTMR11) - mRNA, Homo sapiens chromosome 1 genomic contig - reference assembly, Homo sapiens chromosome 1 genomic contig - alternate assembly (based on HuRef SCAF_1103279188338). **Below,** the alignment of 900bp band query with human chromosome 1 genomic contig (reference assembly). This sequence was expected to be amplified from possible genomic DNA contaminants. As expected, it has the whole sequence from genomic DNA, with both introns spanned. The extra sequences that did not give an alignment with any human DNA or mRNA sequence come from the pGEMT-Easy vector which was used to clone the isolated bands.

CHAPTER 5. DISCUSSION

In this study, we focused on the novel protein phosphatase genes DUSP10 and MTMR11 in HCC. Our starting point for choosing these genes was the result of a microarray study that was performed by our group (Öztürk M et al, unpublished data) for identifying the gene expression changes between the senescent and the immortal Huh7 clones established previously (Öztürk N et al, 2006). In the significant gene list of protein phosphatases representing the most differentially expressed phosphatases between these stable clones, DUSP10 and MTMR11 appeared as the genes that were significantly upregulated in the senescent clones with respect to the immortal clones. Therefore, we decided to analyze DUSP10 and MTMR11 genes.

After a thorough bioinformatics search, we generated the expression data of DUSP10 and MTMR11 in the immortal and senescent clones. RT-PCR results showed that both DUSP10 and MTMR11 were upregulated in senescent clones as compared to immortal clones which is in correlation with the microarray study. We continued by constituting DUSP10 and MTMR11 expression data in HCC and breast cancer cell lines. It was concluded that expression of both genes (and DUSP10 protein) was present in essentially all the cell lines we employed.

Initially we focused our attention on DUSP10. Since the expression data in HCC cell lines did not demonstrate a difference between mesenchymal-like and epithelial-like cell lines, we wanted to see if subcellular localization of DUSP10 might be important in differentiating between the two types of cell lines. We checked the subcellular localization of DUSP10 by immunoperoxidase staining and immunofluorescence. This protein is listed as having a unique distribution in SWISS-PROT Database, as it is said to be seen evenly in both nucleus and cytoplasm. However we observed that while in some cell lines DUSP10 is seen both in nucleus and cytoplasm roughly in similar intensities (Huh7, Hep40, Hep3B-TR, PLC, Focus, SK-Hep1), some cell lines showed strong nuclear DUSP10 (HepG2, Snu182 and Snu398) and some showed predominantly cytoplasmic DUSP10 (Hep3B, Snu387, Snu423, Snu449, Snu475 and Mahlavu). The cytoplasmic DUSP10 seemed to concentrate immediately around nuclei in most cell lines that gave cytoplasmic DUSP10 staining and into cytoplasmic

foci in the rest (Snu449 and SK-Hep1).

We did not observe a colocalization between DUSP10 and Calnexin proteins after confocal microscopy, although the peri-nuclear DUSP10 staining observed in most of the cell lines hinted at its localization to ER. In contrast, we observed that DUSP10 localizes in the cytoplasm. While we could not state that DUSP10 specifically localizes to the ER, its peri-nuclear distribution was still of interest to us as it might have something to do with translocation of DUSP10 to nucleus when needed. It is known that MKPs translocate to nucleus to deactivate MAPKs within the nucleus (Patterson KI et al, 2009).

The observation that predominantly nuclear DUSP10 localization is seen in some cell lines and predominantly cytoplasmic localization in the others drew our attention to the factors that may be changing DUSP10 localization. We tried to correlate a change of DUSP10 localization with induction of senescence. We saw a difference in DUSP10 localization upon comparison of early and late passages of MRC-5 fibroblasts demonstrating that DUSP10 may be translocating to nucleus during replicative senescence. We saw no change in DUSP10 localization was seen upon treatment of Huh7 cells with the senescence-inducing agents, TGF-β and camptothecin, indicating that DUSP10 localization is not changed during premature senescence. Hence although we could not conclude that DUSP10 localization changes upon induction of premature senescence, we can conclude that it changes upon induction of replicative senescence. If the change in DUSP10 localization indicates an important regulatory mechanism, this finding strengthens the microarray study done previously, from which DUSP10 emerged as a replicative senescence-associated phosphatase gene (Öztürk M, unpublished data).

We further reasoned that disruption of JNK and p38 MAPK pathways may affect DUSP10 localization, and used inhibitors of these kinases on selected cell lines. The inhibitors we used were ATP-competitive, preventing their targets to activate downstream elements regardless of their phosphorylation statuses. We chose to work with Huh7, HepG2, Hep3B, Hep3B-TR, Snu182 and Mahlavu cell lines in inhibitor experiments for a number of reasons. The stable clones that form the basis of this research have been established from Huh7 cell line (Öztürk N et al, 2006).

Additionally, the proliferation-inhibitory concentrations of JNK inhibitor V used were measured in Huh7 cell line (Bilget-Güven E et al, unpublished data). We employed HepG2 and Hep3B cell lines as these were well-differentiated cell lines that showed nuclear or cytoplasmic DUSP10 staining, respectively. We employed Snu182 and Mahlavu cell lines for a similar reason, since these were poorly-differentiated cell lines that showed nuclear or cytoplasmic DUSP10 staining, respectively. We also employed Hep3B-TR (TGFβ-Resistant) cell line in the final confocal microscopy experiment, to see if absence of TGFβ receptors I and II causes a difference in the response of cells to JNK inhibitor V, since one of the upstream elements of this pathway is TGFβ-activated kinase 1 (TAK1 or MAP3K7) (Hammaker DR et al, 2007).

Upon inhibitor experiments on Hep3B cell line, we saw that JNK inhibitor V caused translocation of DUSP10 from cytoplasm to nucleus. We treated Snu182 cell line with JNK inhibitor V and p38 inhibitors, too, however did not observe a change in DUSP10 localization. JNK inhibitor V treatment study was expanded to Huh7, HepG2, Snu182 and Mahlavu cell lines, resulting in significant DUSP10 translocation in well-differentiated (epithelial-like) cell lines (Huh7, HepG2, Hep3B), but no significant translocation in poorly-differentiated (mesenchymal-like) cell lines (Snu182, Mahlavu). We also quantified the significance of this translocation, and verified that JNK pathway is inhibited by the used concentration of this inhibitor. Finally we confirmed DUSP10 translocation upon JNK inhibitor V treatment in well-differentiated cell lines, Hep3B and Hep3B-TR, by confocal microscopy compared to the poorly-differentiated cell lines Snu182 and Mahlavu. Effect of JNK inhibitor V on JNK is shown below.

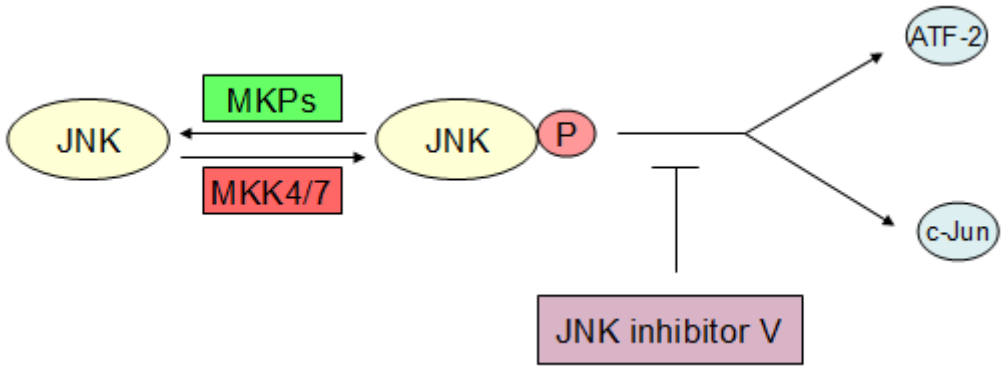

Fig.5.1: Effect of JNK inhibitor V on JNK pathway: JNK inhibitor V competes with ATP to inhibit

phosphorylation of JNK targets by the kinase, regardless of the phosphorylation status of JNK.

Tumor suppressive or oncogenic activity of DUSP10 is not clear in HCC, although it is clear that the chromosomal region DUSP10 gene resides in is a hot spot for chromosomal aberrations in early HCC (see Results chapter, section 4.1.1.1). As mentioned in Introduction chapter, it functions as a tumor suppressor by deactivating the inflammatory MAPK p38 in early prostate cancer. Considering HCC, there is evidence that p38 MAPK may be functioning as a tumor suppressor. Studies with a constitutively active mutant of MKK6 and p38 inhibitors suggested that resistance of human HCC to apoptosis may be resulting due to a reduction in p38 activity (Iyoda K et al, 2003). Another study has shown that IL-6, a p38 target cytokine, mediates G0/G1 growth arrest in HCC cells through STAT3-dependent regulation of cdk2/cdk4 activity and p21 expression (Moran DM et al, 2008). Additionally, p38α has been found to suppress normal hepatocyte and HCC proliferation by antagonizing the JNK-c-Jun pathway, implicating p38α as a tumor suppressor and JNK as an oncogenic protein in HCC (Hui L et al, 2007). Further studies have supported the role of JNK in promoting proliferation in human HCC and chemically induced mouse liver cancers and shown that JNK1-dependent p21 downregulation is responsible for this effect (Hui L et al, 2008). Taking these into consideration, the role of DUSP10 which is able to deactivate both phosphatases, is not clear in HCC.

In this piece of work, we showed that JNKs affect DUSP10 subcellular localization but that p38s do not. This has significant importance since it is known that change in subcellular localization is a way of MKP/DSP regulation in cells, mainly through phosphorylation or myristoylation (Patterson KI et al, 2009). There are also examples of known tumor suppressor or oncogenic proteins which are regulated through subcellular localization and sequestration in specific locations, such as p33ING1b, β-catenin and p53 (Sayan B et al, 2009; Farazi PA, DePinho RA, 2006). Our findings and this information sums up to the possibility that DUSP10 is regulated by JNKs through a change in subcellular localization. Since it is known by large scale studies that DUSP10 isoform a may be phosphorylated in its N-terminus and that according to GPS 2.1 (kinase-specific phosphorylation site prediction), JNKs are among the kinases that may be phosphorylating the predicted residue on DUSP10, the change in subcellular localization may be occuring through this post-translational modification.

Additionally, N-myristoylation sites have been found on DUSP10 according to Motif Scan, however these may not be specific and experimental evidence is required. Furthermore, DUSP10 has an unusual proline-rich N-terminal sequence that is suspected to bear regulatory regions and non-canonical nuclear localization sequences. All of these strengthen the possibility that the change in DUSP10 localization upon inhibition of JNKs is a significant finding that hints at a mechanism of DUSP10 regulation in HCC cells. The finding that DUSP10 may primarily be regulated by JNK in HCC cell lines also implicates that DUSP10 may be acting as a tumor suppressor in HCC, since JNK has been found to act like an oncogenic protein in the study of Hui L et al (Hui L et al, 2007).

On MTMR11 part, after finding out that MTMR11 has two main transcript variants during cloning experiments, and seeing that a new transcript is listed in databases, we were interested in seeing if the expression of these transcript variants change in different cell lines. For HCC cell lines, we wondered if there was a difference between well- and poorly-differentiated cells. For breast cancer cell lines, we wondered if there was a difference between cell lines originating from different breast tissues (basal, mesenchymal or luminal regions). However a significant difference was not observed. Additionally, the microarray studies of Wurmbach and Chen demonstrate MTMR11 upregulation in HCC samples. This might be showing that MTMR11, which emerged as a senescence-associated gene, is not related to senescence functionally. Still, in the microarray results of Wurmbach and Chen, MTMR11's expression seemed to vary between different HCC samples, hence knowledge of the grades and the prognosis of the HCC samples used could be of use in relating MTMR11 to hepatocarcinogenesis. Other than this, we saw that other unknown transcripts may exist considering the region we explored (last two or three exons of MTMR11). One of the unexpected bands, observed as a 550bp band right under the dominant 600bp band, could not be isolated and sent for sequencing. The other unexpected band, observed as a 800bp band under the expected 900bp band, had a surprising sequence which was mainly the same as the 600bp band but had a 200bp insertion of reverse and forward primer repeats. This may render 800bp band as a Taq DNA polymerase error in the PCR conditions used (Methods, section 3.3.7, Table 3.2). Still, the presence of this band in almost all of the cell lines we employed is striking. Finally, 900bp band had the expected sequence of both introns spanned, resembling the sequence that would have

been amplified from genomic DNA. However, this does not completely show that this band has only resulted from genomic DNA amplification. RT-PCR results from HCC cell lines still hint at 900bp band as the sequence amplified from yet another novel transcript, since it is found in varying amounts in different cell lines explored (Fig.4.2.13).

In our study, we worked on DUSP10 and MTMR11 which code for protein phosphatases that we saw to be significantly upregulated in senescent stable clones of Huh7 compared to immortal ones. The gene expression profile changes between these different clones were of great interest, since exploration of genes with differential expression could be a key to reversion of the immortality of cancer cells. Since protein kinases are known to be very important in disease formation and carcinogenesis, their partners in signaling, protein phosphatases should also be important in these processes, although they have started to be appreciated only recently. Hence exploration of protein phosphatases and their genes with differential expression between immortal and senescent clones might provide a mechanism to overcome the immortality of cancer cells. Because overexpression studies could not be done in case of DUSP10 (probably due to the fact that its overexpression is immediately suppressed in cells) and were not done in MTMR11's case (since we first wanted to focus on finding out if different transcript variants are seen in different cell lines), we could not assess whether protein products of these genes function in reversion of the immortal phenotype of Huh7 cell line or not. Still, we reached to important clues in analysis of these genes and their products. For MTMR11, we came to the conclusion that other transcript variants may be present in HCC and breast cancer cell lines, although no connection between MTMR11 and senescence or carcinogenesis is found yet. For DUSP10, we came to the conclusion that the change in DUSP10 subcellular localization may be associated with induction of replicative senescence and that JNKs may be regulating DUSP10 through its subcellular localization in well-differentiated HCC cell lines. Since JNK has also been found to function as an oncoprotein in HCC, this may be hinting at a tumor suppressive role for DUSP10 in hepatocarcinogenesis (Hui L et al, 2007). The significance of the change in DUSP10 localization should be characterized further, before stating that DUSP10 functions in replicative senescence or hepatocarcinogenesis.

CHAPTER 6. FUTURE PERSPECTIVES

Our results indicate DUSP10 and MTMR11 as senescence-upregulated phosphatase genes. Experiments that should be performed for confirmation of preliminary DUSP10 data and for finding out a molecular mechanism for the regulation of DUSP10 localization change by JNK are summarized below:

- Confirmation of DUSP10 localization change in response to JNK inhibitor V by Western blotting of nuclear and cytoplasmic fractions of cells should be done by subcellular fractionation of the cell lines employed (Huh7, HepG2, Hep3B, Hep3B-TR, Snu182 and Mahlavu), followed by DUSP10 Western blotting.

- Experiments with JNK inhibitor V should be performed in other HCC cell lines to verify the difference between well- and poorly-differentiated cell lines.

- Changes in DUSP10 localization should be checked upon JNK activation.

- DUSP10 localization may also be checked in cell lines that have differential JNK activities.

- Co-immunoprecipitation or co-staining experiments with DUSP10 / p38 and DUSP10 / JNK in HCC cell lines should be performed to see if DUSP10 prefers one of these targets in HCC cell lines. DUSP10 targeting JNKs in HCC would be useful in explaining why JNKs regulate DUSP10 subcellular localization.

- RNA interference experiments may be done against JNK, to check DUSP10 localization when JNK expression is knocked-down. This does not necessarily give the same result with the inhibitor, since the inhibitor blocks JNK target phosphorylation and not the expression or activation of JNK itself.

- How DUSP10 translocates to nucleus is also an interesting question. JNK and p38 MAPKs are known to translocate to nucleus upon phosphorylation. Co-immunoprecipitation of DUSP10 with these MAPKs can be done after inhibitor

treatment in well-differentiated cell lines, or without inhibitor treatment in Snu182 cell line since it naturally possesses nuclear DUSP10.

- Another future study may focus on the analysis of DUSP10 promoter sequence to find true AP-1 or ATF-2 sites, and afterwards, check if a transcriptional regulation is asserted on DUSP10 by p38 or JNK through ATF-2 in HCC cell lines.

- Construction of a DUSP10-containing expression vector with an inducible system such as Tetracycline regulated systems, may prove to be useful in overexpression studies of DUSP10, if its ectopic overexpression is prevented by the cells.

Experiments that should be performed for confirmation of preliminary MTMR11 data and for long term studies on this gene and its product are summarized below:

- MTMR11 transcript variants can be checked by RT-PCR in cDNAs from tumor vs non-tumor samples or aging vs young normal cell lines or premature senescence-induced vs normal cell lines.

- Other transcript variants of MTMR11 can be searched for, since the cloning PCR for MTMR11 gives many bands (not shown).

- Yeast-2-hybrid studies for MTMR11 should be done to search for its possible myotubularin phosphatase partners.

- Antibodies should be produced against MTMR11.

- Since MTMR11 is predicted to bind to DNA and have ligand-dependent nuclear receptor activity, this can be confirmed by immunostaining to detect its localization, followed by ChIP to see which sequence it binds to, in normal and cancer cell lines.

REFERENCES

Alonso A, Sasin J, Bottini N, Friedberg I et al. 2004. Protein tyrosine phosphatases in the human genome. Cell 117(6):699-711.

American Cancer Society. Cancer Facts and Figures (2007). American Cancer Society [online] http://www.cancer.org/docroot/home/index.asp.

Arena S, Benvenuti S, Bardelli A. 2005. Genetic analysis of the kinome and phosphatome in cancer. Cellular and Molecular Life Sciences: CMLS 62(18):2092-9.

Begley MJ, Dixon JE. 2005. The structure and regulation of myotubularin phosphatases. Current Opinion in Structural Biology 15(6):614-20.

Ben-Porath I, Weinberg RA. 2004. When cells get stressed: an integrative view of cellular senescence. The Journal of Clinical Investigation 113(1):8-13.

Berman-Golan D, Granot-Attas S, Elson A. 2008. Protein tyrosine phosphatase epsilon and Neu-induced mammary tumorigenesis. Cancer Metastasis Reviews 27(2):193-203.

Bessette DC, Qiu D, Pallen CJ. 2008. PRL PTPs: mediators and markers of cancer progression. Cancer Metastasis Reviews 27(2):231-52.

Breuhahn K, Longerich T, Schirmacher P. 2006. Dysregulation of growth factor signaling in human hepatocellular carcinoma. Oncogene 25(27):3787-800.

Calvisi DF, Pinna F, Meloni F, Ladu S et al. 2008. Dual-specificity phosphatase 1 ubiquitination in extracellular signal-regulated kinase-mediated control of growth in human hepatocellular carcinoma. Cancer Research 68(11):4192-200.

Campisi J. 2005. Suppressing cancer: the importance of being senescent. Science 309(5736):886-7.

Chan G, Kalaitzidis D, Neel BG. 2008. The tyrosine phosphatase Shp2 (PTPN11) in cancer. Cancer Metastasis Reviews 27(2):179-92.

Chen JH, Hales CN, Ozanne SE. 2007. DNA damage, cellular senescence and organismal ageing: causal or correlative? Nucleic Acids Research 35(22):7417-28.

Chen X et al. 2002. Gene expression patterns in human liver cancers. Molecular Biology of the Cell 13(6):1929-39.

Cohen P. 2001. The role of protein phosphorylation in human health and disease. The Sir Hans Krebs Medal Lecture. European Journal of Biochemistry / FEBS 268(19):5001-10.

Collado M, Gil J, Efeyan A, Guerra C et al. 2005. Tumour biology: senescence in premalignant tumours. Nature 436(7051):642.

Combet C, Blanchet C, Geourjon C, Deléage G. 2000. NPS@:Network Protein Sequence Analysis TIBS 25, No 3 291:147-150.

De Toni EN, Kuntzen C, Gerbes AL, Thasler WE et al. 2007. P60-c-src suppresses apoptosis through inhibition of caspase 8 activation in hepatoma cells, but not in primary hepatocytes. Journal of Hepatology 46(4):682-91.

Degos F, Christidis C, Ganne-Carrie N, Farmachidi JP et al. Hepatitis C virus related cirrhosis: time to occurrence of hepatocellular carcinoma and death. Gut 47(1):131-6.

Dickinson RJ, Keyse SM. 2006. Diverse physiological functions for dual-specificity MAP kinase phosphatases. Journal of Cell Science 119(Pt 22):4607-15.

Dimri GP. 2005. What has senescence got to do with cancer? Cancer Cell 7(6):505-12.

Dimri GP, Lee X, Basile G, Acosta M et al. 1995. A biomarker that identifies senescent human cells in culture and in aging skin in vivo. PNAS 92:9363-7.

El-Serag HB, Rudolph KL. 2007. Hepatocellular carcinoma: epidemiology and molecular carcinogenesis. Gastroenterology 132(7):2557-76.

El-Serag HB, Tran T, Everhart JE. 2004. Diabetes increases the risk of chronic liver disease and hepatocellular carcinoma. Gastroenterology 126(2):460-8.

Farazi PA, DePinho RA. 2006. Hepatocellular carcinoma pathogenesis: from genes to environment. Nature Reviews Cancer 6(9):674-87.

Farrell GC, Larter CZ. 2006. Nonalcoholic fatty liver disease: from steatosis to cirrhosis. Hepatology 43(2 Suppl 1):S99-S112.

Fujiwara Y, Hoon DS, Yamada T, Umeshita K et al. 2000. PTEN / MMAC1 mutation and frequent loss of heterozygosity identified in chromosome 10q in a subset of hepatocellular carcinomas. Japanese Journal of Cancer Research 91(3):287-92.

Funayama R, Ishikawa F. 2007. Cellular senescence and chromatin structure. Chromosoma 116(5):431-40.

Gallego M, Virshup DM. 2005. Protein serine/threonine phosphatases: life, death, and

sleeping. Current Opinion in Cell Biology 17(2):197-202.

Goodman ZD. 2007. Neoplasms of the liver. Modern Pathology 20(Suppl 1):S49-60.

Gorbunova V, Seluanov A, Pereira-Smith OM. 2002. Expression of human telomerase (hTERT) does not prevent stress-induced senescence in normal human fibroblasts but protects the cells from stress-induced apoptosis and necrosis. Journal of Biological Chemistry 277(41):38540-9.

Grant PA. 2001. A tale of histone modifications. Genome Biology 2(4):reviews0003.1-0003.6.

Guan XY, Fang Y, Sham JS, Kwong DL et al. 2000. Recurrent chromosome alterations in hepatocellular carcinoma detected by comparative genomic hybridization. Genes, Chromosomes and Cancer 29(2):110-6.

Guermeur Y, Geourjon C, Gallinari P, Deleage G. 1999. Improved performance in protein secondary structure prediction by inhomogeneous score combination. Bioinformatics 15(5):413-421.

Hammaker DR, Boyle DL, Inoue T, Firestein GS. 2007. Regulation of the JNK pathway by TGF-beta activated kinase 1 in rheumatoid arthritis synoviocytes. Arthritis Research & Therapy 9(3):R57.

Hanahan D, Weinberg RA. 2000. The hallmarks of cancer. Cell 100(1):57-70.

Hayashi J, Aoki H, Kajino K, Moriyama M et al. 2000. Hepatitis C virus core protein activates the MAPK/ERK cascade synergistically with tumor promoter TPA, but not with epidermal growth factor or transforming growth factor alpha. Hepatology 32(5):958-61.

Hayflick L. 1965. The limited in vitro lifetime of human diploid cell strains. Experimental Cell Research 37:614-636.

Herbig U, Sedivy JM. 2006. Regulation of growth arrest in senescence: telomere damage is not the end of the story. Mechanism of Ageing and Development 127(1):16-24.

Höpfner M, Schuppan D, Scherübl H. 2008. Growth factor receptors and related signalling pathways as targets for novel treatment strategies of hepatocellular cancer. World Journal of Gastroenterology 14(1):1-14.

Hui L, Bakiri L, Mairhorfer A, Schweifer N et al. 2007. p38alpha suppresses normal and cancer cell proliferation by antagonizing the JNK-c-Jun pathway. Nature Genetics 39(6):741-9.

Hui L, Zatloukal K, Scheuch H, Stepniak E et al. 2008. Proliferation of human HCC

cells and chemically induced mouse liver cancers requires JNK1-dependent p21 downregulation. Journal of Clinical Investigation 118(12):3943-53.

Hunter T. 2007. The age of cross-talk: phosphorylation, ubiquitination, and beyond. Molecular Cell 28(5):730-8.

Inoue H, Nojima H, Okayama H. 1990. High efficiency transformation of Escherichia coli with plasmids. Gene 96:23-8.

Iyoda K, Sasaki Y, Horimoto M, Toyama T et al. 2003. Involvement of the p38 mitogen-activated protein kinase cascade in hepatocellular carcinoma. Cancer 97(12):3017-26.

Janssens V, Goris J, Van Hoof C. 2005. PP2A: the expected tumor suppressor. Current Opinion in Genetics and Development 15(1):34-41.

Jin X, Zimmers TA, Perez EA, Pierce RH et al. 2006. Paradoxical effects of short- and long-term interleukin-6 exposure on liver injury and repair. Hepatology 43(3):474-84.

Jou YS, Lee CS, Chang YH, Hsiao CF et al. 2004. Clustering of minimal deleted regions reveals distinct genetic pathways of human hepatocellular carcinoma. Cancer Research 64(9):3030-6.

Kawamura N, Nagai H, Bando K, Koyama M et al. 1999. PTEN/MMAC1 mutations in hepatocellular carcinomas: somatic inactivation of both alleles in tumors. Japanese Journal of Cancer Research 90(4):413-8.

Keyse SM. 2008. Dual-specificity MAP kinase phosphatases (MKPs) and cancer. Cancer and Metastasis Reviews 27(2):253-61.

Kim SA, Vacratsis PO, Firestein R, Cleary ML et al. 2003. Regulation of myotubularin-related (MTMR)2 phosphatidylinositol phosphatase by MTMR5, a catalytically inactive phosphatase. PNAS 100(8):4492-7.

King RD, Sternberg MJ. 1996. Identification and application of the concepts important for accurate and reliable protein secondary structure prediction. Protein Science 5(11):2298-310.

Kissil JL, Feinstein E, Cohen O, Jones PA et al. 1997. DAP-kinase loss of expression in various carcinoma and B-cell lymphoma cell lines: possible implications for role as tumor suppressor gene. Oncogene 15(4):403-7.

Kitay-Cohen Y, Amiel A, Ashur Y, Fejgin MD et al. 2001. Analysis of chromosomal aberrations in large hepatocellular carcinomas by comparative genomic hybridization. Cancer Genetics and Cytogenetics 131(1):60-4.

Kowluru A. 2008. Emerging roles for protein histidine phosphorylation in cellular signal transduction: lessons from the islet beta-cell. Journal of Cellular and Molecular Medicine 12(5B):1885-908.

Krause DS, Van Etten RA. 2005. Tyrosine kinases as targets for cancer therapy. The New England Journal of Medicine 353(2):172-87.

Krishna M, Narang H. The complexity of mitogen-activated protein kinases (MAPKs) made simple. Cellular and Molecular Life Sciences: CMLS 65(22):3525-44.

La Starza R, Crescenzi B, Pierini V, Romoli S et al. 2007. A common 93-kb duplicated DNA sequence at 1q21.2 in acute lymphoblastic leukemia and Burkitt lymphoma. Cancer Genetics and Cytogenetics 175(1):73-6.

Lang R, Hammer M, Mages J. 2006. DUSP meet immunology: dual specificity MAPK phosphatases in control of the inflammatory response. Journal of Immunology (Baltimore, Md.:1950) 177(11):7497-504.

Lok AS. 2000. Hepatitis B infection: pathogenesis and management. Journal of Hepatology 32(1 Suppl):89-97.

Lu X, Nguyen TA, Moon SH, Darlington Y et al. 2008. The type 2C phosphatase Wip1: an oncogenic regulator of tumor suppressor and DNA damage response pathways. Cancer Metastasis Reviews 27(2):123-35.

Ma DZ, Xu Z, Liang YL, Su JM et al. 2005. Down-regulation of PTEN expression due to loss of promoter activity in human hepatocellular carcinoma cell lines. World Journal of Gastroenterology 11(29):4472-7.

MacKeigan JP, Murphy LO, Blenis J. 2005. Sensitized RNAi screen of human kinases and phosphatases identifies new regulators of apoptosis and chemoresistance. Nature Cell Biology 7(6):591-600.

Maheshwari S, Sarraj A, Kramer J, El-Serag HB. 2007. Oral contraception and the risk of hepatocellular carcinoma. Journal of Hepatology 47(4):506-13.

Majumder M, Ghosh AK, Steele R, Ray R et al. 2001. Hepatitis C virus NS5A physically associates with p53 and regulates p21/waf1 gene expression in a p53-dependent manner. Journal of Virology 75(3):1401-7.

Manning G, Whyte DB, Martinez R, Hunter T. 2002. The protein kinase complement of the human genome. Science 298(5600):1912-34.

Marusawa H, Hijikata M, Chiba T, Shimotohno K. 1999. Hepatitis C virus core protein inhibits Fas- and tumor necrosis factor alpha-mediated apoptosis via NF-kappaB activation. Journal of Virology 73(6):4713-20.

Masuda K, Shima H, Kikuchi K, Watanabe Y et al. 2000. Expression and comparative chromosomal mapping of MKP-5 genes DUSP10/Dusp10. Cytogenetics and Cell Genetics 90(1-2):71-4.

McKillop IH, Moran DM, Jin X, Koniaris LG. 2006. Molecular pathogenesis of hepatocellular carcinoma. The Journal of Surgical Research 136(1):125-35.

Moran DM, Mattocks MA, Cahill PA, Koniaris LG et al. 2008. Interleukin-6 mediates G(0)/G(1) growth arrest in hepatocellular carcinoma through a STAT 3-dependent pathway. Journal of Surgical Research 147(1):23-33.

Nonn L, Duong D, Peehl DM. 2007. Chemopreventive anti-inflammatory activities of curcumin and other phytochemicals mediated by MAP kinase phosphatase-5 in prostate cells. Carcinogenesis 28(6):1188-96.

Nonn L, Peng L, Feldman D, Peehl DM. 2006. Inhibition of p38 by vitamin D reduces interleukin-6 production in normal prostate cells via mitogen-activated protein kinase phosphatase 5: implications for prostate cancer prevention by vitamin D. Cancer Research 66(8):4516-24.

Nousiainen M, Silljé HH, Sauer G, Nigg EA et al. 2006. Phosphoproteome analysis of the human mitotic spindle. PNAS 103(14):5391-6.

Olsen JV, Blagoev B, Gnad F, Macek B et al. 2006. Global, in vivo, and site-specific phosphorylation dynamics in signaling networks. Cell 127(3):635-48.

Oshimura M, Barrett JC. 1997. Multiple pathways to cellular senescence: role of telomerase repressors. European Journal of Cancer 33(5):710-5.

Ozturk M, Arslan-Ergul A, Bagislar S, Senturk S et al. 2008. Senescence and immortality in hepatocellular carcinoma. Cancer Letters [Epub ahead of print].

Ozturk N, Erdal E, Mumcuoglu M, Akcali KC et al. 2006. Reprogramming of replicative senescence in hepatocellular carcinoma-derived cells. PNAS 103(7):2178-83.

Pachiadakis I, Pollara G, Chain BM, Naoumov NV. 2005. Is hepatitis C virus infection of dendritic cells a mechanism facilitating viral persistence? The Lancet Infectious Diseases 5(5):296-304.

Patterson KI, Brummer T, O'Brien PM, Daly RJ. 2009. Dual-specificity phosphatases: critical regulators with diverse cellular targets. The Biochemical Journal 418(3):475-89.

Peehl DM, Shinghal R, Nonn L, Seto E et al. 2004. Molecular activity of 1,25-dihydroxyvitamin D3 in primary cultures of human prostatic epithelial cells

revealed by cDNA microarray analysis. Journal of Steroid Biochemistry and Molecular Biology 92(3):131-41.

Pimienta G, Pascual J. 2007. Canonical and alternative MAPK signaling. Cell Cycle 6(21):2628-32.

Puisieux A, Lim S, Groopman J, Ozturk M. 1991. Selective targeting of p53 gene mutational hotspots in human cancers by etiologically defined carcinogens. Cancer Research 51(22):6185-9.

Ray RB, Lagging LM, Meyer K, Steele R et al. 1995. Transcriptional regulation of cellular and viral promoters by the hepatitis C virus core protein. Virus Research 37(3):209-20.

Rebhan M, Chalifa-Caspi V, Prilusky J, Lancet D. 1998. GeneCards: A novel functional genomics compendium with automated data mining and query reformulation support. Bioinformatics 14:656-664.

Robinson FL, Dixon JE. 2005. The phosphoinositide-3-phosphatase MTMR2 associates with MTMR13, a membrane-associated pseudophosphatase also mutated in type 4B Charcot-Marie-Tooth disease. Journal of Biological Chemistry 280(36):31699-707.

Rost B, Sander C. 1994. Combining evolutionary information and neural networks to predict protein secondary structure. Proteins 19(1):55-72.

Sayan B, Tolga Emre NC, Irmak MB, Ozturk M et al. 2009. Nuclear Exclusion of p33ING1b Tumor Suppressor Protein: Explored in HCC Cells Using a New Highly Specific Antibody. Hybridoma (Larchmt) [Epub ahead of print].

Shay JW, Bacchetti S. 1997. A survey of telomerase activity in human cancer. European Journal of Cancer 33(5):787-91.

Shay JW, Wright WE. 2004. Senescence and immortalization: role of telomeres and telomerase. Carcinogenesis 26(5):867-874.

Sherr CJ, McCormick F. 2002. The RB and p53 pathways in cancer. Cancer Cell 2(2):103-12.

Sherwood SW, Rush D, Ellsworth JL, Schimke RT. 1988. Defining cellular senescence in IMR-90 cells: a flow cytometric analysis. PNAS 85(23):9086-90.

Su AI, Cooke MP, Ching KA, Hakak Y et al. 2002. Large-scale analysis of the human and mouse transcriptomes. PNAS 99(7):4465-4470.

Taki K, Shimozono R, Kusano H, Suzuki N et al. 2008. Apoptosis signal-regulating

kinase 1 is crucial for oxidative stress-induced but not for osmotic stress-induced hepatocyte cell death. Life Sciences 83(25-26):859-64.

Tanoue T, Moriguchi T, Nishida E. 1999. Molecular cloning and characterization of a novel dual specificity phosphatase, MKP-5. Journal of Biological Chemistry 274(28):19949-56.

Tao X, Tong L. 2007. Crystal structure of the MAP kinase binding domain and the catalytic domain of human MKP5. Protein Science 16(5):880-6.

Tarn C, Lee S, Hu Y, Ashendel C et al. 2001. Hepatitis B virus X protein differentially activates RAS-RAF-MAPK and JNK pathways in X-transforming versus non-transforming AML12 hepatocytes. Journal of Biological Chemistry 276(37):34671-80.

Teng DH, Perry WL 3rd, Hogan JK, Baumgard M et al. 1997. Human mitogen-activated protein kinase kinase 4 as a candidate tumor suppressor. Cancer Research 57(19):4177-82.

Theodosiou A, Smith A, Gillieron C, Arkinstall S et al. 1999. MKP5, a new member of the MAP kinase phosphatase family, which selectively dephosphorylates stress-activated kinases. Oncogene 18(50):6981-8.

Thompson JD, Gibson TJ, Plewniak F, Jeanmougin F et al. 1997. The CLUSTAL_X windows interface: flexible strategies for multiple sequence alignment aided by quality analysis tools. Nucleic Acids Research 25(24):4876-82.

Tonks NK. 2006. Protein tyrosine phosphatases: from genes, to function, to disease. Nature Reviews Molecular Cell Biology 7(11):833-46.

Tornillo L, Carafa V, Sauter G, Moch H et al. 2002. Chromosomal alterations in hepatocellular nodules by comparative genomic hybridization: high-grade dysplastic nodules represent early stages of hepatocellular carcinoma. Laboratory Investigation 82(5):547-53.

Tsuboi Y, Ichida T, Sugitani S, Genda T et al. 2004. Overexpression of extracellular signal-regulated protein kinase and its correlation with proliferation in human hepatocellular carcinoma. Liver International 24(5):432-6.

Ventura JJ, Nebreda AR. 2006. Protein kinases and phosphatases as therapeutic targets in cancer. Clinical and Translational Oncology 8(3):153-60.

Villanueva A, Chiang DY, Newell P, Peix J et al. 2008. Pivotal role of mTOR signaling in hepatocellular carcinoma. Gastroenterology 135(6):1972-83, 1983.e1-11.

Wiemann SU, Satyanarayana A, Tsahuridu M, Tillmann HL et al. 2002. Hepatocyte telomere shortening and senescence are general markers of human liver cirrhosis. The FASEB Journal 16(9):935-42.

Wong CC, Wong CM, Tung EK, Man K et al. 2009. Rho-kinase 2 is frequently overexpressed in hepatocellular carcinoma and involved in tumor invasion. Hepatology 49(5):1583-94.

Wurmbach E, Chen YB, Khitrov G, Zhang W et al. 2007. Genome-wide molecular profiles of HCV-induced dysplasia and hepatocellular carcinoma. Hepatology 45(4):938-47.

Xu R, Yu Y, Zheng S, Zhao X et al. 2005. Overexpression of Shp2 tyrosine phosphatase is implicated in leukemogenesis in adult human leukemia. Blood 106(9):3142-9.

Xue Y, Ren J, Gao X, Jin C et al. 2008. GPS 2.0, a tool to predict kinase-specific phosphorylation sites in hierarchy. Molecular and Cellular Proteomics 7:1598-1608.

Yoshida T, Hisamoto T, Akiba J, Koga H et al. 2006. Spreds, inhibitors of the Ras/ERK signal transduction, are dysregulated in human hepatocellular carcinoma and linked to the malignant phenotype of tumors. Oncogene 25(45):6056-66.

Zhang Y, Blattman JN, Kennedy NJ, Duong J et al. 2004. Regulation of innate and adaptive immune responses by MAP kinase phosphatase 5. Nature 430(7001):793-7.

Zhang YL, Dong C. 2005. MAP kinases in immune responses. Cellular and Molecular Immunology 2(1):20-7.

Zhao LJ, Wang L, Ren H, Cao J et al. 2005. Hepatitis C virus E2 protein promotes human hepatoma cell proliferation through the MAPK/ERK signaling pathway via cellular receptors. Experimental Cell Research 305(1):23-32.

Zhao WB, Li Y, Liu X, Zhang LY et al. 2008. Evaluation of PRL-3 expression, and its correlation with angiogenesis and invasion in hepatocellular carcinoma. International Journal of Molecular Medicine 22(2):187-92.